UNIVERSIDADE DE LISBOA

INSTITUTO SUPERIOR TÉCNICO

The effect of a schizophrenia polygenic risk score on brain function during verbal fluency in health, schizophrenia and bipolar disorder

Mariana Génio Balseiro

Thesis to obtain the Master of Science Degree in

Biomedical Engineering

Supervisor: Prof. Dr. Diana Maria Pinto Prata

Co-supervisor: Prof. Dr. Patrícia Margarida Piedade Figueiredo

Examination Committee

Chairperson: Prof. Dr. Maria do Rosário De Oliveira Silva

Supervisor: Prof. Dr. Diana Maria Pinto Prata

Member of Committee: Prof. Dr. Hugo Alexandre Ferreira

November 2017

Agradecimentos

Às minhas orientadoras Diana Prata e Patrícia Figueiredo, um muito obrigada pela dedicação, disponibilidade e flexibilidade que demonstraram ao longo destes meses. Agradeço também por me terem introduzido à imagiologia genética, uma área que me era totalmente desconhecida antes de começar a trabalhar neste projecto e que revelou ser mesmo aquilo que estava à procura quando ingressei há cinco anos no curso de Engenharia Biomédica – um trabalho multidisciplinar e desafiante. Estou grata pelos conhecimentos que partilharam comigo e pelo entusiasmo que sempre me mostraram.

Não poderia deixar de agradecer a todos os meus colegas (e grandes amigos) do DPrata Lab no iMM. Nomeadamente, gostava de agradecer à Vânia Tavares, Mónica Costa, Katja Brodmann, Carina Mendes, Beatriz Simões, Gonçalo Cosme e Gonçalo Oliveira por terem estado presentes nesta caminhada e por se mostrarem sempre disponíveis para me ajudar, mesmo não estando à vontade com o meu trabalho. Obrigada pelas sugestões, pelos desabafos e pelo carinho de vocês todos. Obrigada por fazerem todos os momentos valerem a pena.

Também queria deixar uma mensagem especial a todos os meus amigos do Técnico, em particular à malta do MEBiom12', por terem estado ao meu lado nos bons e nos maus momentos e por não me terem deixado desistir em altura alguma. Passámos juntos por alturas muito complicadas, que teriam sido impossíveis de aguentar sem vocês. Tenho a certeza que amizades como as vossas vão permanecer durante toda a vida. Um F-R-A para todos!

Queria mostrar o meu agradecimento também aos meus amigos de longa data. Vocês provaram que a distância não significa nada quando a amizade existe. Um beijinho em particular para os meus aveirenses preferidos, Samuel Bartolomeu, Inês Reis, Rui Canha, Mariana Pinheiro e Filipe Martinho. Queria agradecer de forma especial ao Nuno Matias, pela paciência, dedicação e pelo tempo que disponibilizou durante este percurso. Estou muito grata por fazeres parte da minha vida.

Por último, gostaria de agradecer à minha família pelo apoio incondicional. O mais difícil neste percurso por Lisboa foi ter de estar longe de vocês nos momentos mais difíceis e não poder celebrar convosco outros momentos tão importantes para mim. Obrigada mãe e pai, por me terem dado sempre o melhor de vocês, obrigada mano chato por me animares, obrigada querida avó e madrinha, por estarem sempre disponíveis para me ajudarem.

Gostaria de dedicar esta tese ao meu avô Gabriel, que sempre me ajudou e acompanhou quase até ao final destes cinco anos. Espero honrar a tua memória da melhor forma possível e espero que, onde quer que estejas, que sintas orgulhoso de mim. Obrigada por tudo.

Resumo

Doenças psicóticas, como a esquizofrenia (SCZ) e a doença bipolar (BD), são hereditárias e apresentam uma arquitetura poligénica. De forma a validar o efeito de variantes genéticos de risco na suscetibilidade para a psicose, o seu impacto em fenótipos intermediários presentes nestas doenças deve ser investigado. Este estudo exploratório testou o efeito de um *score* de risco poligénico (PRS) calculado para a SCZ, que combina o impacto de vários fatores genéticos de risco, na ativação e conectividade funcional cerebrais presentes durante uma tarefa de fluência verbal (VF), um fenótipo intermediário em que doentes com SCZ e BD apresentam alterações. Para tal, imagens de ressonância magnética funcional (fMRI) foram adquiridas numa amostra constituída por controlos (n=39), doentes com BD (n=25) e com SCZ (n=10) e familiares saudáveis (n=27). As imagens foram analisadas usando um método de mapeamento estatístico paramétrico, tendo em conta dos efeitos do diagnóstico e de várias covariáveis sem interesse. Encontrei uma tendência negativa entre o PRS e a ativação da circunvolução frontal inferior esquerda e da ínsula direita em todos os participantes, mas mais predominante nos controlos, possivelmente devido à maior dimensão do grupo. O PRS está também associado, num nível não-corrigido, a uma maior conectividade entre a circunvolução frontal inferior esquerda com a circunvolução angular esquerda (na BD) e com o tálamo esquerdo e a circunvolução lingual direita (nos familiares), áreas relacionadas com a linguagem. Estes resultados indicam que os SCZ-PRSs podem prever alterações da função cerebral, sendo no entanto necessária uma validação num estudo independente.

Palavras-chave: *score* de risco poligénico, esquizofrenia, fluência verbal, fMRI, endofenótipo, imagiologia genética

Abstract

Psychotic disorders, including schizophrenia (SCZ) and bipolar disorder (BD), are highly heritable illnesses with a polygenic and overlapping architecture. To better characterize and validate the effect of previously identified genetic risk variants on psychosis susceptibility, their impact on the intermediate phenotypes of these disorders warrants examination. I investigated for the first time the effect of a polygenic risk score (PRS) for SCZ, which gathers the cumulative impact of several genetic risk factors, on brain activation and connectivity during verbal fluency (VF), an intermediate phenotype showing impairment in SCZ and BD. For this, functional magnetic resonance images (fMRI) were collected from a group of SCZ (n=10) and BD (n=25) patients, their healthy relatives (n=27) and healthy controls (n=39). The fMRI data were analyzed using statistical parametric mapping, in order to identify the effects of PRS on brain activation and on task-modulated connectivity, taking into account the effects of diagnosis as well as a number of nuisance covariates. I found a negative association trend (uncorrected for multiple comparisons) between the SCZ-PRS and the activation of the language-related left inferior frontal gyrus and right insula, effects that were more pronounced in the control group. I also found a positive trend between the SCZ-PRS and the task-modulated connectivity of the left inferior frontal gyrus with the left angular gyrus (in BD) and left thalamus and right lingual gyrus (in relatives), areas also implicated in language. These findings suggest that SCZ-PRSs may preclude changes in brain function during VF – and now warrant independent validation.

Keywords: polygenic risk score, schizophrenia, verbal fluency, fMRI, endophenotype, imaging genetics

Table of contents

List of Figures

List of Tables

List of Abbreviations

3D	Three-dimensional
AAL2	Automated Anatomical Labeling 2
ACC	Anterior cingulate cortex
ANK3	Ankyrin 3
ANOVA	Analysis of variance
APA	American Psychiatric Association
AVOI	Anatomical volume of interest
BD	Bipolar Disorder
BOLD	Blood oxygenation level-dependent
BRC	Biomedical Research Center
CACNA1C	Alpha subunit of the L-type calcium channel
CBF	Cerebral blood flow
COMT	Catechol-o-methyl transferase
df	Degrees of freedom
DGKH	Diacylglycerol kinase eta
dHB	Deoxygenated hemoglobin
DISC1	Disrupted in schizophrenia 1
DLPFC	Dorsolateral prefrontal cortex
DRD2	Dopamine receptor D2
DSM	Diagnostic and Statistical Manual of Mental Disorders
DTNBP1	Dystrobrevin binding protein 1
FGA	First generation antipsychotic
fMRI	Functional magnetic resonance imaging
FWE	Family-wise error
GLM	General linear model
GWAS	Genome-wide association studies
HRF	Hemodynamic response function
HB	Oxygenated hemoglobin
ISC	International Schizophrenia Consortium
IQ	Intelligence quotient
MAF	Minor allele frequency
MNI	Montreal Neurological Institute
NART	National Adult Reading Test
NCAN	Neurocan
NIRS	Near-infrared spectroscopy
NRG1	Neuregulin 1
NRGN	Neurogranin
ODZ4	Odd Oz/teneurin transmembrane protein 4
PC	Principal component
PGC	Psychiatric Genomics Consortium
PPI	Psychophysiological interaction
PRS	Polygenic risk score
RF	Radiofrequency
RFT	Random field theory
ROI	Region of interest
SCZ	Schizophrenia
SGA	Second generation antipsychotic
SNP	Single-nucleotide polymorphism
SPM	Statistical parametric mapping
SVC	Small Volume Correction
SWGPGC	Schizophrenia Working Group of the Psychiatric Genomics Consortium
TCF4	Transcription factor 4
TE	Echo time
TPM	Tissue probability maps

TR	Repetition time
VF	Verbal fluency
VOI	Volume of interest
VLPFC	Ventrolateral prefrontal cortex
WAIS	Wechsler Adult Intelligence Scale
YE	Years of education
ZNF804A	Zinc finger protein 804A

1. Introduction

1.1 Motivation

Psychotic disorders are a group of heterogeneous, polygenic and complex mental illnesses characterized by the presence of psychotic symptoms, namely delusions, hallucinations, disorganized thinking, abnormal motor behavior and negative symptoms such as apathy, reductions in speech or impaired attention (American Psychiatric Association [APA], 2013). Psychotic disorders have a lifetime prevalence of around 3% (Perälä et al., 2007) and represent one of the greatest causes of economic and humanistic burden worldwide (Millier et al., 2014). In the last 100 years, a great effort has been made to understand the etiological factors that contribute to the onset of these disorders such as genetic risk factors. However, the underlying pathways involved on the diseases mechanism are still unknown, compromising the prediction of their development and an early intervention on individuals at risk mental state.

In the 1890s, Emil Kraepelin divided psychosis into two distinct forms: manic depressive psychosis and dementia praecox, diseases with different underlying processes and etiology (Kraepelin, 1896). The first term comprises mood disorders such as bipolar disorder (BD) while the second refers to schizophrenia (SCZ). Although these disorders were earlier considered two distinct extremes of psychosis, evidence from genetic epidemiology suggests that there is a large overlap between them due to the shared susceptibility genes and risk variants, familial coaggregation and symptomatic similarity, even though details about similarities and differences are still not well elucidated. Genome-wide association studies (GWAS) have discovered several risk variants, by identifying new single-nucleotide polymorphisms (SNPs) significantly associated with the risk of developing SCZ (Schizophrenia Working Group of the Psychiatric Genomics Consortium [SWGPGC], 2014) and/or BD (Psychiatric GWAS Consortium Bipolar Disorder Working Group [PCBDWG], 2011), but the impact of these genetic variations on functional mechanisms that lead to psychosis is still not clear.

Imaging genetics is a research approach that aids in the understanding of the unknown disease pathways, by integrating genetics and brain function and structure to discover the risk variations that underlie a relevant biological process associated with a target phenotype or to characterize the neural circuits affected by certain genetic variations. It uses imaging-based phenotypes, called intermediate phenotypes or endophenotypes, that are disease-related and heritable phenotypes, present on a subject independently if the disorder is active or not. Endophenotypes lie closer to the disease pathophysiology than a heterogeneous clinical phenotype, contributing to an increased power to detect the effects of genetic risk variants. Cognitive dysfunction, particularly verbal fluency (VF) impairment, is considered a promising endophenotype for psychotic disorders due to its manifestation on patients and their unaffected relatives, in a smaller extent on the latter (Kim et al., 2015).

As an alternative to studying the individual effect of the disease-related genetic variants found in GWAS studies on brain function, it is possible to analyze the cumulative effect of hundreds or thousands of risk variants concatenated on a polygenic risk score (PRS). A PRS is calculated for each individual as the weighted sum of

multiple risk variants, also called alleles, for a particular disease, explaining thus a larger fraction of heritability when compared to individual SNPs.

The technique of functional magnetic resonance imaging (fMRI) has been used to study the impact of the cognitive impairments present on psychosis, on brain function. fMRI measures the variance in blood flow that follows changes on neuronal activity. Blood flow changes are detectable with fMRI because of the different magnetic properties of hemoglobin, which depends on its binding to the oxygen molecules, and are due to the local increase of oxygenated blood following neural activity. The fMRI images are acquired over a time period in a group of participants and preprocessed to remove artifacts and allow comparisons across them. Statistical parametric mapping is generally used to identify functionally specialized brain regions and it is based on the general linear model (GLM), which estimates the parameters that better fit the data and uses its variance to make inferences about effects of interest.

My work focuses on the investigation of the relationship between a PRS and functional phenotypes (of brain activation and connectivity) exhibited during a VF paradigm, in a group of participants comprising SCZ patients, BD patients, SCZ and BD relatives and healthy controls. I have also analyzed if the effect of a PRS on these endophenotypes depends on the diagnostic groups and if it is associated with the paradigm and in concordance with the previous findings. This is the first study to analyze the effect of PRS on endophenotypes revealed by a VF paradigm and to study the effects of PRS on task-modulated connectivity on psychotic subjects.

1.2 Thesis overview

This thesis is divided on the following chapters:

Chapter 1 (Introduction): This chapter comprises the motivation, theoretical concepts, literature review, objectives, hypotheses, contributions and collaborations. The theoretical background is divided on five sections: psychotic disorders, fMRI, endophenotype, genetics and imaging genetics. Firstly, SCZ and BD are defined and their symptoms are described; the principal results on their genetic background are discussed. A brief summary of the technique of fMRI is made, in order to understand the mechanisms of the MRI signal and to present the model used to explain the data. Then, VF task is introduced as a possible neuroimaging endophenotype for SCZ and BD – the performance and imaging features of those disorders are discussed. The genetics section explains how the PRSs are usually determined and resumes the findings of previous studies that used PRSs. Lastly, the imaging genetics approaches are described and relevant studies on this area are presented. The literature review contains an extensive bibliographic review on the studies of the association between the PRSs and the structural and functional neuroimaging phenotypes.

Chapter 2 (Materials and Methods): This chapter is divided into: participants, genetics and imaging. First, the selection of participants to include on the final sample and their demographic characteristics are described. Genotyping, genetic processing and calculation of the PRSs are then briefly explain. Finally, the paradigm and the acquisition parameters are presented; the preprocessing of fMRI data is explained and

statistical models used to analyze the data are enlightened, particularly, the statistical models used to study the performance of the participants and their regional brain activation and connectivity.

Chapter 3 (Results): This section provides a description of the results found for the task performance and task imaging analyses (encompassing brain activity and brain connectivity analyses). All sections (performance analysis, activation analysis and connectivity analysis) are organized into effect of task, effect of diagnosis and effect of PRS. A section of additional exploratory analysis is provided.

Chapter 4 (Discussion): A discussion of the findings of the previous chapter is made on this section.

Chapter 5 (Conclusions and future works): The main conclusions of this work, existent limitations and future developments that should be included on further studies are summarized.

1.3 Theoretical background

1.3.1 Psychotic disorders

Psychotic disorders are a heterogeneous group of disorders characterized by abnormalities in one or more of the succeeding five domains: delusions, hallucinations, disorganized thinking, grossly disorganized or abnormal motor behavior, defining positive symptoms, and negative symptoms (APA, 2013). Positive symptoms are associated with distortion of the normal functions (qualitative impairment) while negative symptoms reveal a reduction in normal functions (quantitative impairment), particularly in emotions and behaviors (Noll, 2009).

In addition, delusions are defined as fixed beliefs that do not change in the light of contradictory evidence. Hallucinations are sensory experiences that occur in the absence of any external stimulus. Disorganized thinking, formally referred as thought disorder, can be inferred from the subject's speech, as it shows a disconnection on the semantic content. Negative symptoms include diminished emotional expression, avolition (decrease in self-initiated activities) and apathy (APA, 2013; Noll, 2009).

Psychotic disorders not only include SCZ, but also schizophreniform disorder, brief psychotic disorder, schizoaffective disorder, delusional disorder, schizotypal disorder and catatonia. The distinction between these disorders depends on the level and duration of psychosis and the number of symptoms (Heckers, 2016). Psychosis has, as its core elements, the loss of reality testing and the creation of a new reality and can be induced by drugs, medications or other medical condition (Noll, 2009).

The Diagnostic and Statistical Manual of Mental Disorders, Fifth Edition (DSM-5) also considers that bipolar and related disorders are a bridge between the SCZ spectrum and depression disorders in terms of genetic susceptibility, etiology, symptoms and family history (APA, 2013). The first three factors will be discussed in next sections. Family history involves the concept of familial coaggregation between SCZ and BD families, i.e., the association between the two disorders explained by the existence of shared familial factors (Hudson et al., 2008). For example, a manifestation of familial coaggregation is the fact that first-degree relatives of SCZ patients show increased rates of BD when compared to first degree relatives of healthy controls and vice-versa (Van Snellenberg & de Candia, 2009).

Due to these similarities, some authors have proposed a dimensional approach to the psychosis continuum; their results suggest a hybrid model where prototypic SCZ and BD subjects are at two different extremes and several patients lie in a continuum spectrum between those two disorders (Keshavan et al., 2011) (Figure 1.1). The position of an individual on the psychosis continuum and his clinical features depend on the inherited susceptibility genes and on the exposure to several environmental and neurodevelopmental factors. In this dissertation, discussion will focus on functional and genetic differences and similarities between SCZ and BD.

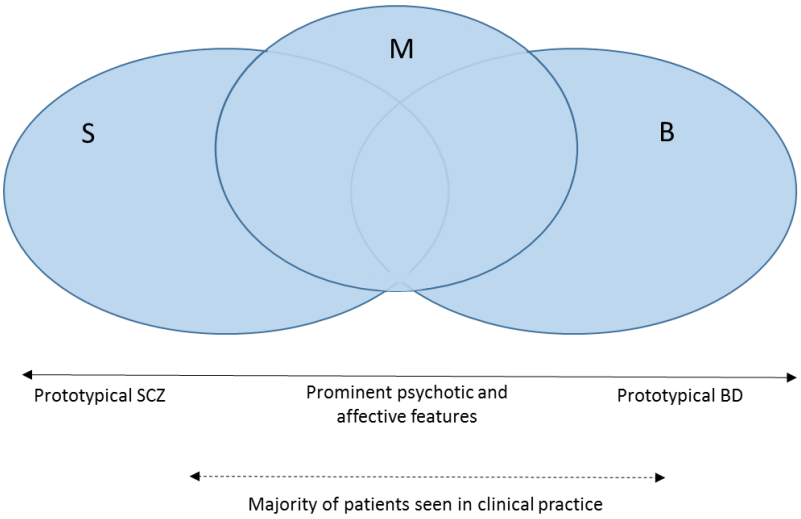

Figure 1.1 - The relationship between the clinical disorders in the psychosis-bipolar spectrum and susceptibility genes specific to SCZ (S), specific to BD (B) and risk genes of schizoaffective disorder, SCZ and BD (M). Adapted from Craddock & Owen, 2005.

1.3.1.1 Schizophrenia

Schizophrenia (SCZ) is a mental illness that affects approximately 1% of the population worldwide (Freedman, 2003). It not only represents an economic burden on society, due to the frequent necessity for patients' hospitalization and for pharmacological treatments, but it is also associated with a humanistic burden because of the usual presence of depressive symptoms and cognitive and social impairment (Millier et al., 2014).

The DSM-5 criteria for SCZ require at least 2 of the 5 characteristic symptoms of psychotic disorders, which were referred before, and that must be on an active phase for a minimum period of one month, as a part of a total duration of the illness of a minimum of six months. One of them must be delusions, hallucinations or disorganized thinking. A social or occupational dysfunction must be present since the onset of the disturbance. Moreover, cognitive deficits are common and strongly linked to functional impairment – these include working memory and language function impairment, slower processing speed and poor memory. The diagnosis depends on the exclusion of the effects of drugs and other somatic disorders (APA, 2013).

The current standard pharmacological treatment of SCZ relies on antipsychotic drugs. There are two classes of antipsychotics: the typical or first generation antipsychotics (FGAs) and the atypical or second generation antipsychotics (SGAs). Both block the dopamine D2 receptor (DRD2), reducing the positive symptoms. Although there are no efficacy differences between both classes, the FGAs are more associated with extrapyramidal side effects, such as dystonic reactions and parkinsonian symptoms, while SGAs confer a higher

risk of weight gain and metabolic disturbances. These differences in adverse side effects may be explained by the slower dissociation of FGAs from the dopamine receptors and by the action of SGAs on additional receptors, such as the 2A receptor of serotonin (Pouget & Müller, 2014).

1.3.1.1.1 Genetic background

In the last 50 years, a considerable amount of studies have shown that genetic factors contribute significantly, but not exclusively, to the risk of developing SCZ. Genetic factors are assumed to account for around 80% of the total variance of SCZ (Cannon, Kaprio, Lönnqvist, Huttunen, & Koskenvuo, 1998). The remaining variance is thought to be explained by neurodevelopmental and environmental factors, which have been proposed as a key feature in the etiology of SCZ. Environmental factors such as social isolation, migrant status or substance abuse, and neurodevelopmental factors that include maternal stress, obstetric complications, low birth weight or maternal infections, are also relevant for the development of SCZ (Owen, Sawa & Mortensen, 2016). The multifactorial polygenic model for SCZ states that the disorder involves an interaction between multiple genetic variants and environmental factors, and it is only expressed in people exceeding a certain threshold of liability. Liability is a continuous variable that describes all factors that contribute to the development of a multifactorial disorder. This model considers that the influence of an environmental factor depends on one or more risk variants, and vice versa. The studies of the interactions between environmental and genetic factors represent several challenges and a variety of approaches can been used (Thomas, 2010).

Molecular genetics methods have showed that SCZ is a heterogeneous and polygenic disorder. The first method applied in this area was linkage analysis, which aims at detecting chromosomal regions constituted by diseased genes that segregate in families. It is based on the fact that genetic markers, which are located physically close on the same chromosome, tend to be inherited together. Meta-analysis studies have found some chromosomal regions that may confer more susceptibility to SCZ, such as the chromosome 2q (119–152 Mb) and chromosome 5q (142–168 Mb) (Lewis et al., 2003; Ng et al., 2009).

The second method applied in this field, the candidate gene approach, aims at finding genes correlated with the illness. This method detects genes with small-effect variants, previously selected based on their position (using results from linkage analysis) or function. The most cited genes include DISC1 (encoding for disrupted in schizophrenia 1), COMT (encoding for catechol-o-methyl transferase), NRG1 (encoding for neuregulin 1), DRD2 and DTNBP1 (encoding for dystrobrevin binding protein 1) (Gejman, Sanders, & Kendler, 2011).

GWAS goal is to find associations between genomic variants and disorders, by comparing healthy controls and patients, without relying on any previous information. GWAS approach is defined by a “common-disease common-variants” hypothesis, which suggests that SCZ is affected by common genetic variations, such as single nucleotide polymorphisms (SNPs), highly numerous but with only minor individual effects (Henriksen, Nordgaard, & Jansson, 2017). Other hypothesis named “common-disease rare-variants” states that uncommon but penetrant genetic variations, such as copy number variations (CNVs) and small insertions and deletions (indels), contribute to the risk of developing SCZ. Both approaches are complementary and demonstrate that the genetic architecture of SCZ is complex and polygenic, as stated by the multifactorial polygenic model.

1.3.1.2 Bipolar disorder

Bipolar disorder (BD) is a mental illness characterized by fluctuations in the mood state and energy, affecting approximately 1% of the world's population. In terms of disability, it can lead to functional and cognitive impairment and increased mortality, especially due to the high risk of suicide (Grande, Berk, Birmaher, & Vieta, 2016).

The DSM-5 criteria for bipolar I disorder (BD-I) is the presence of a manic episode, typically preceded or followed by depressive and hypomanic episodes. Manic and hypomanic episodes vary in severity and duration. A manic episode is a state of elevated mood and increased motor drive, which lasts for at least one week, and may include psychotic symptoms. A hypomanic episode is a less severe manic episode that lasts for at least four days and it is not typically associated with severe impairment or hospital admission.

Around two-thirds of the BD patients were found to have at least one psychotic symptom during manic episodes and the rate of psychotic symptoms may vary between 47-90% (Goodwin & Jamison, 2007). Bipolar II disorder (BD-II) is characterized by one major depressive episode and at least one hypomanic episode. A major depressive episode may include fatigue, diminished interest, weight loss, reduced ability to think and frequent thoughts of death (APA, 2013).

The treatment of BD depends on the patients' mood state since the therapeutic strategies differ for the predominant polarity, the severity of symptoms and other factors such as response to treatment and medical comorbidities. The goal of acute treatment is to stabilize the subject and guarantee his safety. It comprises mood stabilizers (e.g. valproate, lithium and lamotrigine), antipsychotics (e.g. haloperidol and risperidone) and electroconvulsive therapy. The ideal long-term therapy should combine pharmacological, psychological and lifestyle approaches and consider the predominant polarity of the BD patients. For example, subjects with manic predominant polarity respond better to SGAs while subjects with depressive predominant polarity usually have a better response to mood stabilizers, such as lamotrigine, in addition to antidepressants (Grande et al., 2016).

1.3.1.2.1 Genetic background

Epidemiologic studies have showed the importance of genetic factors on conferring risk to develop BD. In fact, the lifetime risks of BD in relatives of a bipolar subject are: monozygotic twin 40-70%, first degree relative 5-10%, unrelated person 0.5-1.5% (Craddock, & Jones, 1999). These values are indicators of the major role that genetic factors play on the pathogenesis of the disorder, although environmental and neurodevelopmental factors also contribute.

Linkage analysis studies in BD did not achieve any positive findings or consistent results, leading to the deduction that there are no risk variations of large effect involved in the etiology of the disorder. In addition, the candidate gene approach has led to inconsistent results, possibly because the underlying biology of BD is still not clear (Craddock, & Sklar, 2009).

GWAS studies have showed a strong evidence for a polygenic contribution to BD, constituted by various risk variants with small effect, partially overlapping with SCZ. Some of the genome-wide significant loci

are located near CACNA1C (encoding the alpha subunit of the L-type calcium channel), ODZ4 (odd Oz/teneurin transmembrane protein 4) and NCAN (encoding for a neurocan core protein) (Craddock, & Sklar, 2013; PCBDWG, 2011). Larger samples are required to confirm additional loci of interest.

1.3.2 Functional magnetic resonance imaging

Functional magnetic resonance imaging (fMRI) is a versatile technique that measures brain activity, usually through the blood oxygenation level-dependent (BOLD) contrast mechanism that is sensitive to the local increase of blood oxygenation following neuronal activity. The changes on the blood oxygenation are a result of blood flow and volume variations. fMRI is a noninvasive technique, with a high spatial resolution, poor temporal resolution and excellent soft-tissue contrast (Webb, 2003).

1.3.2.1 Principles of MRI

Hydrogen nuclei (^{1}H) from the body, mainly present in water and in lipid, have a property called nuclear spin angular momentum. Following the application of a strong and static magnetic field (B_0), these nuclear spins will split into two different energy levels: a lower energy state (aligned parallel to B_0) and a higher energy state (aligned antiparallel to B_0), with a surplus of protons in the lower energy level. These spins precess around the direction of B_0, with a frequency of rotation (Larmor frequency) proportional to the strength of B_0:

$$w_0 = \gamma B_0 \tag{1.1}$$

where γ is the gyromagnetic ratio, a constant for any nucleus. The protons are capable of receiving (and emitting) radiofrequency (RF) energy, when an external magnetic field (B_1) is applied perpendicularly to the B_0 static field. The absorption (and emission) of energy causes the protons to travel to a higher (lower) energy state, respectively. In the presence of B_1, the protons precess coherently, and the sum of all protons magnetic moments, named net magnetization, induces a voltage variation in a receiving coil of wire (Webb, 2003). The detected signal, called free induction decay, oscillates at frequency w_0 and decays over time due to the transverse relaxation.

Initially, the protons' magnetic moments precess randomly distributed around B_0 (in the longitudinal direction). When the RF pulse is applied, the net magnetization tips over to the transversal direction. Upon the removal of the RF pulse, the nuclei return back to their original state, through a longitudinal regrowth and a transversal relaxation, two processes described by exponential functions (associated with two different time constants, T_1 and T_2, respectively). T_1 and T_2 constants depend on the different tissues and are used to differentiate between them.

In practice, the transversal relaxation is described by a T_2*, which takes into account the spatial differences of the magnetic field within the human body and causes a faster signal decay. These spatial variations are due to the fact that the magnet does not produce a homogeneous magnetic field over the entire body and due to the different magnetic susceptibilities of different tissues. Changes in T_2* have an impact in the magnetic resonance signal and are particularly useful to detect changes in the brain hemodynamics that are a result of neuronal activity.

1.3.2.2 Principles of BOLD signal

fMR images are typically obtained using the mechanism of BOLD contrast, which is an indirect measure of the neuronal activity. BOLD imaging is based on the different magnetic susceptibilities of hemoglobin, which depend on if it is on an oxygenated (Hb) or deoxygenated (dHb) state – Hb is a diamagnetic molecule while dHb is paramagnetic (Pauling & Coryell, 1936).

The presence of more Hb molecules in comparison to dHb molecules in a region leads to a growth of the magnetic resonance (MR) signal. This happens because diamagnetic molecules repel the magnetic field while paramagnetic molecules attract the magnetic field. Therefore, when brain areas become active, they stimulate an increase of the metabolic demands and cerebral blood flow (CBF) and volume. Since more oxygen is supplied by the blood flow than is needed to replenish the oxygen used by the activity of neurons (Fox, Raichle, Mintun, & Dence, 1988), there is a local increase of Hb in comparison to the surrounding tissue, thus increasing the MR signal. This effect is explained by the fact that increases in blood oxygenation (decreases in dHb) are associated to an increase of T_2 (Thulborn, Waterton, Matthews, & Radda, 1982) and T_2* (Ogawa, Lee, Kay, & Tank, 1990), leading to a slight signal growth of the T_2 and T_2*-weighted images.

1.3.2.3 Hemodynamic Response Function

The hemodynamic response function (HRF) is the ideal and noiseless time course of the BOLD response that follows an impulse of neuronal activity. There are two important features of HRF that should be considered when performing an fMRI analysis. First, the hemodynamic responses are slow when compared to the neuronal activity. Typically, neuronal activity lasts for some milliseconds while hemodynamic responses last for 12-18s. The BOLD response might be initiated by a negative dip, which occurs 1-2s after the stimulus, and is associated to oxygen consumption before any changes in the CBF and blood volume occur (Buxton, 2001). It is followed by a peak, 4-6s after the stimulus, whose height is related to the amount of neuronal activity in the tissue (Logothetis, Pauls, Augath, Trinath, & Oeltermann, 2001). After the peak, it might show a poststimulus undershoot, which lasts up to 20s after the stimulus and is followed by a return to baseline. The HRF varies significantly across different brain areas and across individuals, with intersubject variability higher than intrasubject variability (Handwerker, Ollinger, & D'Esposito, 2004).

Second, the relationship between the BOLD response and the neuronal activity follows a linear and time invariant (LTI) system properties. This means that if a neural response is scaled by a factor of a, the BOLD response will also be scaled by a factor of a and if the neural response is delayed b seconds, the BOLD response will be delayed b seconds. This property allows the estimation of the BOLD response that follows a particular neural response, by convolving the stimulus time series with an HRF. In fMRI analysis, a canonical HRF is usually used; it is based on the linear combination of two gamma functions, called double-gamma HRF (Figure 1.2) (Friston et al., 1998), which is expressed as:

$$h(t) = A\left(\frac{t^{\alpha_1^{-1}}\beta_1^{\alpha_1}e^{-\beta_1 t}}{\Gamma(\alpha_1)} - c\frac{t^{\alpha_2^{-1}}\beta_2^{\alpha_2}e^{-\beta_2 t}}{\Gamma\Gamma(\alpha_2)}\right), \text{ where } \Gamma(n) = (n-1)!\,(n > 0) \quad (1.2)$$

$\alpha_1, \alpha_2, \beta_1, \beta_2$ and c are predefined constants, A is the unknown amplitude and $\Gamma(n)$ is the gamma function (Lindquist, Loh, Atlas, & Wager, 2009). The first gamma function modulates the initial peak while the second modulates the poststimulus undershoot.

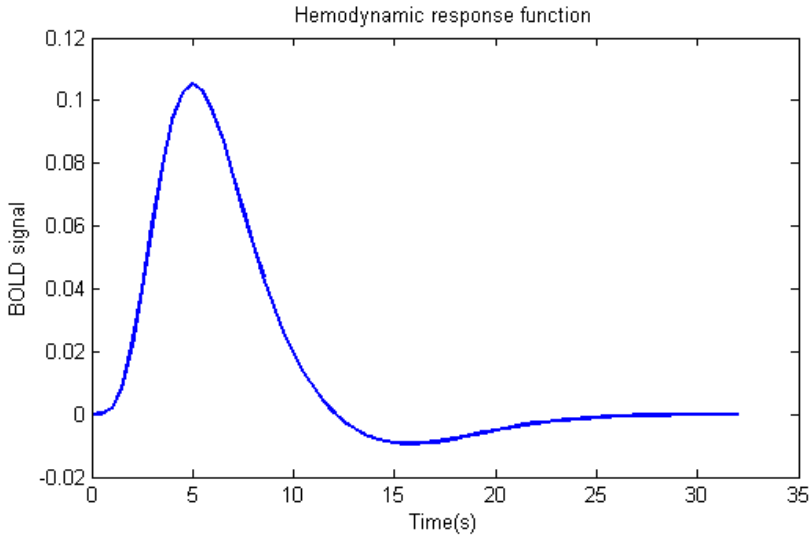

Figure 1.2 - Statistical Parametric Mapping double-gamma HRF.

1.3.2.4 Statistical Parametric Mapping

Statistical Parametric Mapping (SPM) (Friston et al., 1995) is typically used as an analysis method for functional imaging studies, such as regional brain activation studies. SPM involves the formulation of spatially extended statistical processes to test hypotheses on regionally specific effects (Friston, Frith, Liddle, & Frackowiak, 1991). An SPM is an image constituted by voxels, a three-dimensional (3D) analog to a pixel, values that are, under a null hypothesis, distributed according to a known probability density function, commonly the Student's T or F tests. Informally, these are called t- or F-maps. All voxels are analyzed, using a standard mass univariate statistical approach, to test whether a particular voxel time-series is systematically associated to an explanatory variable. A mass univariate approach analyzes each voxel separately. The individually estimated parameters are summarized into an image – the statistical map. This image shows brain activation by color-coding voxels whose t-values overcome a predefined statistical threshold for significance.

SPM analyzes and makes inferences via general linear model (GLM) and random field theory (RFT). The GLM is used to estimate the parameters that explain the continuous data whereas RFT corrects for the multiple comparison problem that appears when all voxels data are concatenated into the statistical map, by adjusting p-values for the search volume.

1.3.2.4.1 General Linear Model

Statistical analysis of imaging data involves the division of the observed neurophysiological responses into components of interest, confounds and error terms and includes the estimation of the variance of each of those partitions in order to make inferences about effects of interest (Friston, 2005). The GLMs can be applied

to different types of analysis, including multiple regressions, one-sample t-test, two-sample t-test, analysis of variance (ANOVA) and analysis of covariance.

For a single voxel, the GLM can be expressed in matrix notation as:

$$Y = X\beta + \varepsilon \tag{1.3}$$

The column vector of the observed response Y (length scans) is a linear combination of explanatory variables (design effects or confounds), combined in a design matrix X (scans×design variables) plus an error vector ε (length scans), an independently and identically distributed Gaussian random term (Friston, 2005). Each column of the design matrix is called explanatory variable, regressor or covariate. The relative contribution of each of these columns to the observed response is expressed in the column vector β (length design variables). These parameters are estimated using a least squares approach. As the explanatory variables can be divided into design effects and confounds, the same logic is used to define the β values. The estimated variance of the parameter estimates is used to make inferences about them.

1.3.2.4.2 Statistical inference

A SPM{T} allows to test the null hypothesis that some particular linear combination (also called contrast) of the estimates is zero. The T statistic is calculated as the contrast or compound (specified by contrast weights) of the parameter estimates divided by the standard error of that compound. These contrasts allow to estimate signal magnitudes in response to a single condition, the difference in magnitude between two conditions or the average magnitude of multiple conditions. A SPM{F} allows to test the null hypothesis that a matrix of contrast weights (a combination of several T contrasts) is zero. Each row of the matrix corresponds to one of the multiple simultaneous tests that one is intended to perform (Friston, 2005).

1.3.2.5 Connectivity analysis

One of the oldest debates of neuroscience deals with the localization of function in the brain. The main interrogation is if mental functions are localized in specific brain regions or if they rely more diffusely upon the entire brain. The first concept, functional segregation, is complementary to the latter, functional integration. Functional integration is an emerging concept that states that function emerges from the flow of information across different brain areas (Ramnani, Behrens, Penny, & Matthews, 2004).

The integration within and between functionally specialized areas is mediated by functional or effective connectivity. Functional connectivity refers to temporal correlations in activity between spatially remote brain regions (Friston, Frith, Liddle, & Frackowiak, 1993) while effective connectivity reflects the direct influence that one neural system exerts over another (Friston, Frith, & Frackowiak, 1993). Functional connectivity does not provide an insight about how the correlations are mediated, thus the results from this analysis should be interpreted with caution.

One particular type of functional connectivity analysis is called psychophysiological interaction (PPI). This method concerns how the functional connectivity is modulated by a task, i.e., it searches for task-specific

changes between the activity in different brain regions (Friston et al., 1997). In a PPI analysis, an additional regressor that describes the interaction between the task and the activity in the seed region is added to the first level analysis, along with the task vector and the time course of the seed. The interaction term is obtained by multiplying the task vector with the deconvolved time course of the seed, that is subsequently reconvolved to be back on the hemodynamic domain (Gitelman, Penny, Ashburner, & Friston, 2003). The deconvolution allows the expression of the observed fMRI signal in terms of the underlying neuronal signal.

The task and the seed vectors are included on the statistical analysis to avoid that the activation observed for the interaction term would be explained by a general effect of the task. However, this results in a lack of power to detect effects in the interaction term, since it might have a similar time-course to the other two vectors and, therefore, a similar variance, which is not assigned to any of the vectors (O'Reilly, Woolrich, Behrens, Smith, & Johansen-Berg, 2012). Another limitation of this analysis is associated with the fact that only one seed region can be specified.

1.3.3 Endophenotype

An endophenotype (also called intermediate phenotype) is a biomarker that reflects the pathway between the genetic vulnerability and a psychiatric illness onset (Gottesman & Gould, 2003). To be considered an endophenotype, a biomarker should be: (1) related with illness in the population; (2) heritable; (3) state-independent (present on a subject independently if the disease is active or not); (4) cosegregated with the illness in families; (5) present in unaffected relatives at a higher rate than in general population (Gottesman & Gould, 2003). Endophenotypes play a fundamental role in understanding the gap between susceptibility genes and complex phenotypes present in psychiatric disorders. Also, they have a simpler etiology and are easier to map than clinical phenotypes.

Cognitive dysfunction, which is associated with most of psychiatric disorders, is considered a promising endophenotype for both SCZ and BD. This is explained by the fact that cognitive function seems to have a genetic etiology (i.e. it is heritable), as it is showed that unaffected relatives have increased cognitive deficits relatively to healthy controls, but in a smaller extent when compared to patients. This deficit is more severe and widespread in SCZ patients when compared to BD patients, although its profile is similar in both diagnostic groups (Vöhringer et al., 2013).

1.3.3.1 Verbal fluency impairment as a candidate endophenotype of SCZ and BD

Verbal fluency (VF) is a cognitive function that assesses the integrity of the lexico-semantic memory and evaluates the capability to retrieve information from memory. VF can be divided into expressive (comprising phonemic and semantic fluency) and perceptual fluency (associated to verbal stimulus recognition) (Tyburski, Sokołowski, Chęć, Pełka-Wysiecka, & Samochowiec, 2015). Phonemic fluency tests are assessed by asking the subject to produce words beginning with a particular given letter whereas semantic fluency tests involve the generation of words that belong to a certain category. A phonemic fluency task was implemented on this project.

In a recent meta-analysis study, a set neurocognitive endophenotypes were compared between SCZ and BD. These included VF, working memory, verbal learning and memory, executive function, and others. This study suggested that VF is a potential endophenotype for only SCZ, as there were significant differences between the SCZ patients and controls on the performance of this task, for both phonemic and semantic fluency tests. However, this difference was not replicated for the BD patients group (Kim, Kim, Koo, Yun, & Won, 2015). On the other hand, another meta-analysis study has concluded that BD patients show a medium VF impairment, with euthymic patients (i.e. patients not experiencing a depressed or elevated mood) scoring worse than manic patients, on a semantic fluency task, showing that mood states may influence the performance on VF tests (Raucher-Chéné, Achim, Kaladjian, & Besche-Richard, 2017). Thus, there is a pronounced impairment in VF for SCZ patients, which is shared with BD in a moderate fashion, suggesting the presence of a common mechanism. There is also evidence that unaffected relatives of SCZ and BD patients score intermediately between both types of probands and healthy controls (Kim et al., 2015), suggesting that VF is a plausible endophenotype for SCZ and might be as well for BD.

1.3.3.2 Verbal fluency performance and neural correlates in SCZ and BD

Schizophrenic subjects generate fewer words and produce more errors than controls in VF tasks. Lower performance of SCZ patients is also characterized by the creation of fewer clusters (successive words organized in groups) in semantic tests, suggesting a dysfunction in the semantic system and poor access mechanisms to stored information (Neill, Gurvich, & Rossell, 2014; Sung et al., 2012). Also, SCZ patients show an impairment in generating new clusters and in switching (ability to switch between clusters), dysfunctions that are linked to executive function disorders (Moore, Savla, Woods, Jeste, & Palmer, 2006; Robert et al., 1998).

In healthy individuals, VF task is linked to the activation of a network of cortical and subcortical areas, such as the anterior cingulate cortex (ACC) and left inferior frontal, middle frontal, the insular, the precentral and parietal cortices, areas that have been systematically associated with word generation in several studies (Costafreda, David, & Brammer, 2009; Fu et al., 2002; Fu et al., 2005). The inferior frontal gyrus comprises the Broca's area, a region with functions linked to the speech production and its control.

In general, fMRI studies have showed in SCZ patients a deficit in the left hemisphere structures of the brain, relevant for language processing (Li, Branch, & DeLisi, 2009). Previous findings have showed that the reduced VF performance in SCZ is associated with attenuated activations of the ACC, left inferior, left middle and right middle frontal gyri, temporoparietal cortices, thalamus and bilateral cerebellum (Fu et al., 2005; Lurito, Kareken, Lowe, Chen, & Mathews, 2000; Smee et al., 2011; Yurgelun-Todd et al., 1996). This reduced activation showed by SCZ when compared to healthy participants is essentially present when the performance accuracy is not matched, i.e., when the incorrect trials are not regressed out from the analysis. This effect is explained by the poor performance and lack of attention of SCZ patients, which results in a disengagement with the task (Prata, 2008). However, Curtis et al. found that SCZ patients also show attenuated activation on insula, parietal cortex and frontal regions (effect referred to as hypofrontality) when the performance is matched between the groups (Curtis et al., 1998).

Other studies found that the prefrontal dysfunction may be associated with a greater activation instead of a deactivation, mostly when the task performance is matched, suggesting that extra activation is necessary to sustain a normal performance (Callicott et al., 2000; Costafreda et al., 2011). Also, prefrontal impairment is associated with symptoms severity, since as the positive symptoms decrease, the activation in the left middle frontal gyrus normalizes (Smee et al., 2011). Moreover, the difficulty of the task also influences the activation of the brain regions, as increasing task demand is associated with more activation in several brain areas (such as left anterior and posterior insula and left putamen), and thus the impairment becomes more evident (Fu et al., 2005). Therefore, differences in activation between patients and controls differ across studies and seem to be associated with the severity of symptoms at the time of scanning, the difficulty of the task and additionally the consumption of antipsychotics (Keefe, Silva, Perkins, & Lieberman, 1999).

BD subjects show a medium impairment in VF, producing fewer words and making more errors than healthy subjects but with a better performance when compared to SCZ patients (Krabbendam, Arts, van Os, & Aleman, 2005; Vöhringer et al.,2013). fMRI studies have found that BD patients show increased activation in the bilateral inferior frontal and insular cortices, bilateral precuneus, left superior temporal cortex, thalamus and dorsal ACC, when compared to healthy controls (Costafreda et al., 2011; Yoshimura et al., 2015). Moreover, the VF paradigm was also associated with a reduced activation in the precuneus, posterior cingulate and left dorsolateral prefrontal cortex (DLPFC) (Costafreda et al., 2011; Nishimura et al., 2014). Near-infrared spectroscopy (NIRS) is a technique that detects changes in Hb and dHB in micro vessels in the brain. When measuring hemodynamic responses in the prefrontal cortex during a VF task using NIRS, Hb increases were found to be significantly smaller in remitted BD patients when compared to controls, in a VF task. This findings suggest that BD is associated with a bilateral hypofrontality of the prefrontal region, which might be due to vascular regulation (Matsuo, Watanabe, Onodera, Kato, & Kato, 2004). Moreover, as referred previously, these impairments are dependent on the mood state during the acquisition and on the nature of the task (phonemic or semantic) (Raucher-Chéné et al., 2017).

1.3.4 Genetics

GWAS studies have identified several SNPs that individually explain a limited heritability of complex disorders. PRS analyses allow to combine the effect of several risk variants found to be more common in patients than in the healthy population into one quantifiable score.

A PRS is calculated for each individual as the weighted sum of his multiple risk variants for a particular disease. The weights are given by the effect size of each variant (usually the logarithm of odds ratio taken from case-control analysis), which are estimated using the results of large GWAS studies. The genetic variants used in the calculation of the score are selected using a pre-specified p-value threshold. A PRS includes information from GWAS-SNPs and also SNPs that do not meet genome-wide significance, enabling the presence of false positives, although it is considered that true positives still contribute with useful information (Wray et al., 2014).

The first study where the PRS method was applied revealed that a polygenic component explains a substantial fraction of the heritability of SCZ, with considerable similarities with BD (International Schizophrenia

Consortium [ISC], 2009). This polygenic nature of both disorders is explain by thousands of variants with very small effect. With increased samples, studies have found new genome-wide significant variants, which explain a higher proportion of variance in SCZ (Schizophrenia Psychiatric GWAS Consortium, 2011; Ripke et al., 2013). The most recent study has collected 108 variants (83 of which have not been previously reported) and reached a significant increase in proportion of variance (Nagelkerke R^2), from 3% (ISC,2009) to 18.4% (SWGPGC, 2014). These variants are associated with genes involved in glutamatergic neurotransmission, synaptic plasticity, and voltage-gated calcium channel subunits (SWGPGC, 2014).

1.3.5 Imaging genetics

Imaging genetics is a research method that integrates structural and functional imaging technologies and genetics to study the impact that genetic variations have on brain structure and function. The neuroimaging phenotypes are called endophenotypes (see 1.3.3), since they are located in the pathway between susceptibility genes and the psychiatric disorder. Imaging genetics involves the use of two different approaches (Figure 1.3). The first uses imaging genetics as a tool to discover risk genes for a given psychiatric disorder (green arrows); the second uses imaging genetics to characterize the neural circuits affected by certain genetic variants (orange arrows) (Hashimoto et al., 2015). The later involves the search for polymorphisms which may have an impact on a function of a relevant biological process (associated with a target phenotype).

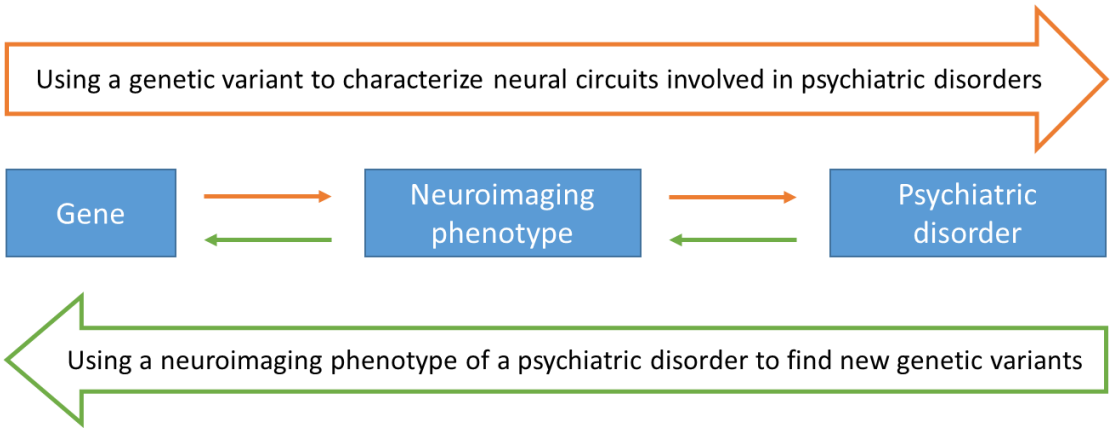

Figure 1.3 - The three elements of imaging genetics (gene, neuroimaging phenotype and psychiatric disorder) and the two approaches used in imaging genetics. Adapted from Hashimoto et al., 2015.

1.3.5.1 Imaging genetics of SCZ and BD

Numerous studies have focused on structural and functional imaging as intermediate phenotypes for SCZ and BD. Typically, the approaches used are candidate gene analysis, GWAS or PRS analysis. Imaging genetic studies that analyze the effect of susceptibility genes or variants on task-modulated brain function usually use VF, working memory, face processing, cognitive control and episodic memory paradigms.

Candidate gene analysis comprise a variety of studies using COMT, DISC1, NRG1, DTNBP1, and other genes. For example, participants (SCZ and BD patients and controls) with the high-risk variant of NRG1 showed a decreased activation of the left precuneus during a VF task. Particularly in SCZ patients with the high-risk variant, there was an increased activation of the inferior frontal gyrus, and BD patients with the high-risk variant showed

greater activation in the right posterior orbital gyrus (Mechelli et al., 2008). Another study found a greater activation in the right hemispherical brain (including the ACC, superior and middle temporal gyrus) in participants carrying a genetic variant rs1018381 in the DTNBP1 gene, during a VF paradigm (Markov et al., 2009).

Gurung and Prata reviewed the impact of GWAS studies of SCZ and BD risk genes on brain function and structure. In summary, they found several neuroimaging phenotypes affected by risk variations: structural phenotypes, such as white-matter integrity (affected by ANK3 and ZNF804A), volume (affected by CACNA1C and ZNF804A) and density (affected by ZNF804A); grey-matter (CACNA1C, NRGN, TCF4 and ZNF804A) and ventricular (TCF4) volume; cortical folding (NCAN) and thickness (ZNF804A) – and functional phenotypes – regional activation during executive tasks (ANK3, CACNA1C, DGKH, NRGN and ZNF804A) and functional connectivity during executive tasks (CACNA1C and ZNF804A and others (Gurung & Prata, 2015). Particularly for VF tasks, the A allele of the rs1006737 risk variant of the CACNA1C gene (overrepresented in SCZ/BD patients) was associated with the performance of a semantic VF task, as the participants with the risk variant show increased activation in the left inferior frontal gyrus and in the left precuneus (Krug et al., 2010). Moreover, three genetic variations of the DGKH gene have been associated with increased activation in the prefrontal cortex, left precuneus and right parahippocampal gyrus (Whalley et al., 2012a).

The findings revealed by PRS approach in imaging studies will be discussed in the following sections 1.4.1 and 1.4.2.

1.4 Literature review

1.4.1 PRS in structural imaging studies of SCZ and BD

So far, several studies have reported associations between the PRSs and structural neuroimaging phenotypes. A summary of the results on SCZ, BD and psychosis are presented in Table 1.1. Although some studies did not find an effect of PRS on brain volume (grey and white matter volume) and cortical thickness, the others found a consistent negative association between SCZ-PRSs and structural phenotypes, i.e., an increasing PRS is linked with reduced brain volumes or cortical thickness. This effect was found independently of the diagnosis in almost all studies, except for the one of Neilson et al.

The study of Terwisscha van Scheltinga et al. found a negative association between a SCZ-PRS and the total brain and white matter volume, in a sample constituted by SCZ patients and healthy controls. However, they did not find an effect of PRS on the grey matter volume (Terwisscha van Scheltinga et al., 2013). The group of Papiol et al. calculated two different PRS, one with SNPs associated with the risk of developing SCZ and other with SNPs most associated with changes in the white matter volume. There was not any association between any of the scores and the total brain volume, white matter volume and grey matter volume, in a group of healthy controls (Papiol et al., 2014). Another study has found that a SCZ-PRS is negatively associated with the white matter volume, in a group of participants that included SCZ patients and first-degree relatives, BD patients and controls. Moreover, this effect was replicated in another independent sample of healthy controls (Oertel-Knöchel et al., 2015). Harrisberger et al. found that a SCZ-PRS is associated with decreased hippocampal volume in a

group of at-risk mental state and first episode psychosis patients. Additionally, they also found that a higher PRS is linked with a larger likelihood that a participant would be allocated to the first episode psychosis group relatively to the at-risk mental state group (Harrisberger et al., 2016). A study from Voineskos et al. found that there is no association between a SCZ-PRS and the frontal and temporal thickness of a group of healthy controls (Voineskos et al., 2016). Finally, Neilson et al. found that a SCZ-PRS is associated with decreased cortical thickness in a group of SCZ and BD patients, effect that is not replicated in the healthy control group (Neilson et al., 2017).

Table.1.1 - List of previous studies with association findings between PRSs and structural neuroimaging phenotypes.

Author	Scanner magnetic field	Diagnostic groups	Phenotypes (association direction)
Terwisscha van Scheltinga et al. (2013)	1.5T	SCZ patients (n=152) Controls (n=142)	Total brain volume (-) White matter volume (-) Grey matter volume (null)
Papiol et al. (2014)	3T	Controls (n=122)	Total brain, white or grey matter volume association (null)
Oertel-Knöchel et al. (2015)	3T	SCZ patients (n=24) SCZ first-degree relatives (n=12) BD patients (n=20) Controls (n=38)	White matter volume (-)
		Controls (n=89)	
Harrisberger et al. (2016)	3T	At-risk mental state patients (n=38) First episode psychosis (n=27)	Hippocampal volume (-) (both groups together and individually)
Voineskos et al. (2016)	1.5T	Controls (n=107)	Frontal and temporal cortical thickness (null)
Neilson et al. (2017)	3T	SCZ and BD patients (n=43)	Cortical thickness (-)
		Controls (n=32)	-

1.4.2 PRS in functional imaging studies of SCZ and BD

The use of PRS method in functional imaging studies of regional brain activation is a promising approach to identify individuals at risk of developing a psychiatric disorder. The first study published in this area showed that a SCZ-PRS is positively and significantly associated with neural activity in the left DLPFC and left pars triangularis of the inferior frontal gyrus during a working memory task, in both SCZ patients and healthy controls. This study found no significant diagnosis by PRS effects (Walton et al., 2012). A more recent study from the same group, using the same paradigm, confirmed the positive correlation between a SCZ-PRS and the activity in the DLPFC and in the left ventrolateral prefrontal cortex (VLPFC) and additionally left frontal medial cortex, including ACC, across all participants. On this study, the PRS included more genetic variations than their previous study PRS (comprising over than 600 SNPs, instead of 41 SNPs from the former study) (Walton et al., 2013). Kauppi et al. found that a SCZ-PRS is negatively associated with activation in areas including the inferior frontal gyrus, the middle and superior prefrontal cortex and the right middle temporal gyrus, across SCZ patients and control group. This effect was found in a contrast between high and low working memory load (2-back > 0-back). Moreover, when using the contrast 2-back > baseline, increasing SCZ-PRS was found to be associated with decreasing brain

activation in the ACC, right inferior frontal gyrus and insula and in the bilateral postcentral gyrus (Kauppi et al., 2014). Lancaster et al. found a negative association between a SCZ-PRS and the activation in the right frontal lobe, on a whole-brain analysis, and an association between the PRS and the activation in the ventral striatum pointing in the same direction, on a region of interest (ROI) analysis. This was found in the trials reflecting choice behavior (shift > stay contrast, after reward and punishment cues were reversed) during a probabilistic learning paradigm assessed in healthy controls (Lancaster et al., 2016a). A study from Cosgrove et al. revealed that increasing PRS, constructed using variants on the downstream pathway of MIR137 (a region in chromosome 1 highly associated with SCZ risk (Ripke et al., 2013)) in healthy controls was associated with increasing activation of a cluster on the right inferior occipital gyrus and right middle temporal gyrus and other on the medial parietal region, during a spatial working memory task. However, using another paradigm (face processing), there was not any association between the MIR137 polygenic risk and the cortical activation (Cosgrove et al., 2017).

PRSs for BD have also been used to study the relation between brain function and the genetic risk for this disorder. Whalley et al. found in both healthy controls and unaffected relatives of BD a positive association between a BD-PRS and the activation of the subgenual portion of the ACC (at the whole-brain level, corrected for multiple comparisons) and of the right amygdala (after applying small volume correction [SVC]), both limbic regions involved in emotion regulation, during a language-based executive task. There were no statistically significant associations between PRS and group interaction effects (Whalley et al., 2012b). Using the same paradigm and diagnostic groups, the same group studied the associations between a cross-disorder PRS (based on the genetic risks for five psychiatric disorders) and a single-disorder PRS (computed for a single one of them). Although there were no significant effects between the cross-disorder PRS and brain activation across all groups, they found a significant cross-disorder PRS × group interaction in the frontal cortex (in an area including the left inferior frontal gyrus, precentral and postcentral gyri), effect that was driven by the healthy controls and that was not significant on the familial group; this association was also statistically significant when considering only the SCZ single PRS (Whalley et al., 2014). Tesli et al. found that a BD-PRS is positively associated with activation in the right inferior frontal gyrus during a face processing task, for BD patients and controls, with no evidence of an interaction effect between diagnostic group and PRS on brain activation (Tesli et al., 2015). Moreover, they also found that the PRS is negatively correlated with the activation of the right postcentral gyrus, although their results were not statistically significant. Lastly, the most recent study on BD-PRS showed that it is negatively associated with activation in the visual cortex during a facial affect processing task and also negatively associated with activation in the VLPFC and DLPFC and in the parietal cortex during a working memory task, across three groups (BD patients, BD first degree-relatives and controls) (Dima, de Jong, Breen, & Frangou, 2016).

Using a PRS for psychosis and searching for activation within a ROI encompassing the ventral striatum, Lancaster et al. found a positive association between the PRS and the ventral striatum BOLD signal in the group of healthy participants, assessed during a monetary incentive delay task. This association was present in both reward and anticipation contrasts (Lancaster et al., 2016b).

Table 1.2 - List of previous studies with association findings between PRSs and functional neuroimaging phenotypes. Blue: working memory task; yellow: executive language-base task; green: facial processing task; orange: probabilistic learning; pink: monetary incentive delay.

Author	Task	Scanner magnetic field	Diagnostic groups	Analysis	Brain areas (association direction)
Walton et al. (2012)	Working memory	1.5T	SCZ patients (n=79) Controls (n=99)	Whole-brain	Left DLPFC (+) Left inferior frontal gyrus, pars triangularis (+)
Whalley et al. (2012b)	Executive language-based	1.5T	BD relatives (n=87) Unrelated controls (n=71)	Whole-brain	Subgenual ACC (+)
				ROI analysis (SVC)	Right amygdala (+)
Walton et al. (2013)	Working memory	1.5T	SCZ patients (n=92) Controls (n=114)	Whole-brain analysis	Left DLPFC and left VLPFC (+) Left frontal medial cortex (including ACC) (+)
Kauppi et al. (2014)	Working memory	1.5T	SCZ patients (n=63) Controls (n=118)	Masking using main effect of task contrast	Right inferior frontal gyrus (-) Middle and superior PFC (-) Right middle temporal gyrus (-)
Whalley et al. (2014)	Executive language-based	1.5T	BD relatives (n=82)	Whole-brain analysis	-
			Unrelated controls (n=57)		Frontal cortex, precentral and postcentral gyri (+) **(PRS×group interaction)**
Tesli et al. (2015)	Facial processing	1.5T	BD patients (n=85) Controls (n=121)	Whole-brain analysis	Right inferior frontal gyrus (+) Right postcentral gyrus (-) (not statistically significant)
Dima et al. (2016)	Facial processing	1.5T	BD patients (n=41) BD relatives (n=25) Unrelated controls (n=46)	Whole-brain analysis	Visual cortex (-)
	Working memory				Ventromedial prefrontal cortex (+)
Lancaster et al. (2016a)	Probabilistic learning	3T	Controls (n=83)	Whole-brain analysis	Right frontal pole (-)
				ROI analysis	Left ventral striatum (-)
Lancaster et al. (2016b)	Monetary incentive delay	3T	Controls (n=1841)	ROI analysis	Ventral striatum (+)
Cosgrove et al. (2017)	Spatial working memory	3T	Controls (n=108)	Whole-brain analysis	Right inferior occipital gyrus and middle temporal gyrus (+) Medial parietal region (+)
	Facial processing		Controls (n=83)		-

1.5 Scopes and objectives

The main objective of this dissertation is to combine the advances in molecular genetics and functional neuroimaging to study the effect of a SCZ-PRS, i.e. a PRS based on susceptibility risk variations of SCZ, on brain activation and connectivity in a group of participants, during a VF task. Moreover, within this objective it is also proposed to analyze if the effect of PRS on brain activation and connectivity depends on the diagnostic group and if it is associated with the paradigm and consistent with previous findings. More general goals are to study the patterns of task-modulated brain activation and connectivity and to understand if these patterns allow to differentiate SCZ from BD and healthy control groups. Additionally, it was studied if the effect of PRS on brain activation and connectivity depends on VF task difficulty and on the presence of the diagnosis factor. In terms of methodology, one of the goals is to assess the impact of the inclusion of covariates of no interest to single and group models as well as the influence of preprocessing steps choices on the statistical significance of the results found and on brain activation patterns.

1.6 Hypotheses

The underlying hypothesis for this work was that a SCZ-PRS has an effect on regional brain activation and connectivity and that it can be detected by a VF-related fMRI paradigm. My hypothesis was that an increasing PRS would be associated with inefficient performance during the task, i.e. increased activation, given the same performance level. This would occur particularly in areas that are associated with the task or associated with SCZ or areas associated with a SCZ-PRS, even with other cognitive executive paradigms.

I was also expecting that the positive association of PRS with brain activation would be greater on SCZ and BD groups, given that these groups are likely to be in the presence of other genetic factors, not captured by the PRSs, and/or environmental factors that also make them more susceptible to the detrimental effects of the PRS on cognitive executive brain function.

1.7 Innovative contributions

The main contribution of this dissertation includes the use of a pioneering paradigm to study the association between PRSs and brain activation and connectivity. Although VF tasks have been widely use to study cognitive deficits of SCZ and BD and the effect of individual SNPs on brain activation, this is the first study using a VF paradigm to include a score that aggregates the effect of almost 18000 SNPs that confer risk to SCZ. A great proportion of the studies reviewed from the literature use working memory or facial processing paradigms.

Additionally, this is the first study to analyze the effects of PRSs on task-modulated brain connectivity. As described on literature review, the previous studies only focused on investigating the association of PRSs with regional brain activation phenotypes, present during a specific paradigm.

Furthermore, this is the first study in the field of imaging genetics searching for an association between PRSs and functional biomarkers to compare both SCZ and BD patients, diseases with heterogeneous phenotypes that share several similarities in terms of genetic etiology and cognitive impairments. Usually, this association is only studied on a group of healthy participants or on a case vs. control comparison study, comparing a group of SCZ or BD patients or BD relatives with a group of healthy controls.

1.8 Collaborations

The data used in this dissertation were collected and processed by researchers working at the Institute of Psychiatry, Psychology & Neuroscience (IoPPN) from King's College London, United Kingdom. Cynthia Fu, Chris Chaddock, Marco Picchioni, Sri Kalidindi, Fergus Kane, Colm McDonald, Elvira Bramon and Timi Toulopoulou participated in subject recruitment, acquired the functional and structural images and performed the clinical and neuropsychological assessments. Genomic DNA was extracted and genotyped by Social Genetic and Developmental Psychiatry laboratory technicians. Evagelos Vassos (investigator at the Medical Research Council, Social, Genetic and Developmental Psychiatry Centre at IoPPN) was responsible for processing the genetic data (including the quality control steps) and for constructing the PRSs – a more detailed explanation about these processes can be found in section 2.2.

The image and statistical analysis was performed by me, under the supervision of Prof. Diana Prata (Group Leader at Instituto de Medicina Molecular [iMM], Lisboa) and Prof. Patrícia Figueiredo (Assistant Professor at Institute for Systems and Robotics, Department of Bioengineering, Instituto Superior Técnico).

2. Materials and Methods

2.1 Subject recruitment

2.1.1 Participants

In this project, a total number of 134 subjects were studied. Initially, I excluded 16 participants due to the absence of structural data, required for the coregistration step in the preprocessing of functional images. These 118 participants' data were preprocessed and underwent to the estimation of single level parameters and contrast definition. Afterwards, I removed 4 subjects from the sample as their PRS was calculated using a different DNA chip from the rest of the participants. Finally, before running the group level analysis, I excluded 13 participants due to the presence of relatives within the same diagnostic group. This step was included to guarantee that all individuals in the sample could be considered statistically independent between each other – my criteria was to select the relative with more detailed demographics or choose at random. The 101 subjects left were divided into 4 different groups:

1) Unrelated healthy controls (n=39) were subjects with no previous history of mental illness and no first degree relatives with a psychotic disorder, assessed using the Family Interview for Genetic Studies.
2) BD type I patients (n=25), 22 with psychosis.
3) SCZ patients (n=10).
4) Healthy relatives (n=27) of subjects with BD or SCZ. 12 subjects in this group have family members on BD or SCZ groups of the final sample. 20 participants are relatives of BD subjects and the remaining 7 are relatives of SCZ patients.

Some of the functional and structural neuroimaging data from this project overlaps with data examined in previous studies (Costafreda et al., 2011; Mechelli et al., 2012; Prata, 2008). All participants were native English-speakers and Caucasian. Participants were recruited as part of the Biomedical Research Centre (BRC) at South London and Maudsley National Health Service Trust. The diagnosis was established by a qualified psychiatrist using a structured diagnostic interview (Wing, 1990), to assess the criteria of the DSM-4 edition (APA, 1994). All SCZ and BD patients were in a stable clinical state. Exclusion criteria were applied to participants with a history of significant head injury and recent substance dependency, according to DSM-4 diagnostic criteria.

This project was approved by the National Health Service South East London Research Ethics Committee, UK (Project Mental Health Genetics and Psychosis) reference number 047/04 and all volunteers gave written informed consent at the time of participation.

2.1.2 Demographics

Intelligence quotient (IQ) scores were obtained using the Wechsler Adult Intelligence Scale-III (WAIS-III) (Wechsler, 1997), the Wechsler Adult Intelligence Scale–Revised (WAIS-R) (Wechsler, 1981), the Wechsler Abbreviated Scale of Intelligence – Full Scale IQ (WASI-FSIQ-4) (Wechsler, 2008) or the National

Adult Reading Test (NART) (Nelson & Willison, 1991). The values were standardized to Z-scores to allow comparison between different tests (Appendix A).

I performed the analysis of demographic differences between diagnostic groups using Excel (Microsoft Word, 2013) and MATLAB 8.1.0.604 (Table 2.1). Chi-square (χ^2) tests were used for categorical variables and Kruskal-Wallis tests for continuous variables, as the groups had small sizes (with less than 20 participants). There were no significant differences between diagnostic groups in age, IQ (z-scores), Years of Education (YE), gender or handedness.

Table 2.1 – Participants demographics per diagnostic group. Age, IQ (z-scores) and YE are presented as mean (standard deviation).

Participants demographics	Controls (n=39)	BD (n=25)	SCZ (n=10)	Relatives (n=27)	Statistic, degrees of freedom (df), p-value
Age (years)	40.14(14.49)	41.72 (11.91)	40.93 (12.53)	39.65 (11.39)	χ^2= 0.56, df=3, p=0.91
IQ (z-scores)	0.10 (0.96)	-0.33 (1.74)	-0.69 (1.36)	0.28 (0.94)	χ^2= 4.5, df=3, p=0.21
YE	14.70 (2.77)	14.72 (3.39)	13.70 (2.79)	15.41 (2.80)	χ^2= 3.6, df=3, p=0.31
Gender (M/F)	18/21	10/15	2/8	15/12	χ^2= 4.0, df=3, p=0.26
Handedness (R/L/M)	33/6/0	22/1/2	9/1/0	27/0/0	χ^2= 12, df=6, p=0.06

To understand if the groups differed in terms of PRS, a Kruskal Wallis test was also performed. The medians of the groups are not equal (χ^2= 11; p=0.011), although it is not possible to conclude, using this test, which pairs of medians are significantly different and which are not. Therefore, a multiple comparison test was performed, by applying the Bonferroni method. The only means that are statistically different are the ones from controls and SCZ (p=0.027), with an estimated mean difference of 0.98.

On Figure 2.1, it is showed a box plot of the participants PRS, separated per diagnostic group. It is possible to conclude that the PRS median is greater on the SCZ group, followed by relatives, BD and control groups. The PRS median is larger on the Relatives group when compared to the BD group possibly because of the contribution of both diagnosis types (i.e., the PRS median of SCZ relatives patients is larger than on BD relatives (see Figure 2.2)). Moreover, PRS from BD and controls show a relatively symmetric distribution, with the median placed on the center of the box, while the distributions of SCZ and relatives PRS are more asymmetric. There is only one outlier in the whole sample – a BD patient (with PRS equal to 1.9). The minimum PRS value is the lowest on controls, followed by relatives, BD and SCZ. As for the maximum value, it is lower on SCZ and controls, with a minimum equal to 1.6, followed by BD (excluding the outlier) and relatives.

The Pearson's correlation coefficients were calculated for the pairs PRS- (Age/ IQ(z-scores)/ YE/ Gender) and the respective p-values were determined (Appendix B). The PRS did not correlate with age, IQ (z-scores), YE or handedness for the groups combined, although it correlated with gender (p=0.015).

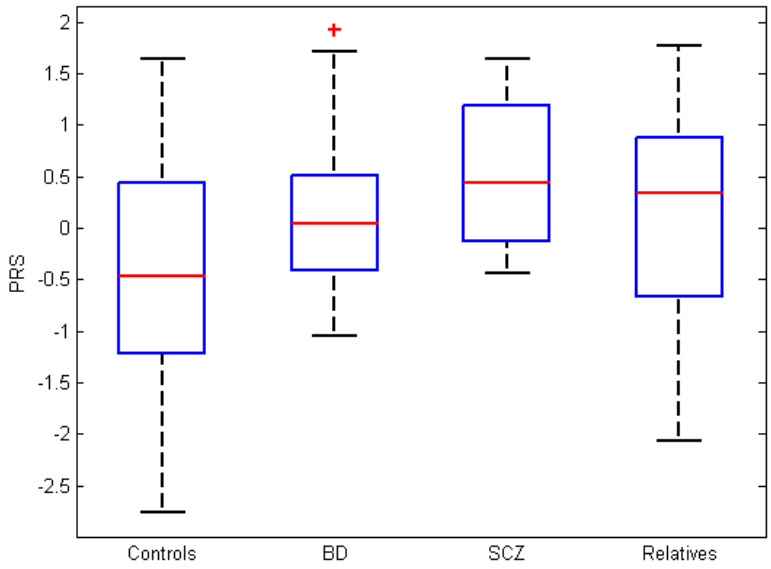

Figure 2.1 - Box plot of the participants PRS per diagnostic group (controls, BD, SCZ and relatives).

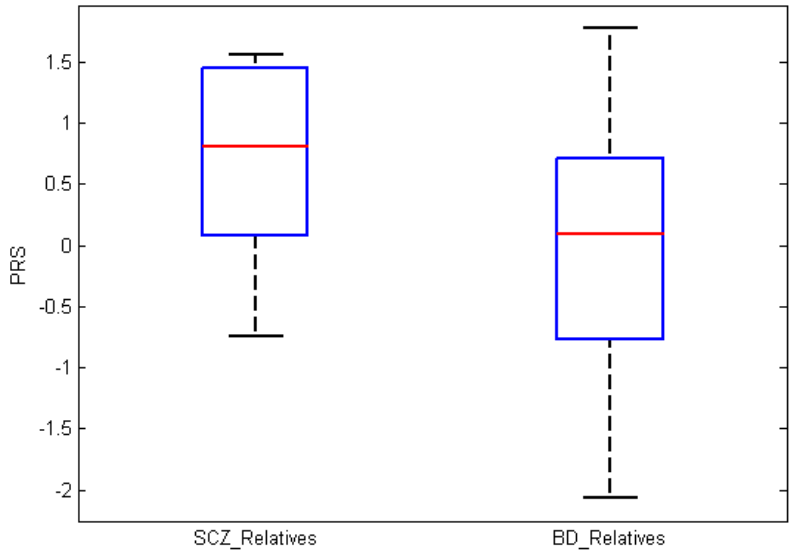

Figure 2.2 - Box plot of the relatives group PRS divided on SCZ and BD relatives.

2.2 Genetics

2.2.1 DNA extraction and genotyping

DNA was obtained from the participants using blood or buccal swabs. All participants were genotyped at the South London and Maudsley Trust/ King's College London BRC Genomics Laboratory on the Illumina HumanCore Exome BeadChip. The GenomeStudio Analysis software 2011.1 (Illumina Inc., San Diego, California) was used to process the genotypes.

Quality control was performed using PLINK 1.9 (https://www.cog-genomics.org/plink2) (Chang et al., 2015). It included the exclusion of SNPs with minor allele frequency (MAF) <1%, when they were

missing in >1% of the sample or when the Hardy Weinberg equilibrium (HWE) < 10^{-5} in controls. Participants were excluded when their genotypic failure >1% or had discordant gender information. A detailed description of the genetic samples processing can be find elsewhere (Vassos et al., 2016).

2.2.2 Polygenic risk scores

The PRSs were generated with the PRSice software (http://prsice.info/) (Euesden, Lewis, & O'Reilly, 2014), using the most recent Psychiatric Genomics Consortium (PGC) SCZ meta-analysis as a discovery sample (SWGPGC, 2014). This GWAS study detected several risk variants and their effect sizes on a large discovery sample, which was constituted by a maximum of 36989 cases and 113075 controls (SWGPGC, 2014). The target sample is constituted by the participants included on this project. There was not overlap between discovery and target samples, which could have led to an inflation of the results.

The PRSs were calculated for each individual of the target sample as the sum of the risk variants weighted by log odds ratio of the discovery sample($\ln(OR_{SNP(i)})$):

$$PRS = \sum_{i=1}^{n} \ln(OR_{SNP(i)}) X_{SNP(i)} \quad (2.1)$$

Where $X_{SNP(i)}$ is the number of risk variants for each SNP (0, 1 or 2).

A logistic regression was used to analyze the association between the calculated PRS (independent variable) and the disease trait (i.e. case-control status). The results for the PRS association, calculated for a set of thresholds (p_T = 0.00000005; 0.00001; 0.0001; 0.001; 0.01; 0,05; 0.1; 0.2; 0.5; 1) are present on Table 2.2. Notice that for larger thresholds, the number of SNPs included on the score increases. The PRSs used on this project were obtained at a threshold of 0.1, as it has reached the greatest proportion of variance between PRS and the case-control status (9.3% calculated as the Nagelkerker's pseudo-R^2). Thus, the SNPs with a p-value below a 0.1 were identified on the target sample and the individual PRSs were generated.

To guarantee that the SNPs included on the PRSs are informative, another selection was made using MAF>10% and INFO score>0.9, according to the PGC protocol (SWGPGC, 2014), including only one SNP from the Major Histocompatibility Complex region of the genome (hg19; chr6:27-33Mb). Principal component (PC) analysis was used to model population structure and exclude any outlier individuals. Ten PCs were used as covariates in the genetic analysis, to control for population stratification.

Table 2.2 - Results of PRS association with case-control status. The thresholded p-value, the p-value of the association, R^2 and number of SNPs are listed.

p_T	p-value	R^2	SNPs
0.00000005	0.0067	0.0309	106
0.00001	0.0205	0.0221	353
0.0001	0.0015	0.0419	781
0.001	0.0001	0.0651	1889
0.01	5.78×10^{-5}	0.0703	5513
0.05	1.75×10^{-5}	0.0802	12479
0.1	4.20×10^{-6}	0.0927	17965
0.2	7.10×10^{-6}	0.0878	26161
0.5	1.20×10^{-5}	0.0829	41866
1	1.77×10^{-5}	0.0793	55013

2.3 Imaging

2.3.1 Paradigm

The participants performed a VF task in response to a letter that was presented visually every 4 seconds. An “easy” and a “hard” set of letters were showed alternately to the subjects. The “easy” set of letters were: T, L, B, R, S or T, C, B, P, S and the “hard” set of letters were O, A, N, E, G or I, F, N, E, G. The task required the generation of a word that started with the letter presented and it was contrasted with a repetition condition, in which the subjects were presented visually with the word “rest” and were asked to say “rest” also within a period of 4 seconds.

The conditions were arranged in a block design, in which letters and “rest” conditions were presented in blocks of seven (except for the first and last word repetition blocks). The same letter was presented in the consecutive seven trials between each “rest” condition. Each participant performed two different runs: one easy and one hard. A run consisted of 69 trials, with 35 word generation blocks and 34 repetition condition blocks (Figure 2.3). In total, 74 volume images were acquired for each condition and the first 5 acquisitions were discarded from the analysis since they were considered dummy scans.

The verbal responses were recorded using a MRI-compatible microphone. Incorrect responses were considered situations where the subject did not generate any response or generated proper names, repetitions, grammatical variations of the previous word and “pass” responses.

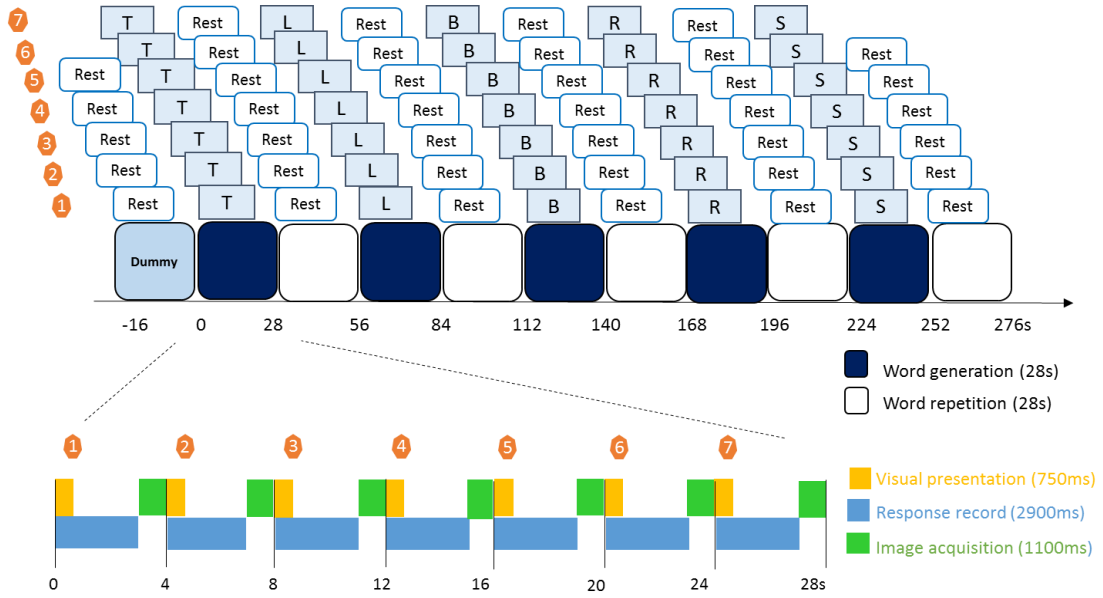

Figure 2.3 - Schematic representation of the block design used. The first word generation trial is zoomed to exemplify the acquisition timeline, which is similar in the other blocks. A run consisted of 69 trials, with 35 word generation blocks and 34 repetition condition blocks.

2.3.2 Image acquisition

Seventy-four T_2*-weighted functional images were acquired on a 1.5T GE LX System (General Electric, Milwaukee, USA), with echo planar imaging capability, at the Maudsley Hospital, London, UK. Twelve non-contiguous axial planes (with 7mm thickness, 1mm slice gap and 64×64 matrix size) parallel to the anterior commissure-posterior commissure line were collected over 1100ms in a clustered acquisition (echo-time (TE)=40ms, flip angle=70°, and voxel size = 3.75×3.75×8mm^3). During one repetition time (TR= 4000ms), a letter (or the "rest" word) was presented during a period of 750ms and a single overt verbal response could be made during a period of 2900ms, followed by image acquisition over 1100ms (Figure 2.3).

The T_1-weighted structural images were acquired on the same equipment, using a spoiled gradient-echo sequence, in axial and coronal slicing acquisition. In 33 participants, the structural images were acquired using axial slice acquisition and in the remaining 68 participants the structural images were acquired through coronal slicing acquisition. All images had similar parameters (1.5mm slice thickness, no slice gap, flip angle=20° and 256×256 matrix size), varying in TE (5000ms for axial slicing and 5800ms for coronal slicing) and TR. The voxel size for the images acquired in the axial plane was 0.9375×0.9375×1.500mm^3 size while for the images acquired in the coronal plane the voxel size was 0.8594×0.8594×1.500mm^3.

A forehead strap was used to reduce head movement. The subjects also wore noise-insulated headphones. To make sure that subjects heard their responses clearly, their speech was amplified and relayed using an acoustic MRI sound system (Ward Ray, Hampton Court, UK). All subjects' responses were

recorded for posterior evaluation of their performance, to distinguish between incorrect and correct trials.

2.3.3 Image analysis

2.3.3.1 Preprocessing

Before starting the preprocessing of functional images, the coronal slicing structural volumes were reordered to axial slicing, using the FSL 5.0.8 tools `fslorient` and `fslwapdim` (https://fsl.fmrib.ox.ac.uk/fsl/fslwiki/Fslutils).

I preprocessed the functional volumes using SPM12 (Wellcome Trust Centre for Neuroimaging, University College London, UK; http://www.fil.ion.ucl.ac.uk/spm), running under MATLAB 8.1.0.604. The preprocessing involved five steps: realignment, coregistration, segmentation, normalization and smoothing (Figure 2.4).

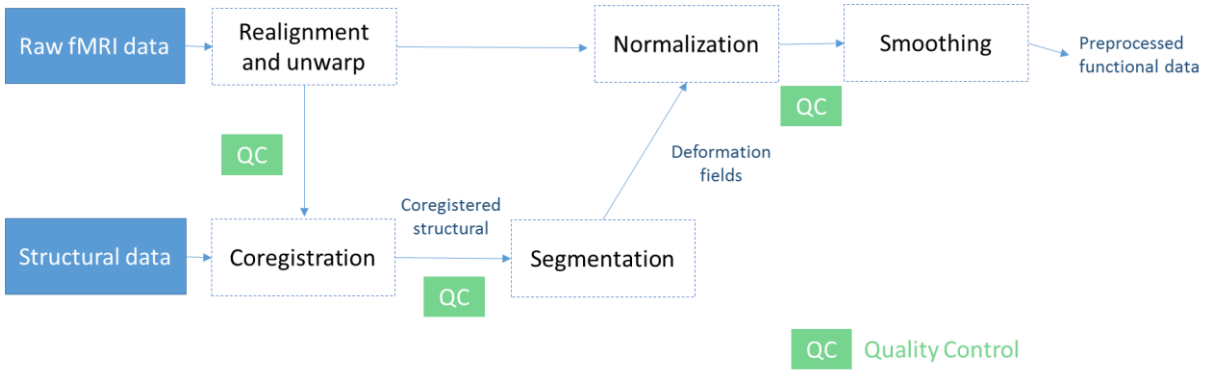

Figure 2.4 – Image preprocessing stream. It involves five steps: Realignment and unwarp, Coregistration, Segmentation, Normalization and Smoothing. Functional scans were realigned, spatially normalized and smoothed. Deformation fields used in normalization were obtained after the coregistration of the structural scans to the mean functional realigned image. Appropriate quality control steps were made at different time points.

2.3.3.1.1 Realignment and unwarp

All functional images were realigned and unwarped using the first image as a reference, through a least squares approach. This procedure is used to remove movement related artifacts and it is based on a six parameter (rigid body) transformation (3 translational parameters and 3 rotational parameters). The rigid body transformation assumes that the size and shape of the volumes are the same. The realignment parameters for each session were saved in a file and posteriorly used on the first level model as confounding covariates.

2.3.3.1.2 Coregistration

A coregistration between the structural (source) image and the mean realigned functional (reference) image was applied, maximizing the mutual information between both images (Collignon et al., 1995). The aim of this step is to map the functional information into the structural space, with greater resolution. This is also done using a rigid body transformation.

2.3.3.1.3 Segmentation

The structural coregistered image was segmented using the SPM default tissue probability maps (TPM) as priors. TPMs used in SPM are based on averaging multiple T_2-weighted and proton-density-weighted scans from the IXI dataset (http://www.brain-development.org/ixi-dataset/). This step segments the image into gray matter, white matter, cerebrospinal fluid, bone, soft tissue and air/background and creates deformation fields, which convert the shapes of the subjects' brain into the reference brain (Ashburner, 2009). Therefore, the normalization is done via segmentation, in a process named unified segmentation (Ashburner & Friston, 2005), in the sense that it combines both voxel intensity and prior spatial knowledge of TPMs to determine the tissue class.

2.3.3.1.4 Normalization

The realigned functional images were spatially normalized into the Montreal Neurological Institute (MNI) space and resampled to $2 \times 2 \times 2\text{mm}^3$ voxel size, using the deformation fields obtained from the segmentation step. The aim of this step is to increase sensitivity and allow inter-subject averaging.

2.3.3.1.5 Smoothing

The normalized scans were spatially smoothed through a convolution with an 8mm full-width at half maximum 3D Gaussian kernel. This process increases the signal-to-noise ratio (SNR) and mitigates the effects of the variability in the spatial location of functional regions across subjects, which were not corrected by normalization.

2.3.4 Statistical analysis

2.3.4.1 Performance analysis

The performance of the participants during the task was evaluated by the number of incorrect trials. A higher performance corresponds to a reduced number of incorrect trials. The goal of this analysis was to understand the effect of difficulty, group and genotype on the performance of the participants during the task. To do so, I performed a Mann-Whitney U-test and a Kruskal-Wallis test to study the effect of difficulty and diagnostic groups on the participant's performance, respectively. I have also determined a Pearson's correlation coefficient to analyze the effect of genotype on the performance.

2.3.4.2 Regional activation analysis

Statistical analysis of fMRI data on SPM uses a mass univariate data analysis based on GLMs. Statistical analysis involves the specification of the GLM design matrix, the estimation of the GLM parameters using a classical method and hypothesis testing through the generation of contrast vectors. The GLM can be expressed as in matrix notation as:

$$Y = X\beta + \varepsilon, \varepsilon \sim \mathcal{N}(0, \sigma^2 I) \quad (2.2)$$

Where Y is the image data (scans × voxels), in which the scans are acquired along a time period and all voxels constitute a three-dimensional image, X is the design matrix (scans × design variables), β are the parameters to be estimated (design variables × voxels) and ε is an error matrix. It is assumed that the error is normally distributed, such that ε has a mean of 0, a variance of σ^2 and any two elements of the error term are uncorrelated.

2.3.4.2.1 First-level analysis

After preprocessing, I performed the statistical analysis for each subject independently. Here, five different conditions (easy word generation, word repetition in easy runs, hard word generation, word repetition in hard runs and incorrect trials) were defined and six regressors (the individual movement parameters estimated in the realignment step in the preprocessing) were added to the model and considered covariates of no interest. A constant term was also added since it allows to model small fluctuations relative to the baseline signal. The resultant design matrix is depicted on Figure 2.5. The participants' smoothed images were concatenated and filtered using a high pass filter with 128s cutoff, to remove low-frequency trends, and serial correlations were taking into consideration by using the first order autoregressive model. Each experimental condition was convolved with a canonical HRF.

The GLM for a single voxel i, considering this single-level model, can be written as:

$$Y_i = \beta_{0,i} + X_1\beta_{1,i} + X_2\beta_{2,i} + \cdots + X_{11}\beta_{11,i} + \varepsilon_i \quad (2.3)$$

The first four variables (X_1, X_2, X_3 and X_4) are considered variables of interest while the rest are considered variables of no interest. X_5 was defined to exclude the trials were the participant did not respond properly and $X_6, \ldots, X_{11}$ constitute the three translational parameters (x,y,z) and three rotational parameters (pitch, roll and yaw) added to the model to remove the variance associated with motion. For each subject, a contrast image "easy + hard > rest" was computed using *t*-tests, excluding the wrong responses. Only the correct trials were taken into account on the second-level analysis to avoid the existence of performance differences as confounding factor, which might have influenced activation differences. On the other hand, as less trials are used on the group-level analysis, it might be associated with a loss of power to detect effects. The percentage of trials excluded per diagnostic group is found on section 3.1.

Subjects with more than 3mm translation or more than 3° rotation parameters were selected for graphical inspection of their estimated time-series translation and rotation. In total, 15 subjects were selected and in 4 of them, specific volumes (in which there was an abrupt displacement) were removed from the analysis, by adding a new binary regressor into their first-level analysis (with a 1 in the position of the volume being excluded and 0 otherwise). A graphical example of movement parameters of a subject where a volume was excluded is presented on Figure 2.6.

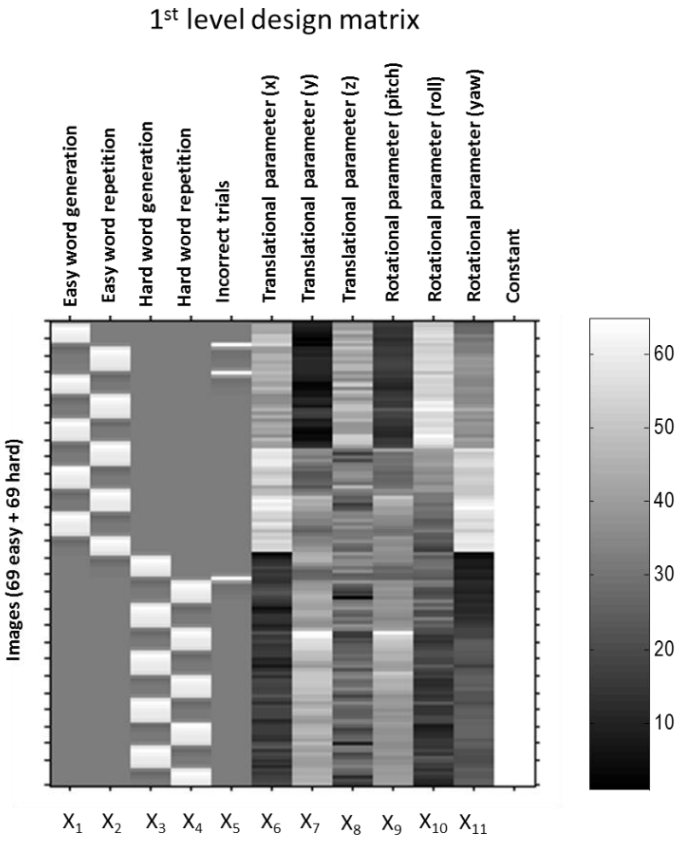

Figure 2.5 - Single-level (1st level) design matrix, composed by 11 column vectors (4 parameters of interest and 7 of no interest). The rows of the matrix are the individual functional scans obtained after preprocessing.

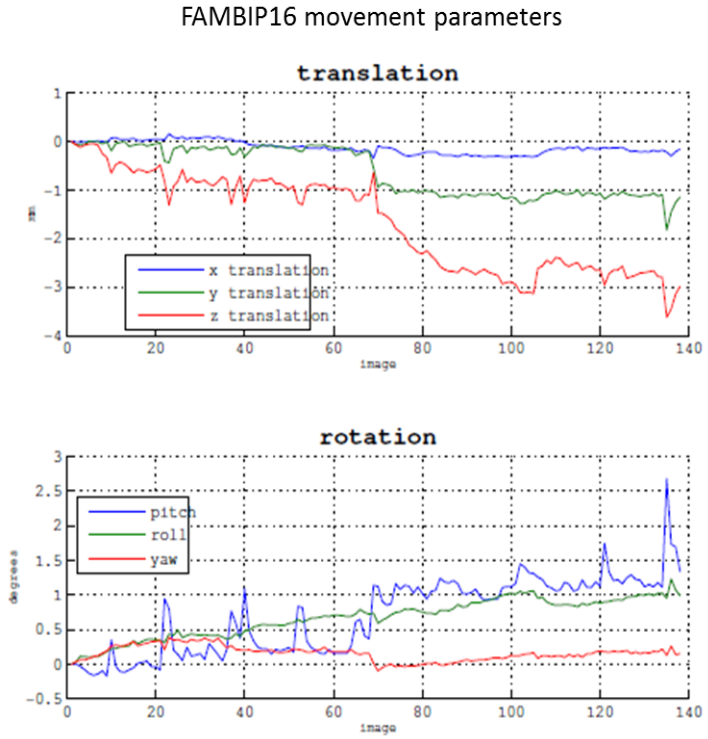

Figure 2.6 - Graphical display of the movement parameters of subject FAMBIP16. The volume 135 (final peak) was removed from the analysis.

2.3.4.2.2 Second-level analysis

To perform a group level analysis, subject-specific contrast images "easy + hard > rest" were entered into a full factorial ANOVA. This design allowed the localization of brain structures activated by easy or hard generation trials relatively to repetition trials and the study of their connectivity, for each diagnostic group. Additionally, it also permitted the study of the effect of diagnosis and the effect of PRS (main effect, diagnosis-specific effect and its interaction with each diagnostic group) during word generation relatively to repetition.

In the ANOVA model used here, one factor (diagnosis) was defined and divided into four levels: controls, BD, SCZ and relatives. Five covariates were included in the model: the covariate of interest (PRS) and four covariates of no interest (Age, IQ (z-scores), Gender and YE). These non-genetic factors were considered on this model as they usually have greater effects when compared to genetic factors (Muñoz, Hyde, & Hariri, 2009). The covariate of interest was entered as a single regressor per group. Therefore, this model included 12 design variables (Figure 2.7).

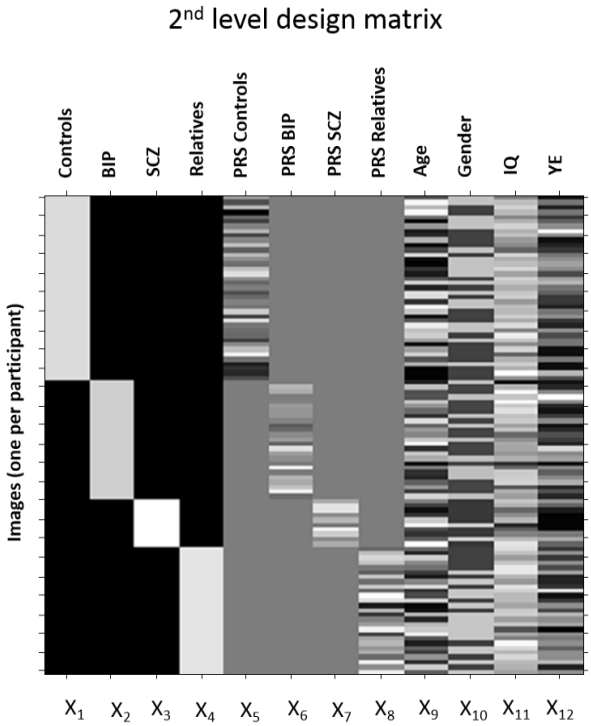

Figure 2.7 - Group-level (2nd level) design matrix, composed by one factor (divided into 4 levels), a covariate of interest (PRS; separated for each factor level) and 4 covariates of no interest (age, gender, IQ, YE).

The contrast images defined at this step can be divided into three different groups: effect of task, effect of diagnosis and effect of PRS. For the generation of contrast images, it is required the definition of the contrast vectors constituted by 1s (more activation), -1s (less activation) and 0s (hypothesis-free). For instance, the contrast vector for the main effect of PRS was defined as [0 0 0 0 1 1 1 1 0 0 0 0] for the positive effect and [0 0 0 0 -1- 1 -1 -1 0 0 0 0] for the negative effect. For the effect of PRS on the diagnostic groups, the contrast vectors for controls were defined as [0 0 0 0 1 0 0 0 0 0 0 0] for the positive effect and [0 0 0 0 -1 0 0 0 0 0 0 0] for the negative effect. On the diagnosis × PRS interaction contrasts, for

example, the contrast vectors for the comparison of the effect of PRS between controls and SCZ were [0 0 0 0 1 0 -1 0 0 0 0 0] and [0 0 0 0 -1 0 1 0 0 0 0 0], for the opposite association.

On the regional activation and connectivity analysis, the statistical maps were inspected at a voxel-wise $p<0.001$ (uncorrected for multiple comparisons) and regions were considered statistically significant when surviving a voxel-wise $p<0.05$ corrected using family-wise error (FWE) rate for multiple comparisons across the whole brain. The FWE rate method measures the probability of making one or more false positives, when performing multiple tests. The FWE rate implemented on SPM12 combines the use of a Bonferroni approach, in which the desired threshold is divided by the number of tests being made, and the use of RFT. RFT is a less conservative method that allows the adjustment of the p-value, considering that neighboring voxels are not independent, due to the continuity of the original data and due to its smoothness (Worsley, Taylor, Tomaiuolo, & Lerch, 2004). The results presented were analyzed at a whole-brain level, except for the section 3.4.1, where the search for regional activation was restricted to several ROIs.

2.3.4.3 Connectivity analysis

PPI analysis focus on task-dependent changes between activity in different brain structures and a seed region. PPI relies on the definition of three vectors: the influencing region time series, the task vector (that incorporates stimulus signal changes) and the product of the two terms (the interaction term). It looks for voxels that are more correlated with the seed during task blocks than during rest blocks, i.e., that will show a positive correlation with the PPI interaction term (Friston et al., 1997).

The connectivity analysis started by the definition of the coordinates of the "general" seed, which corresponded to the global maximum of the contrast image of the main effect of task (-42, 10, 26), located on the left inferior frontal gyrus. Afterwards, a volume of interest (VOI) was defined individually for each subject, by searching for the local maxima of each participant on a sphere of 6mm radius around the peek coordinates previously found. Using the SPM function *eigenvariate*, the BOLD time series of the first eigenvariate of this region (the 6mm-sphere around the coordinates of the maxima, which differ from subject to subject) was extracted. This BOLD time series corresponds to the physiological vector used on the new first-level PPI analysis. This step was included to account for inter-subject differences regarding the localization of anatomical structures.

2.3.4.3.1 First-level analysis

The PPI tool implemented in SPM was used to obtain the psychological vector (correspondent to the "easy+hard>rest" contrast vector) and the interaction term. The interaction term is created by multiplying the deconvolved physiological time-course with the psychological vector (Gitelman, Penny, Ashburner, & Friston, 2003). These three vectors (PPI interaction term, physiological and psychological vectors) were added to a new single-subject level analysis, including also as covariates of no interest the

individual six movement parameters (Figure 2.9). A contrast image of the interaction term against baseline was created for a single subject, which corresponds to the contrast vector [1 0 0 0 0 0 0 0 0].

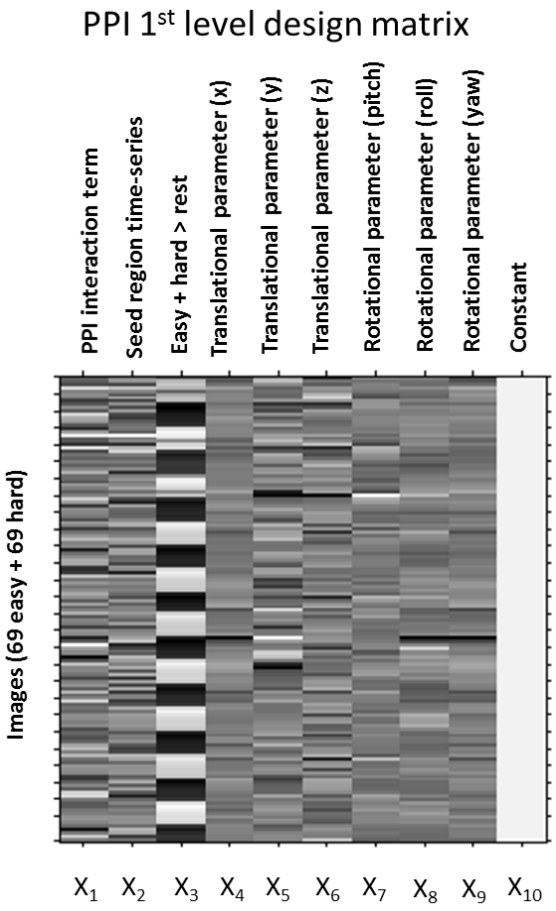

Figure 2.8 – Single-level (1st level) design matrix of the PPI analysis. It is composed by 9 covariates, the 3 regressors required for the PPI analysis (interaction term, seed region time-series and task vector) and 6 movement parameters.

2.3.4.3.2 Second-level analysis

Subsequently, a contrast image per participant was entered into a second level analysis, defined using a full factorial ANOVA. This model included the diagnosis as a factor, divided in four levels, and the PRS as a covariate of interest, entered as a single regressor per group. Besides that, the model also incorporated age, IQ (z-scores), YE and gender as covariates of no interest. This analysis enabled the study of the overall effect of task, the detection of diagnostic group differences and the understanding of the influence of the PRS, on the task-modulated connectivity with the seed region.

2.3.4.4 Additional analyses

The additional analyses included the use of a ROI approach on the PRS contrasts, the analysis of a multiple regression model where the diagnosis factor was not taken into account and an analysis of the task difficulty effect on the areas recruited by the task and on the areas associated with PRS.

The ROI analysis was added to avoid the problem of multiple comparisons of the whole-brain analysis and to understand if the VOIs of previous findings and task-modulated networks are associated

with the PRS. Two different approaches were used for this analysis. Firstly, by listing the peak coordinates of anatomical/functional structures from the literature studies on the application of PRS on functional endophenotypes (Table 1.2 on section 1.2.4.2) and applying SVC into a sphere of 8mm radius around those coordinates (Table 2.3), and searching for regional activation. Secondly, by applying inclusively into the different contrast images a mask of the main effect of task (obtained at $p<0.05$ FWE corrected) and searching for significant regional activation.

On the un-modelled diagnosis analysis, the five covariates defined previously were added to the model and the effects of PRS on regional activation were analyzed. The design matrix is not showed due to its simplicity.

On the task difficulty analysis, a new full factorial ANOVA was defined. New single-level contrast images were generated for each participant, one "easy > rest_easy" and other "hard > rest_hard". The images were entered on a design composed by two factors, diagnosis and difficulty, and divided on 8 different levels (four for the diagnostic groups multiplied by the two difficulty levels) (Figure 3.15). The five covariates included on the previously defined 2nd level models were also added, with the difference that PRS was entered as a single regressor per group and per difficulty level (i.e., entered separated by 8 vectors) in order to study its interaction with difficulty and diagnosis (Figure 2.9).

Table 2.3 - List of the peak coordinates of the functional endophenotypes where an association with PRS was previously found. Blue: working memory task; yellow: executive language-base task; green: facial processing task; orange: probabilistic learning; pink: monetary incentive delay.

Author	Task	Brain regions	Peak MNI coordinates (x, y, z)
Walton et al. (2012)	Working memory	DLPFC	-26, 50, 8
Whalley et al. (2012b)	Executive language-based	Subgenual portion of the ACC	2, 40, -6
		Right amygdala	18, -6, -14
Walton et al. (2013)	Working memory	Left DLPFC and left VLPFC	−6, 38, 48
		DLPFC	−12, 48, 30
		Anterior cingulate gyrus	−4, 46, -18
Kauppi et al. (2014)	Working memory	Right inferior frontal gyrus	48, 18, −10
		Right middle/ superior prefrontal cortex	38, 46, −16
		Right middle temporal gyrus	72, −40, −4
Whalley et al. (2014)	Executive language-based	Left inferior frontal gyrus, precentral and postcentral gyri	−58, −14, 38
Tesli et al. (2015)	Facial processing	Right inferior frontal gyrus	52, 18, 12
		Right postcentral gyrus	54, -20, 50
Dima et al. (2016)	Facial processing	Visual cortex	−32,−88, 2
	Working memory	Medial prefrontal cortex	22, 48 -14
Lancaster et al. (2016a)	Probabilistic learning	Right frontal pole	34, 58, 0
		Left ventral striatum	-4, 4 -12
Lancaster et al. (2016b)	Monetary incentive delay	Left ventral striatum	-12, 2, -8
Cosgrove et al. (2017)	Spatial working memory	Right inferior occipital gyrus and middle temporal gyrus	48, −76, −2
		Medial parietal region	3, −34, 16
	Facial processing	-	-

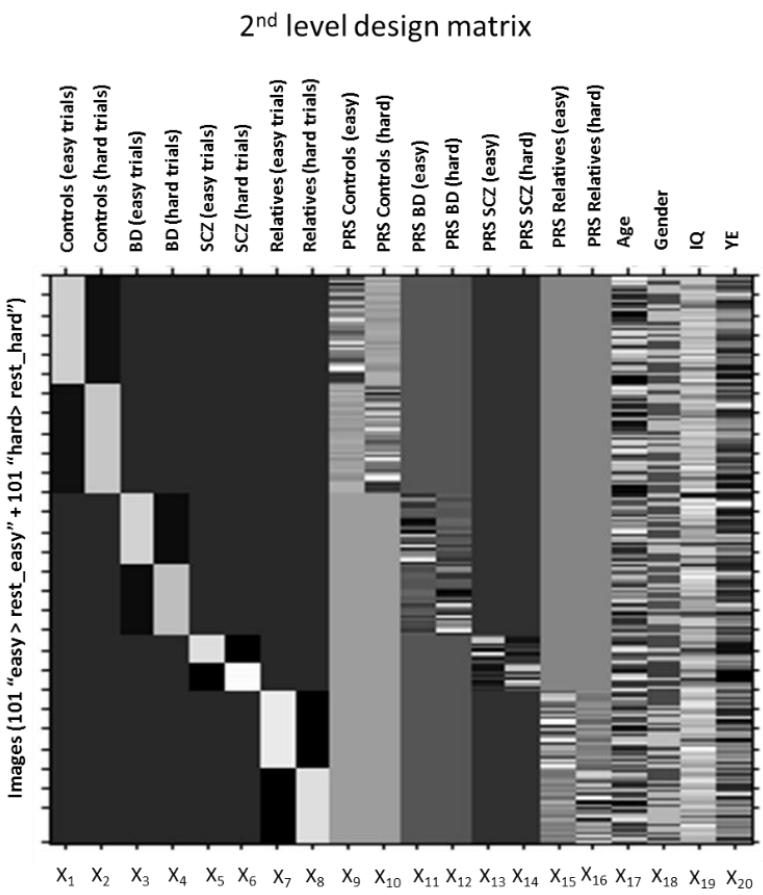

Figure 2.9 - Group-level (2nd level) design matrix of the task difficulty analysis. The model comprises two factors (diagnosis and difficulty), the PRS interacting with both factors and the 4 covariates of no interest.

3. Results

3.1. Performance analysis

Overall, the percentages of incorrect trials for both difficulty trials combined are 16% for controls, 16% for BD, 15% for SCZ and 12% for relatives. These percentages represent the proportion of trials that were not included on the group-level analysis, for each group separately.

3.1.1. Effect of VF difficulty

I conducted this analysis to understand if the number of incorrect responses is statistically different on the two difficulty levels of the task. Since the sample is constituted by groups with small sizes (<20 participants) and as the number of incorrect responses in each group does not follow a normal distribution, Mann-Whitney U-tests were conducted on MATLAB R2014a. The histogram plots of the number of incorrect trials are presented on Appendix C.

The `ranksum(x,y)` function of MATLAB performs the Mann-Whitney U-test, by testing the null hypothesis that data in `x` and `y` are samples from continuous distributions with equal medians, assuming that they are both independent, with identical distributions. This test suggests the rejection of the null hypothesis of equal medians, as the hard task seems to induce more errors than the easy version (U=4043; p=0.014). For each diagnostic group analyzed individually, controls (U=610; p=0.13), BD (U=267; p=0.38), SCZ (U=33; p=0.21) and relatives (U=284; p=0.16), there were no statistical differences for the two versions of the task.

3.1.2. Effect of diagnosis

To understand if the diagnosis has an effect on the distribution of the number of errors (Table 3.1), I conducted a Kruskal-Wallis test, using the MATLAB function `kruskalwallis(x)`, where `x` is a matrix with columns representing the independent samples being tested. This test assumes the null hypothesis that each column of `x` comes from the same distribution. There is no effect of the diagnosis on the number of incorrect trials, for the easy (χ^2=1.20, p=0.80), the hard (χ^2=0.92, p=0.82) and both versions combined (χ^2=0.70, p=0.87).

Table 3.1 - Number of incorrect responses during the task presented as mean (standard deviation), for the easy, hard and both versions of the task combined, divided per diagnostic group.

	Controls (n=39)	BD (n=25)	SCZ (n=10)	Relatives (n=27)
Easy (mean(SD))	4.87 (4.86)	5.00 (5.10)	4.20 (4.26)	3.44 (2.90)
Hard (mean(SD))	6.33 (5.63)	6.32 (5.86)	6.00 (3.68)	5.07 (3.99)
Easy + Hard (mean(SD))	11.21 (9.75)	11.32 (9.48)	10.20 (6.75)	8.52 (4.99)

3.1.3. Effect of PRS

The goal of this analysis is to understand if the PRSs are associated with a worse performance of the participants during the task. The Pearson's correlation coefficient between these two variables is r =

0.0037, with a p-value of 0.97, meaning that these variables are not linearly related, as can be showed on Figure 3.1.

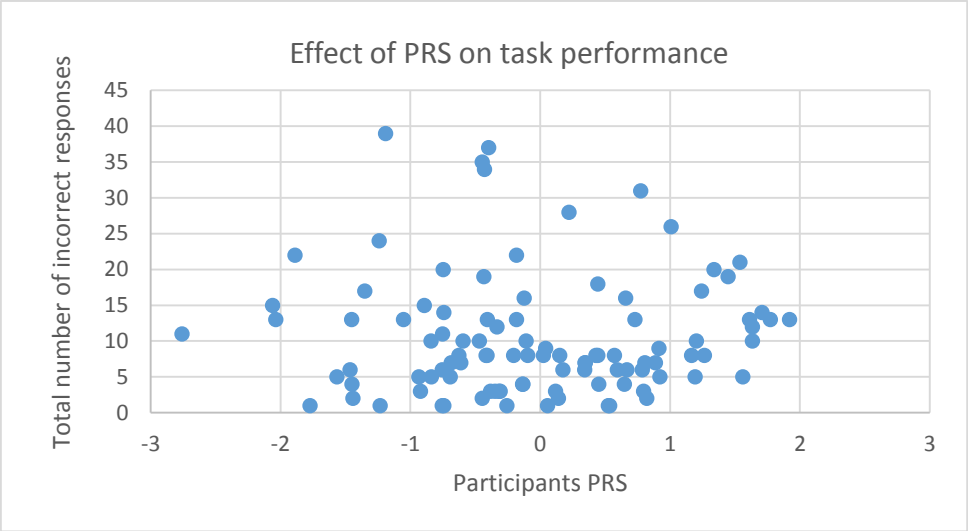

Figure 3.1 - Graphical display of the total number of incorrect responses as function of the PRS.

3.2. Regional activation analysis

The results that I have obtained for brain activation and connectivity analysis (listed on this section and on section 3.3, respectively) will be presented on the form of a table, usually followed by a visual representation of the regions where an effect was found, where the color bars represent the intensity of T-values. The voxels that survived the significance threshold defined initially, at a voxel level, of 0.05 FWE corrected or 0.001 uncorrected for the images with no corrected results, are characterized by the cluster extent k, the maximal activation peak coordinates, the peak T-value and the abbreviations of the clusters labeling provided by Automated Anatomical Labeling 2 (AAL2) (Rolls, Joliot, & Tzourio-Mazoyer, 2015), with the percentage of intersection between the activation clusters and the anatomical VOI (AVOI) of the parcellation defined by this software. The abbreviations used on the cluster labelling correspond to anatomical descriptions, which are listed on Appendix D. The automated labeling of regions was confirmed using an anatomical human atlas (Netter, 2006). Often, SPM reports several peaks that are more than 8mm apart on the same cluster, information that might be useful when the cluster has a great extent. The label of the main maxima of each cluster (the one with the largest T-value) is the structure bolded in each row. I defined previously the minimal cluster extent as k=10, except for the main effect of task where I defined as k=20.

3.2.1. Effect of VF task

On this subsection, the goal is to understand the areas associated with the VF task, for both word generation > repetition (i.e. easy + hard > rest) contrast and the opposite contrast word repetition > generation (i.e. rest > easy + hard), across the whole sample and independently of the risk score, using a minimum cluster extent of 20 voxels and a p-value of 0.05 FWE corrected. The paradigm was associated with activation of the left inferior frontal gyrus (both pars opercularis and triangularis), bilateral anterior

insula, right caudate nucleus and left middle temporal gyrus (Table 3.2; Figure 3.2). Moreover, contrasting word repetition with word generation revealed an increased activation on a network of areas including the bilateral precuneus, angular gyrus and posterior insula and right rolandic operculum and putamen (Table 3.3; Figure 3.3).

Table 3.2 – Significant regions at p<0.05 FWE corrected, for the effect of task during word generation > repetition.

Task-modulated networks: word generation > repetition					
Cluster extent (k)	T-value	Peak MNI coordinates			Cluster labeling
		x {mm}	y {mm}	z {mm}	
1827	12.13	-42	10	26	**Frontal_Inf_Tri_L (25.51%)** Insula_L (25.01%) Frontal_Inf_Oper_L (21.46%) Unknown (14.34%) Precentral_L (9.41%) Frontal_Inf_Orb_2_L (3.45%) Rolandic_Oper_L (0.71%) Temporal_Pole_Sup_L (0.11%)
	9.24	-32	20	4	
	6.49	-42	28	16	
1274	7.35	20	6	20	Unknown (48.35%) **Caudate_R (22.92%)** Thalamus_L (8.48%) Cerebelum_4_5_L (6.91%) Caudate_L (4.40%) Vermis_3 (4.24%) Vermis_4_5 (2.90%) Thalamus_R (1.33%) Cerebelum_3_L (0.24%) Putamen_L (0.16%) Lingual_L (0.08%)
	7.19	14	0	16	
	6.52	-2	-8	12	
291	6.67	34	22	4	**Insula_R (81.79%)** Unknown (9.97%) Frontal_Inf_Orb_2_R (3.78%) Frontal_Inf_Oper_R (3.78%) Frontal_Inf_Tri_R (0.69%)
36	5.32	-20	-46	16	**Unknown (100.00%)**
67	5.03	-48	-30	-8	**Temporal_Mid_L (73.13%)** Unknown (26.87%)
51	4.97	28	-46	14	**Unknown (100%)**

Table 3.3 - Significant regions at p<0.05 FWE corrected, for the effect of task during word repetition > generation.

Task-modulated networks: word repetition > generation					
Cluster extent (k)	T-value	Peak MNI Coordinates			Cluster labeling
		x {mm}	y {mm}	z {mm}	
2839	12.17	2	-54	36	**Precuneus_R (31.95%)** Precuneus_L (25.18%) Cingulate_Post_L (8.24%) Cuneus_L (6.83%) Cingulate_Mid_R (6.09%) Cingulate_Mid_L (5.42%) Cingulate_Post_R (5.24%) Cuneus_R (5.11%) Unknown (2.40%) Calcarine_R (2.11%) Calcarine_L (1.34%) Occipital_Sup_L (0.07%)
728	8.94	50	-56	32	**Angular_R (53.85%)** Temporal_Mid_R (27.75%) Temporal_Sup_R (9.62%) SupraMarginal_R (3.43%) Occipital_Mid_R (3.30%) Unknown (2.06%)
977	7.90	34	-16	6	Rolandic_Oper_R (30.91%) **Insula_R (26.00%)** Putamen_R (18.12%) Unknown (10.24%) SupraMarginal_R (9.72%) Heschl_R (2.66%) Temporal_Sup_R (1.74%) Pallidum_R (0.61%)
	5.80	58	-26	22	
	5.42	50	-4	12	
1002	7.62	-38	-14	2	**Insula_L (29.64%)** Rolandic_Oper_L (18.56%) Temporal_Sup_L (17.76%) Heschl_L (15.87%) Putamen_L (8.88%) Unknown (8.78%) Pallidum_L (0.50%)
	5.21	-48	-24	8	
98	7.17	-46	-60	30	**Angular_L (91.84%)** Temporal_Mid_L (4.08%) SupraMarginal_L (4.08%)

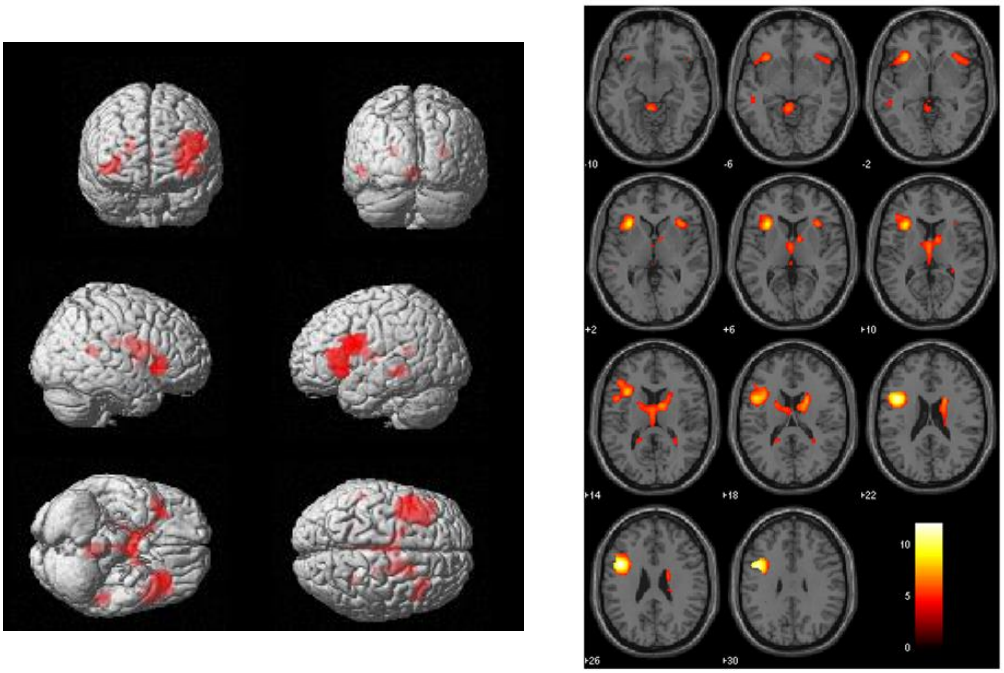

Figure 3.2 – Rendering and axial slices of the significant regions at p<0,05 FWE corrected, for the effect of task on brain activation during word generation > repetition independently of the diagnostic group. The predominance of activation (higher T-value) on the left hemisphere and on frontal lobe is evident on this rendering (color bars indicate T-values).

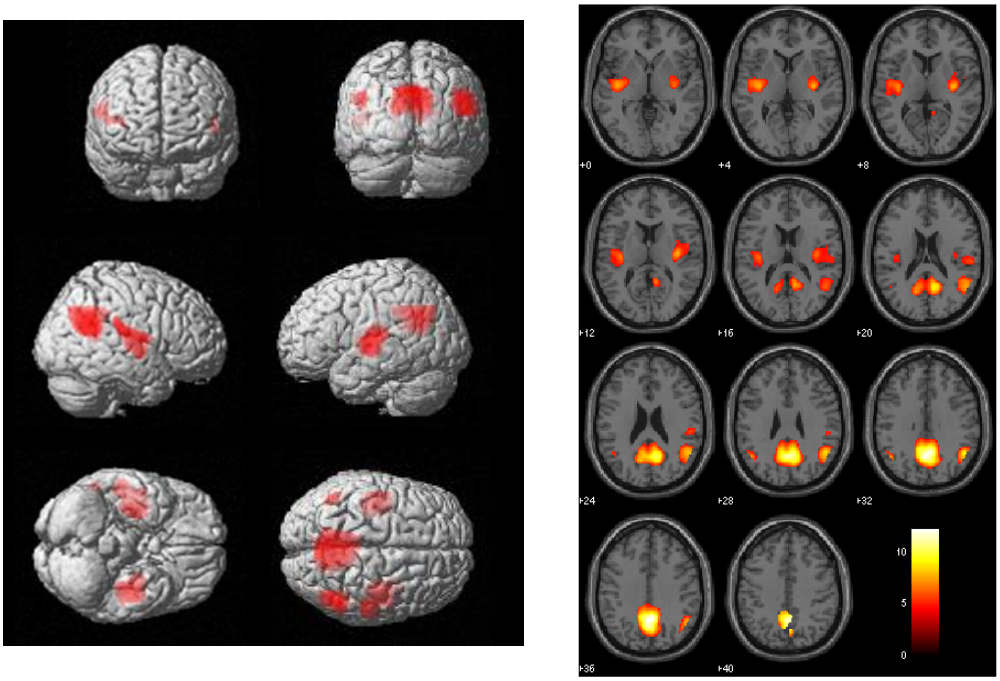

Figure 3.3 - Rendering and axial slices of the significant regions at p<0,05 FWE corrected, for the effect of task on the contrast word repetition > generation, independently of the diagnostic group. There is a predominance of activation on the right hemisphere and parietal lobe (higher T-value) (color bars indicate T-values).

3.2.2. Effect of diagnosis

As there were no corrected regions for the diagnostic group differences contrasts, the results presented on this section were obtained at p=0.001 uncorrected and k>10. For the contrasts where patients activate more than health (i.e. SCZ/BD > controls/relatives) (Table 3.4), I found that SCZ patients activated more the right parahippocampal gyrus than controls and relatives, analyzed separately, and additionally they showed greater activation of the left middle temporal gyrus and right temporal pole of the superior temporal gyrus when compared to the control group (Figure 3.4). There were no areas more activated in BD patients than in healthy groups. As for the cases where healthy groups activated more than patients groups (Table 3.5), all contrasts analyzed included activation of areas that are not defined by AAL2, effect that is particularly evident in the contrasts controls > SCZ and relatives > patients groups. Moreover, the controls activated more than BD in an area including the left hippocampus, cerebellar vermis and left cerebellum.

There were no areas more activated in controls than in relatives and vice-versa. SCZ activated more than BD in a network of areas including the right parahippocampal gyrus, the right calcarine fissure and surrounding cortex (from now on, abbreviated to calcarine) and the left supramarginal gyrus. BD activated more than SCZ in regions localized outside the parcellation defined on AAL2 (Table 3.6).

All these contrasts suggested that the task has an effect on the right parahippocampal gyrus, which seems to be particularly different in the SCZ group when compared to the others. To understand this effect, I extracted a graphical plot of the contrast estimates on the coordinates (32,-32, 14), peak of maximal activation located on this area (Figure 3.5). The plot indicates that the task is negatively correlated with activation of the right parahippocampal gyrus in controls, BD and relatives while in SCZ it is positively correlated with the activation of this region.

Table 3.4 – Uncorrected regions at p<0.001, for the effect of task during word generation > repetition on contrasts patients > health.

Effect of task during word generation > repetition for patients > health contrasts					
Cluster extent (k)	T-value	Peak MNI coordinates			Cluster labeling
		x {mm}	y {mm}	z {mm}	
Effect of task in SCZ > Effect of task in controls					
25	3.94	32	-32	-14	**ParaHippocampal_R (88.00%)** Hippocampus_R (12.00%)
70	3.90	-56	-42	0	**Temporal_Mid_L (100%)**
11	3.57	48	2	-18	Temporal_Pole_Sup_R (63.64%) Unknown (18.18%) **Temporal_Pole_Mid_R (9.09%)** Temporal_Mid_R (9.09%)
Effect of task in SCZ > Effect of task in relatives					
35	4.36	32	-32	-14	**ParaHippocampal_R (77.14%)** Hippocampus_R (22.86%)

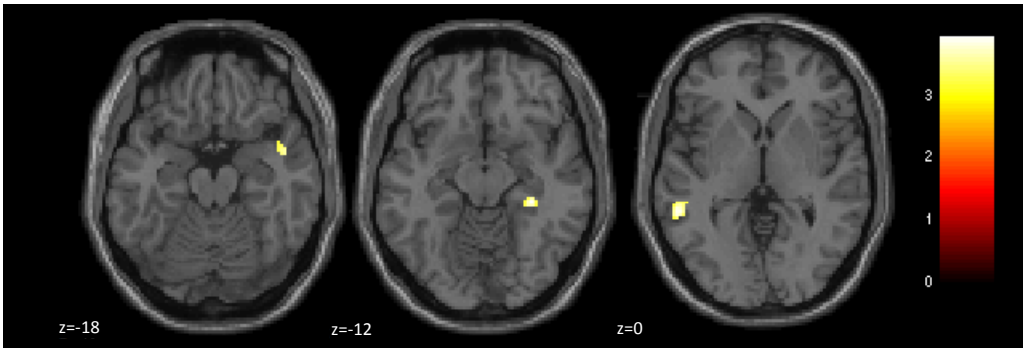

Figure 3.4 – Uncorrected regions at p<0,001, for the effect of task on the contrast SCZ > controls. During word generation > repetition, SCZ patients activate more the right temporal pole of the superior temporal gyrus (z=-18), the right parahippocampal gyrus (z=-12) and the left middle temporal gyrus (z=0) when compared to controls (color scale indicate T-values).

Table 3.5 - Uncorrected regions at p<0,001, for the effect of task during word generation > repetition on contrasts healthy < patients.

Effect of task during word generation > repetition for health > patients contrasts					
Cluster Extent (k)	T-value	Peak MNI coordinates			Cluster labeling
		x {mm}	y {mm}	z {mm}	
Effect of task in controls > Effect of task in SCZ					
67	4.01	4	22	2	**Unknown (91.04%)**
	3.80	14	28	0	Caudate_R (8.96%)
Effect of task in controls > Effect of task in BD					
45	3.95	-38	-36	-4	**Unknown (88.89%)** Hippocampus_L (11.11%)
26	3.69	-16	-34	26	**Unknown (100%)**
20	3.49	-2	-56	0	**Vermis_4_5 (55.00%)** Cerebelum_4_5_L (20.00%) Lingual_L (15.00%) Calcarine_L (10.00%)
Effect of task in relatives > Effect of task in SCZ					
235	4.72	6	22	2	**Unknown (84.26%)** Caudate_R (13.62%) Caudate_L (1.70%) Olfactory_R (0.43%)
	4.52	14	28	0	
	3.74	-20	34	0	
31	3.93	-26	-34	18	**Unknown (100.00%)**
27	3.69	-12	-32	16	**Unknown (96.30%)** Cingulate_Post_L (3.70%)
10	3.37	-20	14	24	**Unknown (100.00%)**
Effect of task in relatives > Effect of task in BD					
124	4.11	-16	-36	26	**Unknown (100.00%)**
214	3.99	22	-28	20	**Unknown (100.00%)**
72	3.61	-32	-44	4	**Unknown (80.56%)** Hippocampus_L (11.11%) Lingual_L (5.57%) ParaHippocampal_L (2.78%)
	3,31	-30	-46	-4	

Table 3.6 - Uncorrected regions at p<0.001 on contrasts where SCZ patients activated more than BD during the task and vice-versa.

Effect of task during word generation > repetition for SCZ>BD and vice-versa					
Cluster extent (k)	T-value	Peak MNI coordinates			Cluster labeling
		x {mm}	y {mm}	z {mm}	
Effect of task in SCZ > Effect of task in BD					
58	4.62	34	-32	-12	**ParaHippocampal_R (55.17%)** Hippocampus_R (39.66%) Fusiform_R (3.45%) Unknown (1.72%)
54	4.10	18	-82	6	**Calcarine_R (98.15%)** Cuneus_R (1.85%)
30	3.88	-58	-30	26	**SupraMarginal_L (93.33%)** Temporal_Sup_L (6.67%)
Effect of task in BD > Effect of task in SCZ					
81	4.10	18	30	-2	**Unknown (72.84%)**
	3.84	8	24	2	Caudate_R (27.16%)
64	3.87	-18	32	0	**Unknown (100.00%)**

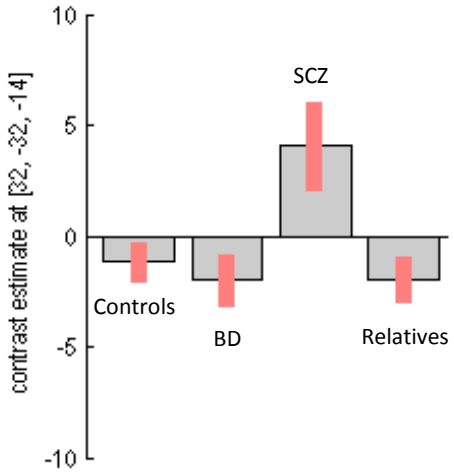

Figure 3.5 - Plot of the contrast estimates on the right parahippocampal gyrus. The word generation > repetition contrast is negatively correlated with the activation of this area in controls, BD and relatives while in SCZ patients it is positively correlated with this region.

3.2.3. Effect of PRS

3.2.3.1. Main effect of PRS

There were only uncorrected results for the main effect of PRS on brain activation, and in particular all the associations found were pointing out in the negative direction (Table 3.7). Moreover, I found a negative association of the PRS with the activation on a network of regions including the left inferior frontal gyrus, the left middle temporal gyrus, the bilateral insula, the right putamen, right thalamus and right caudate nucleus (Figure 3.6).

Table 3.7 - Uncorrected regions obtained at p<0.001, for the main effect of PRS on regional brain activation.

Main effect of PRS on regional brain activation					
Cluster extent (k)	T-value	Peak MNI coordinates			Cluster labeling
		x {mm}	y {mm}	z {mm}	
Negative effect of PRS on activation					
192	4.71	-32	10	22	**Unknown (53.13%)** Frontal_Inf_Oper_L (33.33%) Frontal_Inf_Tri_L (10.94%) Precentral_L (2.08%) Insula_L (0.52%)
83	4.06	-48	-28	-6	Temporal_Mid_L (51.91%) **Unknown (48.19%)**
244	3.92	34	-4	12	**Insula_R (57.79%)** Rolandic_Oper_R (13.52%) Temporal_Sup_R (11.89%) Unknown (9.02%) Putamen_R (7.38%) Heschl_R (0.41%)
	3.84	40	-10	4	
	3.71	50	-4	0	
40	3.74	18	16	-2	**Putamen_R (52.50%)** Caudate_R (25.00%) Unknown (22.50%)
21	3.72	6	-22	-2	Unknown (61.90%) **Thalamus_R (38.10%)**
23	3.62	-58	-42	-2	**Temporal_Mid_L (100.00%)**
13	3.37	-38	4	-4	**Insula_L (69.23%)** Unknown (30.77%)

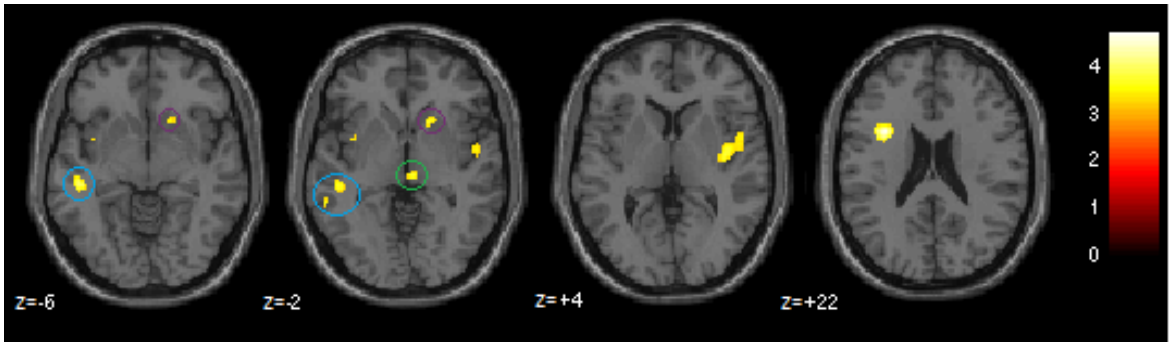

Figure 3.6 - Axial slices obtained at p<0.001 uncorrected, where a main effect of PRS on brain activation during word generation > repetition was found. PRS was negatively associated with activation of the left middle temporal gyrus (z=-6 and z=-2, blue circle), right putamen (z=-6 and z=-2, purple circle), right thalamus (z=-2, green circle), right insula (z=+4) and left inferior frontal gyrus (z=+22; peak of maximal activation).

3.2.3.2. Diagnosis-specific effect of PRS

There are no positive effects of PRS in either diagnostic group at p<0.001 uncorrected. As for the negative effects of PRS, two corrected clusters were found on regions outside the parcellation areas defined by AAL2, in control group.

Other negative effects of PRS were found at an uncorrected threshold for all diagnostic groups (Table 3.7) (Figure 3.7). In controls, PRS is negatively associated with the activation of areas outside the AVOIs defined by AAL2, areas that were overlapping with the left inferior frontal gyrus, right cingulate and paracingulate gyri (shortened to cingulate from now on) and left insula. In SCZ patients, PRS is negatively

correlated with the activation of the right calcarine and the left middle temporal gyrus. In BD patients, PRS was negatively associated with the activation of a cluster incorporating right inferior frontal gyrus (pars orbitalis and triangularis). The clusters found in relatives reside in areas outside the regions identified by AAL2.

Table 3.8 – Uncorrected regions obtained at p<0.001 for the diagnosis-specific effect of PRS on brain deactivation. The cluster size, as well as the coordinates of the peaks with maximal activation, peak T-values and cluster labeling are also described.

PRS effect on brain activation for each diagnostic group					
Cluster extent (k)	T-value	Peak MNI coordinates			Cluster labeling
		x{mm}	y {mm}	z {mm}	
Negative effect of PRS on brain activation in SCZ					
39	4.13	18	-82	6	**Calcarine_R (100.00%)**
29	3.77	-48	-32	-4	**Unknown (55.17%)** Temporal_Mid_L (44.83%)
Negative effect of PRS on brain activation in BD					
177	4.15	38	34	-8	**Frontal_Inf_Orb_2_R (64.41%)** Unknown (23.73%) Frontal_Inf_Tri_R (6.78%) Insula_R (5.08%)
Negative effect of PRS on brain activation in controls					
1214	5.17*	-30	12	22	**Unknown (90.03%)** Frontal_Inf_Oper_L (4.53%) Caudate_L (1.40%) Frontal_Inf_Tri_L (1.40%) Cingulate_Ant_L (0.99%)
	4.92**	-26	0	32	
	4.62	-30	-6	28	
274	4.66	24	-4	28	**Unknown (98.18%)** Cingulate_Mid_R (1.09%) Caudate_R (0.73%)
	4.45	32	-10	28	
45	3.72	-34	6	0	**Unknown (57.78%)** Insula_L (42.22%)
12	3.69	10	6	30	**Unknown (66.67%)** Cingulate_Mid_R (16.67%) Cingulate_Ant_R (16.67%)
23	3.68	-22	-46	36	**Unknown (100.00%)**
Negative effect of PRS on brain activation in relatives					
22	3.67	28	-42	22	**Unknown (100.00%)**
25	3.63	-26	-56	20	

* peak-level p_{FWE} = 0.006 ; **peak-level p_{FWE}=0.014

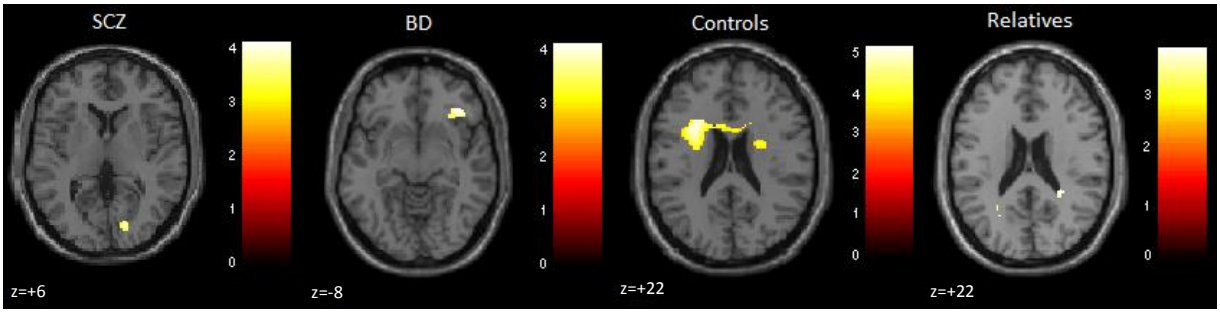

Figure 3.7 - Axial slices obtained at p<0.001 uncorrected, depicting the global maximum of the diagnosis-specific effect of PRS on brain activation. In SCZ the global maximum is on the right calcarine (z=+6), in BD is on the right inferior frontal gyrus (z=-8) and in controls and relatives, tested separately, it covers a portion of the white matter (z=+22).

3.2.3.3. Diagnosis x PRS interaction

There were no significant effects for the interaction between the diagnosis and the PRS. At an uncorrected level, I found a diagnosis x PRS interaction on the bilateral calcarine, right parahippocampal gyrus and right lingual gyrus (Table 3.9). PRS is associated with greater activation of the right calcarine and right parahippocampal gyrus in controls than in the SCZ patients. Moreover, PRS is associated with greater activation in controls of the bilateral calcarine and lingual gyrus than in SCZ and BD patients. PRS has a greater effect in relatives and BD (tested separately) than in SCZ on the right calcarine. The results found on these four different contrasts suggest that PRS is more negatively correlated with activation on right calcarine on the SCZ group than it is on any other. This is confirmed by the plot of the contrast estimates on that area, specifically at the coordinates of the peak with greatest T-value, (16,-84, 6) (Figure 3.8). PRS is negatively associated with the activation of the right calcarine for SCZ and slightly positively correlated with the activation of this area in controls and BD groups.

Table 3.9 – Uncorrected regions obtained at p<0.001, for the diagnosis x PRS interaction on brain activation.

Diagnosis x PRS interaction on brain activation					
Cluster extent (k)	T-value	Peak MNI coordinates			Cluster labeling
		x {mm}	y {mm}	z {mm}	
PRS effect in controls > PRS effect in SCZ					
70	4.01	16	-84	6	**Calcarine_R (100.00%)**
13	3.61	16	-38	-8	**ParaHippocampal_R (61.54%)** Lingual_R (23.08%) Cerebelum_4_5_R (15.38%)
PRS effect in controls > PRS effect in SCZ and BD					
79	3.55	6	-86	4	**Calcarine_R (83.54%)** Calcarine_L (11.39%) Lingual_R (5.06%)
18	3.49	-6	-58	4	**Calcarine_L (72.22%)** Lingual_L (22.22%) Precuneus_L (5.56%)
PRS effect in relatives > PRS effect in SCZ					
10	3.57	18	-82	6	**Calcarine_R (100.00%)**
PRS effect in BD > PRS effect in SCZ					
12	3.69	18	-82	6	**Calcarine_R (100.00%)**

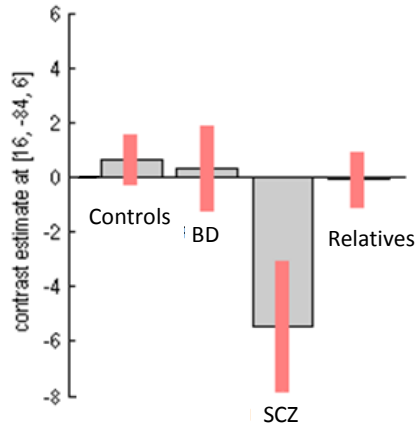

Figure 3.8 – Plot of the contrast estimates on the right calcarine. PRS is negatively correlated with activation of the right calcarine in SCZ and slightly positively correlated with the activation of this region in controls and BD groups.

3.3. Connectivity analysis

3.3.1. Effect of VF task

At an uncorrected threshold of 0.001, the PPI analysis revealed that the connectivity between the left inferior frontal gyrus (seed region) and the right caudate nucleus and left middle and superior temporal gyrus is greater during word generation trials than during word repetition trials. Conversely, the connectivity between the seed and the right thalamus, left cuneus and left superior occipital cortex is greater during word repetition trials than during word generation trials (Table 3.10; Figure 3.9). To understand if there is any group driving the effect found in the left superior temporal gyrus, I extracted a plot of the contrast estimates at (-56,14,0). The plot shows that in all groups there is a slight positive correlation of this area with the interaction term and the correlation is considerably greater on SCZ (Figure 3.10).

Table 3.10 - Uncorrected regions obtained at p<0.001, for the main effect of the task on the task-modulated connectivity analysis.

Effect of VF task on task-modulated connectivity analysis					
Cluster extent (k)	T-value	Peak MNI coordinates			Cluster labeling
		x {mm}	y {mm}	z {mm}	
Effect of task on PPI analysis during word generation > repetition					
29	3.79	14	2	6	**Unknown (86.21%)** Caudate_R (13.79%)
37	3.77	-56	-14	0	**Temporal_Sup_L (67.57%)** Temporal_Mid_L (29.73%) Heschl_L (2.70%)
30	3.63	24	-36	12	**Unknown (100.00%)**
Effect of task on PPI analysis during word repetition > generation					
26	3.69	4	-22	-2	**Unknown (84.62%)** Thalamus_R (15.38%)
18	3.68	-18	-78	38	Cuneus_L (66.67%) **Occipital_Sup_L (33.33%)**

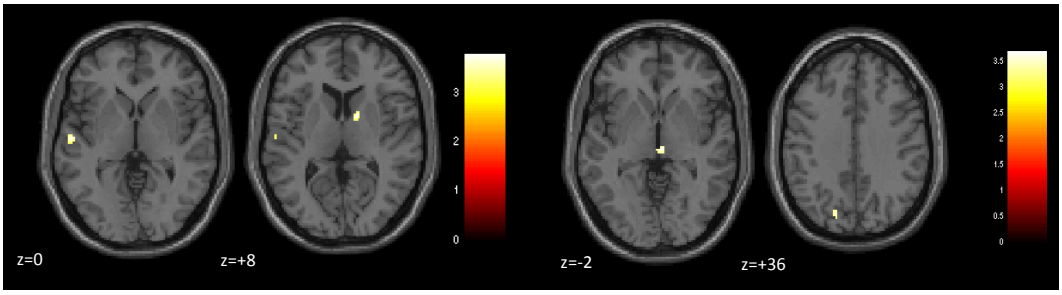

Figure 3.9 - Axial slices depicting the uncorrected regions found at p<0.001, for the main effect of task on the connectivity with the left inferior frontal gyrus. The connectivity of the left inferior frontal gyrus with the left temporal gyrus (z=0) and right caudate (z=8) is greater during word generation than word repetition (left figures). The connectivity of the left inferior frontal gyrus with the right thalamus (z=-2) and the left cuneus and left superior occipital cortex (z=+36) is greater during word repetition than word generation (right figures).

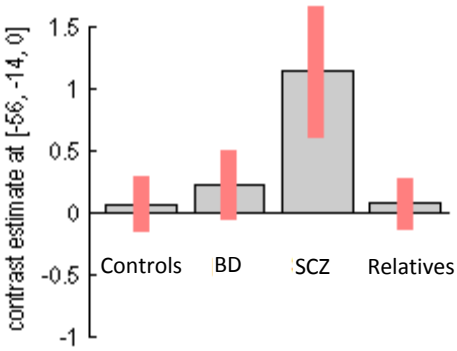

Figure 3.10 - Plot of the contrast estimates on the left superior temporal gyrus. There is a slight positive correlation of this area with the interaction term in all diagnostic groups whereas SCZ shows a strong correlation with the interaction term.

3.3.2. Effect of diagnosis

There were no corrected results for the effect of diagnosis on the task-modulated connectivity analysis. At an uncorrected level (Table 3.11; Figure 3.11), I found that the correlation between the left pallidum and left putamen with the seed region is greater during word generation than word repetition in controls. Moreover, in SCZ patients, the correlation between the seed and the left postcentral gyrus, the left superior temporal gyrus, the precentral gyrus and the left inferior frontal gyrus (pars opercularis) was greater during word generation than during word repetition. In relatives the seed was correlated with the right putamen and left insula, an association that was greater during word generation than during word repetition trials. As for the areas more correlated with the seed during word repetition than generation, I found this effect in SCZ on the left cuneus and on the left superior occipital gyrus. In BD patients, I found that the right inferior frontal gyrus is negatively correlated with the interaction term (i.e., showed greater correlation with the seed during word repetition trials than generation).

Table 3.11 - Uncorrected regions obtained at p<0.001, for the effect of diagnosis on the task-modulated connectivity analysis.

Effect of diagnosis on the task-modulated connectivity analysis					
Cluster extent (k)	T-value	Peak MNI coordinates			Cluster labeling
		x {mm}	y {mm}	z {mm}	
Areas positively correlated in controls on the task-modulated connectivity					
30	4.16	-26	-10	-4	**Pallidum_L (56.67%)** Putamen_L (36.67%) Unknown (6.67%)
Areas positively correlated in SCZ on the task-modulated connectivity					
140	3.80	-58	-8	20	**Postcentral_L (40.00%)** Temporal_Sup_L (31.43%) Precentral_L (22.14%) Heschl_L (5.00%) Temporal_Mid_L (1.43%)
	3.72	-56	-14	4	
	3.61	-52	-4	24	
30	3.69	16	-22	28	**Unknown (100.00%)**
12	3.32	-56	8	18	**Frontal_Inf_Oper_L (91.67%)** Precentral_L (8.33%)
Areas positively correlated in relatives on the task-modulated connectivity					
36	4.17	30	12	2	**Putamen_R (86.11%)** Unknown (13.89%)
36	3.89	-34	-22	20	**Insula_L (72.22%)** Rolandic_Oper_L (19.44%) Unknown (8.33%)
Areas negatively correlated in SCZ on the task-modulated connectivity					
39	4.19	-18	-76	40	Cuneus_L (76.92%) **Occipital_Sup_L (23.08%)**
Areas negatively correlated in BD on the task-modulated connectivity					
30	3.57	48	22	14	**Frontal_Inf_Tri_R (70.00%)** Frontal_Inf_Oper_R (26.67%) Unknown (3.33%)

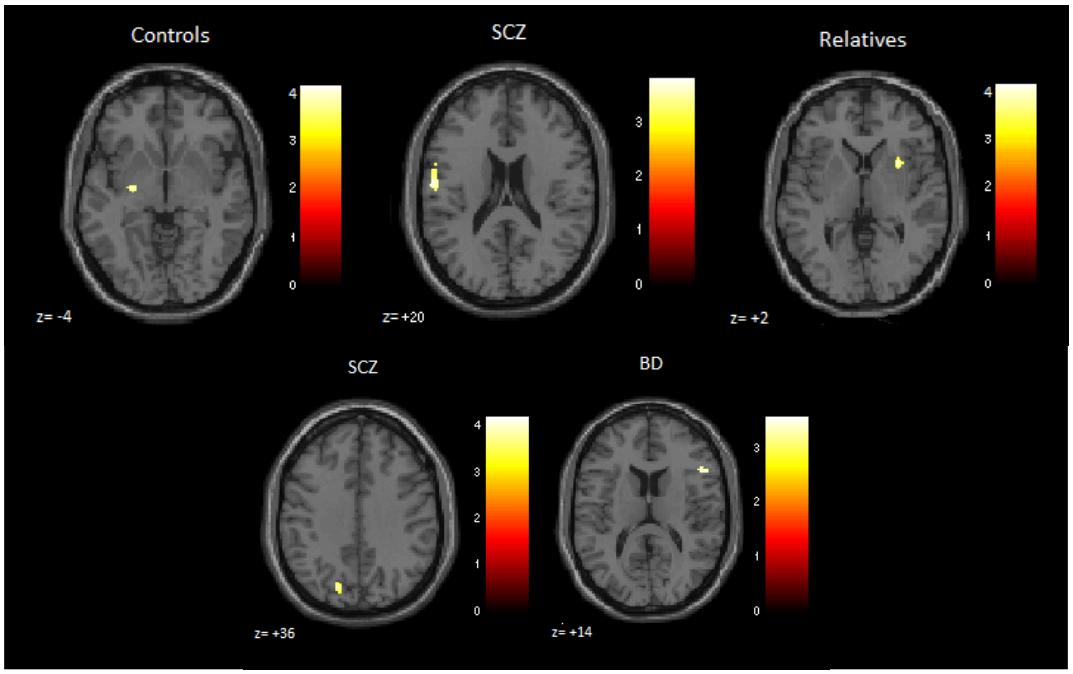

Figure 3.11 - Uncorrected regions found at p<0.001, for the diagnosis-specific effect of the task in all groups, on the PPI analysis.
***Top**: Areas positively correlated with the interaction term during word generation > repetition. Left: in controls, the left pallidum and left putamen (z=-4); Middle: in SCZ, the left postcentral gyrus, the left superior temporal gyrus, the precentral gyrus (z=+20); Right: in relatives, the right putamen (z=+2).*
***Down**: Areas negatively correlated with the interaction term during word generation > repetition. Left: in SCZ, the left cuneus and the left superior occipital gyrus (z=+36); Right: in BD, the right inferior frontal gyrus (z=+14).*

There were no corrected results for the diagnostic group differences on the task-modulated connectivity analysis. I found that the left postcentral and precentral gyri, a portion of the left inferior frontal gyrus and an area outside the AAL2 are more correlated with the interaction term in SCZ group than in controls. Also, the opposite effect was found in the left cuneus and superior and middle occipital gyrus, areas are more correlated with the seed in controls than in SCZ during word generation trials than word repetition (Table 3.12; Figure 3.12). I did not find other uncorrected effects for the other contrasts tested.

Table 3.12 - Uncorrected regions obtained at p<0.001, for the diagnostic-group differences on the task-modulated connectivity analysis.

Diagnostic-group differences on the task-modulated connectivity analysis					
Cluster extent (k)	T-value	Peak MNI coordinates			Cluster labeling
		x {mm}	y {mm}	z {mm}	
Regions more correlated in SCZ than in controls on the task-modulated connectivity					
69	3.73	-58	-8	20	**Postcentral_L (55.07%)**
	3.41	-56	8	14	Precentral_L (23.19%) Frontal_Inf_Oper_L (21.74%)
14	3.52	16	-22	28	**Unknown (100.00%)**
Regions more correlated in controls than in SCZ on the task-modulated connectivity					
14	3.60	-18	-76	38	Cuneus_L (64.29%) **Occipital_Sup_L (35.71%)**
11	3.54	-24	-56	34	Unknown (81.82%) **Occipital_Mid_L (18.18%)**

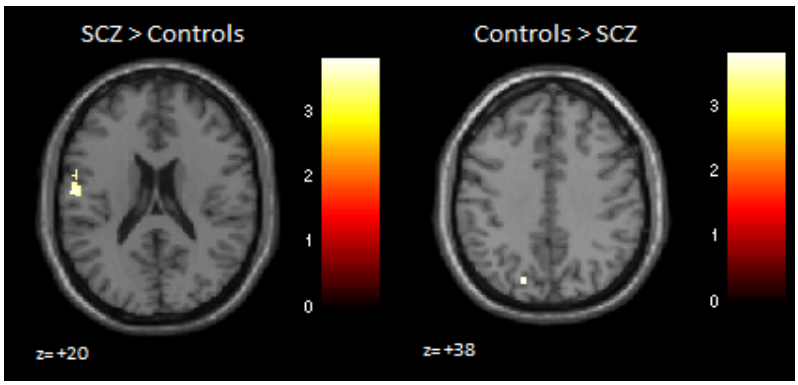

Figure 3.12 - Uncorrected regions obtained at p<0.001 for the diagnostic-group differences on the task-modulated connectivity analysis
***Left**: The left postcentral and precentral gyri and a portion of the left inferior frontal gyrus are more correlated with the seed during task blocks than rest blocks in SCZ than in controls (z=+20).*
***Right**: The left cuneus and superior and middle occipital gyrus are more correlated with the seed during task blocks than rest blocks in SCZ than in controls (z=+38).*

3.3.3. Effect of PRS

3.3.3.1. Main effect

There were no uncorrected results for the main effect of PRS on the correlation with the interaction term.

3.3.3.2. Diagnosis-specific effect

At an uncorrelated level, I found a diagnosis-specific effect of PRS on the correlation between the seed and the cerebellar vermis, right occipital gyrus, left angular gyrus, left thalamus, right lingual gyrus and right calcarine, effects that were different between word generation and repetition (Table 3.13; Figure 3.13). In SCZ, PRS had a negative effect on the correlation of the cerebellar vermis and the right occipital gyrus with the interaction term. In BD, PRS was associated with greater correlation between the left angular gyrus and the seed during word generation than word repetition. In relatives, PRS had a positive effect on the correlation between the left thalamus, right lingual gyrus and right calcarine, and the interaction term. There were no effects of PRS on the task-modulated connectivity in controls.

Table 3.13 - Uncorrected regions obtained p<0.001, for the effect of PRS on the task-modulated connectivity analysis.

Effect of PRS on the task-modulated connectivity analysis					
Cluster extent (k)	T-value	Peak MNI coordinates			Cluster labeling
		x {mm}	y {mm}	z {mm}	
Negative correlation of PRS on the task-modulated connectivity in SCZ					
18	3.73	2	-58	-4	**Vermis_4_5 (100.00%)**
15	3.68	16	6	6	**Unknown (73.33%)** Pallidum_R (20.00%) Caudate_R (6.67%)
10	3.60	38	-80	0	**Occipital_Mid_R (90.00%)** Occipital_Inf_R (10.00%)
	3.28	32	-86	0	
Positive correlation of PRS on the task-modulated connectivity in BD					
10	3.34	-46	-54	26	**Angular_L (100.00%)**
Positive correlation of PRS on the task-modulated connectivity in relatives					
48	3.77	-10	-12	0	**Thalamus_L (100.00%)**
21	3.62	0	14	16	**Unknown (100.00%)**
19	3.56	12	-54	2	**Lingual_R (100.00%)**
12	3.50	28	-60	4	**Calcarine_R (91.67%)** Lingual_R (8.33%)

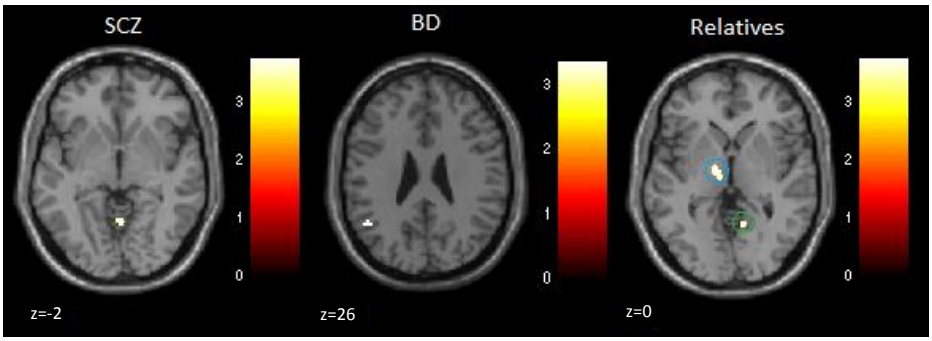

Figure 3.13 - Axial slices depicting the global maximum of the diagnosis-specific effect of PRS on brain connectivity, obtained at p<0-001 uncorrected. PRS has a negative effect on the correlation of the interaction term with the cerebellar vermis (left figure, z=-4) in SCZ, a positive effect on the correlation of the interaction term with the left angular gyrus (middle figure, z=+26) in BD, and in relatives (right figure, z=0), a positive effect on the correlation of the left thalamus (blue circle) and the right lingual gyrus (green circle) with the interaction term.

3.3.3.3. Diagnosis x PRS interaction

There were no uncorrected results for the diagnosis x PRS interaction contrasts on the task-modulated connectivity analysis. There were, however, uncorrected results for this interaction on the cerebellar vermis, on the right occipital gyrus, on the left thalamus, bilateral calcarine, bilateral lingual gyrus and right caudate nucleus (Table 3.14). PRS had a larger effect in controls and relatives, tested separately, than in SCZ patients on the correlation between the cerebellar vermis and the interaction term. Moreover, PRS had also a more pronounced effect in relatives than in SCZ on the correlation of the right middle and inferior occipital gyrus with the interaction term. PRS was more associated with the correlation of the interaction term and the left thalamus, bilateral calcarine and bilateral lingual gyrus in relatives than in controls. Finally, PRS had a greater effect in BD than in SCZ on the correlation of a portion of the right caudate nucleus with the interaction term.

Table 3.14 - Uncorrected regions obtained at p<0.001, for the diagnosis x PRS interaction on the task-modulated connectivity analysis.

Diagnosis x PRS interaction on the task-modulated connectivity analysis					
Cluster extent (k)	T-value	Peak MNI coordinates			Cluster labeling
		x {mm}	y {mm}	z {mm}	
PRS effect in controls > PRS effect in SCZ on the task-modulated connectivity					
10	3.39	2	-58	-4	**Vermis_4_5 (100.00%)**
PRS effect in relatives > PRS effect in SCZ on the task-modulated connectivity					
18	3.89	38	-80	0	**Occipital_Mid_R (77.78%)** Occipital_Inf_R (16.67%) Unknown (5.56%)
	3.56	32	-86	0	
32	3.84	2	-56	-2	**Vermis_4_5 (100.00%)**
PRS effect on relatives > PRS effect in controls on the task-modulated connectivity					
69	4.34	2	12	18	**Unknown (100.00%)**
26	3.65	-10	-10	-2	**Thalamus_L (84.62%)** Unknown (15.38%)
15	3.60	-6	-62	10	**Calcarine_L (100.00%)**
37	3.58	-8	-72	2	**Lingual_L (45.95%)** Calcarine_L (43.24%) Lingual_R (5.41%) Calcarine_R (5.41%)
	3.51	2	-68	10	
20	3.55	12	-54	4	**Lingual_R (100.00%)**
11	3.37	26	-58	4	**Calcarine_R (100.00%)**
PRS effect in BD > PRS effect in SCZ on the task-modulated connectivity					
25	3.74	16	6	6	**Unknown (64.00%)** Caudate_R (24.00%) Pallidum_R (12.00%)

3.4. Additional analyses

3.4.1. ROI analysis

I did not find any active clusters inside the spheres of 8-mm radius defined around the peak coordinates listed on Table 2.2. Only one voxel of the contrast of the negative effect of PRS on brain activation on BD was localized inside of one of those spheres, particularly the one around the coordinates (48, 18, −10), on the right inferior frontal gyrus.

Regarding the results of masking the PRS contrasts with the main effect of task contrast, several regions were found using a minimum cluster extent of k=10. On the main effect of PRS, two uncorrected activated regions were found, one with peak coordinates at (32,10,22) had k=176, $p_{FWE} = 0.028$ peak-level and T=4.71, located outside the AAL2 (48.86%) and also on the left inferior frontal gyrus (48.29%) and other with peak coordinates at (-48,-28,-8), with k=17, $p_{FWE}=0.22$ and T= 4.02, located mostly outside the areas defined by AAL2 (64.71%) and on left middle temporal gyrus (35.29%) (Figure 3.14).

On the diagnosis-specific effect of PRS on the different diagnostic groups, in SCZ I found that PRS is negatively correlated with the activation of area close to left temporal gyrus (peak coordinates at (-48, -30, -6), T=3.60); in controls, PRS is negatively correlated with the activation on a region encompassing the left inferior frontal gyrus and the insula, as well as a cluster near the right caudate. On the other groups, no effects were found inside the mask. I did not find any regions inclusively masked by the main effect of task contrast for the diagnosis x PRS interaction. On the areas found to be engaged with the left inferior frontal gyrus (the seed region) during the task-modulated connectivity, I found a cluster on an area covered by the mask, at the main effect of task during word generation > repetition. This cluster was predominantly on the white matter (81.25%), but included a small portion of the right caudate nucleus (18.75%) (peak coordinates at (14,2,6), T= 3.79). All other contrasts were tested and no results were found.

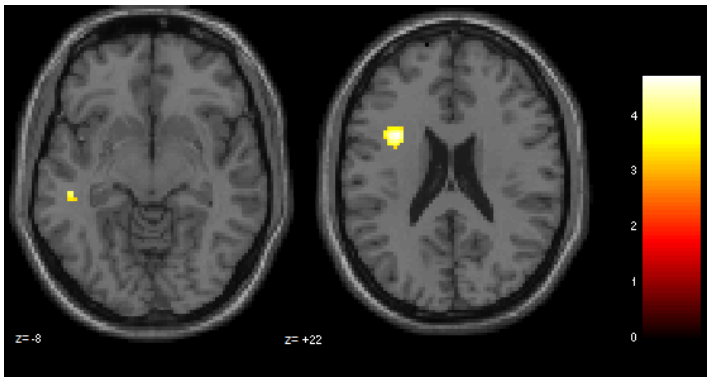

Figure 3.14 - Uncorrected regions found at p<0.001 uncorrected for the main effect of PRS after masking with the contrast image of the main effect of task (word generation > repetition).

3.4.2. Un-modelled diagnosis analysis

The purpose of this analysis was to understand if the effect of PRS on regional activation is influenced by the presence of the diagnosis factor. To do so, I performed a new 2nd-level analysis using a multiple regression model, where five covariates were included: PRS, Age, IQ (z-scores), YE and Gender. Previously, on the full factorial ANOVA used for the regional activation analysis, the main effect of PRS was only negatively associated with brain activation and there were no statistically significant regions.

On the multiple regression model used here, both positive and negative effects of PRS on brain activation were analyzed. As before, at a p=0.001 uncorrected no results were found for the positive effect. Nevertheless, at a k>10, one region was below the voxel-wise FWE corrected threshold of 0.05. This region had peak coordinates at (32, 10, 22) had k=45, p_{FWE} = 0.004 and T=5.22, located mostly on the white matter (91.11%) and also on the left inferior frontal gyrus (8.89%). This region is included on the global maximum of the main effect of PRS found previously at an uncorrected level (Table 3.7). When the threshold was lowered to 0.001 uncorrected, I found effects on the previously reported regions, with the difference that the cluster sizes were larger and p_{FWE} were smaller.

3.4.3. Task difficulty analysis

The purpose of this analysis was to understand if the effect of PRS on brain activation depends on the task difficulty and also to confirm that there were no differences between the easy and hard trials in terms of regional activation.

I did not find significant differences between easy and hard trials for the main effect of task. Also, when the groups were tested separately, I did not find any differences between the difficulty levels in terms of brain activation in all groups. As for the PRS, there were no significant differences between both difficulty levels on the main effect of PRS, not even when an uncorrected voxel-wise p-value of 0,001 was chosen. There were, however, significant differences on the diagnosis-specific effect of PRS in controls, for the contrast "PRS controls (hard) > PRS controls (easy)" (Table 3.15; Figure 3.15). PRS had a larger effect during hard trials on the activation of a part of the left postcentral gyrus than on easy trials (p_{FWE}= 0.0014). There were no significant differences on the other diagnosis-specific effect of PRS contrasts.

Table 3.15 - Corrected results for the effect of task difficulty on the diagnosis-specific effect of PRS on brain activation.

Effect of task difficulty on the diagnosis-specific effect of PRS on brain activation					
Cluster extent (k)	T-value	Peak MNI coordinates			Cluster labeling
		x {mm}	y {mm}	z {mm}	
PRS effect in controls during hard trials > PRS effect in controls during easy trials					
54	5.34	-46	-16	30	**Postcentral_L (75.93%)** Unknown (16.67%) Precentral_L (7.41%)
	4.87	-54	-8	28	
	4.72	-40	-8	28	

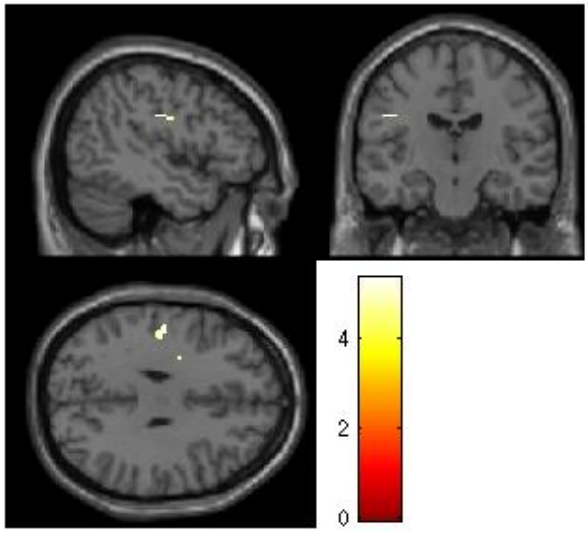

Figure 3.15 - Corrected regions found at p<0.05 FWE corrected for the effect of task difficulty on the diagnosis-specific effect of PRS on the regional activation. PRS has a greater effect during hard trials than on easy trials on the activation of the left postcentral gyrus.

4. Discussion

The main purpose of this project was to study the effects of a PRS, generated based on susceptibility risk variations for SCZ, on task-modulated brain activation and connectivity during VF, in a group of healthy participants, SCZ and BD patients and their relatives. I have investigated the main effects of PRS, diagnosis-specific effects as well as PRS by diagnosis interactions across the whole brain. Complementarily, I also performed analyses within regions of interest and within the regions activated by the task. The assumptions made were that the effect of PRS on brain function is observable with fMRI and during a VF paradigm, as it is showed to be an adequate endophenotype for SCZ and BD.

4.1 Main effect of task

The VF paradigm activated a brain network comprising areas involved in language processes such as the left inferior frontal gyrus (both pars opercularis and triangularis), bilateral anterior insula, right caudate nucleus and left middle temporal gyrus. All these areas have previously associated with VF tasks (Baldo, Schwartz, Wilkins, & Dronkers, 2006; Birn et al., 2010; Meinzer et al., 2009; Phelps, Hyder, Blamire, & Shulman, 1997). Other areas that were expected to be associated with the task were the anterior and posterior cingulate cortex, superior temporal, inferior parietal cortex and bilateral thalamus (Costafreda et al., 2011; Fu et al., 2005; Prata, 2008). The activation was moderately left lateralized, as showed by the superior number of regions found on the left areas and their superior size and T-value when compared to right lateralized activation, a finding that is also consistent with the previous studies (Costafreda et al., 2011; Prata, 2008).

The areas more engaged during word repetition than generation were the bilateral precuneus, angular gyrus and posterior insula, right rolandic operculum and right putamen. Both precuneus and angular gyrus belong to a network of areas that are activated and intrinsically correlated when the human brain is at rest and not focused on any particular task (Utevsky, Smith, & Huettel, 2014). This network of areas is called default mode network and it has been showed to be usually deactivated during the task (Prata et al., 2012). The putamen has been previously linked to VF (Baldo et al., 2006) and consequently it was expected to be activated during the opposite contrast. The only association of right rolandic operculum, adjacent to the Broca's area, with VF tasks was a differential activation between boys and girls during a fMRI experiment, although its association with VF is still not clear (Soleman et al., 2013).

Furthermore, on the PPI analysis, I found a trend on the correlation of the left inferior frontal gyrus (seed region) with the right caudate nucleus and left superior temporal gyrus that is greater during word generation trials than during word repetition trials. The left inferior frontal gyrus and left superior temporal gyrus are positively correlated across all groups but their correlation is particularly strong in the SCZ patients group, as showed by Figure 3.10. Lesions on both inferior and temporal regions have been found to be associated with language dysfunctions (Baldo et al., 2006). Particularly in SCZ, the connectivity between the left inferior frontal gyrus and left superior temporal gyrus is dysfunctional, i.e., weaker when

compared to healthy controls, a finding that is not consistent with this work but reveals that the interaction between these two regions is abnormal in SCZ (Jeong, Wible, Hashimoto, & Kubicki, 2009).

On a sentence completion task, a recent study from Li et al. that used a PPI analysis revealed that the connectivity between the left superior temporal and frontal regions is greater between sentence completion and pseudo-sentence completion trials, a finding that is consistent with this work (Li et al., 2017). However, in another study that used a silent phonemic VF task, the left inferior frontal gyrus did not show task-modulated connectivity with the left superior temporal gyrus. The left inferior frontal gyrus was more correlated with the supplementary motor area, bilateral parietal lobule, thalamus and occipital areas during the onset of task block than during its end (La et al., 2016). Also, during an overt phonemic VF task, Boksman et al. found that the ACC is more connected with the left temporal lobe during word generation trials than during rest, suggesting that the temporal lobe during VF tasks is highly connected with task-related networks (Boksman et al., 2005). Although the connectivity between frontal and temporal regions during VF tasks is still not clear, both regions are consistently found to be associated with these tasks and specifically frontal regions are more associated with phonemic VF while temporal regions are more associated with semantic VF (Baldo et al., 2016). As for the right caudate nucleus, it was not correlated with the left inferior frontal gyrus on previous VF studies, though it has been reported to be activated during VF paradigms, suggesting that the basal ganglia structures are important for the VF performance (Fu et al., 2002; Fu et al., 2005; Thames et al., 2012).

A trend was also found on the connectivity between the left inferior frontal gyrus and right thalamus, left cuneus and left superior occipital gyrus that is greater during word repetition trials than during word generation trials, across all participants. This may suggest that these areas show an impaired connectivity with the frontal gyrus, that is overactivated during the task to compensate for the decreased connectivity with these regions, that were often showed to be associated with the VF task (Li et al., 2017; Prata, 2008), but surprisingly not on this study.

4.2 Effect of diagnosis

All results reported on this section were considered trends due to the fact that they were obtained at an uncorrected significance threshold of $p<0.001$. The task is associated with a greater activation of the right parahippocampal gyrus in SCZ when compared to controls and relatives analyzed separately, and additionally it is also associated with increased activation of the left middle temporal gyrus and right temporal pole of the superior temporal gyrus in SCZ when compared to controls. The increased activation of the parahippocampal gyrus was also present on SCZ relatively to BD, during the task. A plot of the contrasts estimates revealed that this area is highly positively correlated with the task on SCZ while it is negatively correlated with the task on the other groups. This increased activation the parahippocampal gyrus during a VF paradigm on SCZ has not been reported previously, although it has been reported on an emotional auditory paradigm, along with increased activation of other limbic region,

the amygdala. This effect was particular robust in SCZ patients with auditory hallucinations (Escartí et al., 2010).

On previous studies, the differential diagnostic group activations on VF task of SCZ compared to the other diagnostic groups, found at FWE corrected thresholds, were usually restricted to frontal regions, ACC and insula (Costafreda et al., 2011; Prata, 2008). These effects were not reproduced on this work, possibly due to the small group size of the SCZ group (n=10), which does not give power to find significant associations. Moreover, SCZ show a less pronounced impairment on phonemic fluency tasks when compared to semantic ones, so a great power would be reached if the task nature was semantic (Henry & Crawford, 2005).

On the contrast word generation > repetition BD group did not show a greater activation than controls and relatives. As for the cases where healthy groups activated more than patients groups, in all contrasts analyzed the regional brain activation was found in areas not covered by the AAL2 atlas. By visual inspection these areas were found to belong to white matter. Although it is widely known that fMRI signal can capture considerably better the BOLD signal on grey matter than on white matter, due to its increased cerebral blood volume and flow, there is not a clear evidence against regional activation on white matter (Gawryluk, Mazerolle, & D'Arcy, 2014). Additionally, the number of studies reporting white matter activation keeps rising. However, as this effect is still controversial and there are no reports of white matter activation during VF paradigms, it will be regarded as an artifactual result. As none of the activation regions did not pass the voxel-wise significance threshold, these effects may be considered false positives. In addition, on previous studies there were no areas more activated on healthy controls than on patient groups (Costafreda et al., 2011; Prata, 2008).

The trends found for the diagnosis-specific effect of the task on the connectivity of the seed revealed a positive effect of the task on the correlation of different regions with the interaction term, such as the left pallidum and left putamen in controls; the left postcentral, superior temporal, inferior frontal (pars opercularis) and precentral gyri in SCZ; the right putamen and left insula in relatives. This findings suggest that the task is associated with greater connectivity of the left inferior frontal gyrus with regions found to be associated with VF paradigms (left putamen, left superior temporal gyrus, right putamen and left insula) (Costafreda et al., 2011; Fu et al., 2005). The study of Boksman et al. was the only study found in literature to use a PPI analysis on a word fluency task with SCZ patients and healthy controls. The results may be considered consistent with their work as they also found an association between the seed (on their case, the ACC) and the left superior temporal gyrus, the left inferior frontal gyrus and precentral gyrus on the SCZ group, association that was greater during VF scans than during the baseline condition (Boksman et al., 2005). However, other areas that they reported did not pass the uncorrected significance threshold on this work. These regions include as the cingulate gyrus, the fusiform gyrus, occipital lobe and the cerebellum. The areas found to be negatively correlated with the left inferior frontal gyrus during the task were the left cuneus and the left superior occipital gyrus in SCZ and the right inferior frontal gyrus in BD.

The diagnostic group differences trends on the task-modulated connectivity were restricted to controls and SCZ groups: the left postcentral and precentral gyrus and a small portion of the left inferior frontal gyrus are more correlated with the interaction term in SCZ group than in controls; the left cuneus and superior and middle occipital gyrus are more correlated with the interaction term on controls than in SCZ. Boksman et al. only reported the regions where the activation was greater in SCZ than in controls and the only region that overlaps between the studies is the left inferior frontal gyrus. Moreover, they also found that the right thalamus, bilateral insula, right temporal gyrus, right fusiform gyrus and right inferior occipital gyrus are more correlated with the seed during word generation than baseline conditions, on SCZ than on controls (Boksman et al., 2005).

4.3 Effect of PRS

4.3.1 Main effect of PRS

The results for the main effect of PRS on brain activation were exclusively pointing on the negative direction, in contrast to the hypothesis defined initially. In fact, I found that the PRS is negatively associated with the activation of a network including the left inferior frontal gyrus, the left middle temporal gyrus, the bilateral insula, the right putamen, right thalamus and right caudate nucleus, areas that have all been previously associated with VF paradigms and showed to have a robust association with language processes (Baldo et al., 2006; Birn et al., 2010; Meinzer et al., 2009). It is also important to highlight that a reasonable proportion of brain regions activated by this contrast were localized on the white matter, an effect that as previously discussed is herein considered an artifact.

This finding suggests that PRS has an effect on task-modulated networks instead of have an effect on single regions not related with the task, as the study of Dima et al. proposes (Dima et al., 2016). The negative effect of PRS on brain activation might indicate that the subjects with increased risk for developing SCZ show decreased flexibility in the recruitment of neuronal resources during the word generation process.

Although the effects on the left inferior frontal gyrus and right insula are not considered statistical significant, as they have a voxel-wise threshold $p>0.05$ FWE corrected, the association between PRSs and these structures is interesting. These areas not only have been previously linked to VF paradigms, as they were additional found to be strongly associated with the task during this study. The insula, particularly its anterior region, is important for articulatory coordination of the speech (Dronkers, 1996). The left inferior frontal gyrus is associated with word recognition and processing on both semantic and phonemic VF tasks, as it is involved in processes related to the sound of words and its meaning (Fiez, 1997). Moreover, the left inferior frontal gyrus and the insula alterations have also been linked to SCZ. Namely, physiological alterations of the frontal structures on SCZ include an impairment in DLPFC activity and increased activity in other prefrontal areas, prefrontal cortex circuit dysfunction that results in an increased risk of suicidal thoughts, reductions in fractional anisotropy between the orbitofrontal cortex and the ACC, and so on (Mubarik & Tohid, 2016). Structural prefrontal changes have also been observed

in SCZ, as the frontal lobe volume is usually reduced. On the other hand, people with insula dysfunction show impaired emotional identification of faces and speech and difficulty in distinguishing external sensory inputs from self-generated information, deficits that observable on SCZ patients. Due to these effects, hallucinations on SCZ are thought to be a consequence of insular dysfunction (Wylie & Tregellas, 2010).

The hypothesis defined initially during this work was that the PRS would be associated with regions that are engaged during the task and regions that were found to be previously associated with SCZ-PRSs. SCZ-PRSs were found to be positively associated with the left DLPFC and the left inferior frontal gyrus (pars triangularis) on the first study of Walton et al. (Walton et al., 2012), positively associated with a region including the left DLPFC and VLPFC and other including the left frontal medial cortex (comprising the ACC) on the second study of the same group (Walton et al., 2013) and negatively associated with the activation of the right inferior frontal gyrus, middle and superior PFC and right middle temporal gyrus (Kauppi et al., 2014). It is important to notice that on the first two studies, the PRS is associated with the frontal regions during a working memory paradigm, on a positive direction, as hypothesized on this work, supporting the concept of SCZ inefficiency (i.e. an increased risk for SCZ is associated with an hyperactivation of brain areas, in order to recruit additional neuronal resources required to sustain a normal performance during the task). On the third study, however, the PRS is negatively correlated with the activation of frontal areas during a working memory paradigm; an effect that does not depend on task performance. These three studies indicate that PRS might be associated with hypo- or hyperactivation of frontal regions and that the direction of the association does not depend on the task, as working memory paradigms were always used. Moreover, frontal regions (such as inferior frontal gyrus and prefrontal cortex) seem to have a strong relationship with the SCZ-PRSs, highlighting the importance of frontal structures and its impairment in SCZ.

On the task-modulated connectivity analysis, no voxels survived the significance threshold of p=0,001 uncorrected for the main effect of PRS. Possibly, this was due to a lack of power of PRSs to produce effects on the connectivity between the left inferior frontal gyrus and other regions in the brain and lack of power of the PPI analysis. First, the p-value that was chosen to select the SNPs was the one associated with the optimal discrimination between cases and controls. Nevertheless, the PRSs only explained a very small proportion of the variance of the disease trait, 9.3% and only takes into account common variants, excluding the rare variants with large effect. Second, the lack of power of the PPI analysis is due to the fact that the interaction term and the time-series of the seed are two correlated vectors that might share some variance. Thus, the GLM model won't assign the variance to either, resulting in a small power to detect PPI effects (O'Reilly et al., 2012).

4.3.2 Diagnosis-specific effect of PRS

There were no positive effects of PRS on brain activation for each diagnostic group. There were, however, negative effects of PRS on brain activation across all groups. As for the results below the voxel-

wise p_{FWE} of 0,05, two corrected clusters were found on regions outside the parcellation areas defined by AAL2, in control group. This effect is considered artifactual as white matter activation is a controversial result, as discussed on section 4.2.

In controls, increasing PRS was correlated with a decreased activation of areas outside the AVOIs defined by AAL2, areas that were overlapping with the left inferior frontal gyrus, right cingulate and and left insula. In SCZ patients, an increasing PRS was correlated with activation of the right calcarine and the left middle temporal gyrus. In BD patients, there was an effect of PRS on the deactivation of a cluster incorporating right inferior frontal gyrus (pars orbitalis and triangularis). The clusters found in relatives reside in an area outside the regions identified by AAL2.

First, these results are against the initial hypothesis, as a greater effect of PRS was expected on the diseased groups and particularly in SCZ, due to the use of a specific PRS for this disorder and to the frequent presence of other genetic and environmental factors that make these patients more susceptible to cognitive impairments, thought to be captured by the PRS. The predominance of PRS effects on controls is indicated by the larger cluster sizes when compared to the other groups and the existence of FWE corrected regions. These results might be explained by the increased size of this group (n=39 participants versus n=10 for SCZ, n= 25 for BD and n=27 for relatives), which is associated with a greater power to detect effects. Also, as seen on the boxplot of the PRS on Figure 2.1, the PRSs on controls are distributed across a wider range than on the other groups, i.e., PRS is more spread out, possibly indicating that it can capture more effects on controls.

Second, another key point is that the brain regions where a diagnosis-specific effect of PRS was found have been previously linked to SCZ. This might suggest that the SCZ dysfunctions (as discussed on section 4.3.1), particularly the ones on the insula and left inferior frontal gyrus are heritable and present in individuals with increased risk, rather than being a secondary effect of the illness, as suggested by the greater effect of PRS on the brain activation in controls than in SCZ and/or BD (Whalley et al., 2014).

Third, the lack of power of the diseased groups might be associated with the heterogeneous manifestation of SCZ and BD. The etiology, symptoms and underlying mechanisms of these disorders may vary between individuals, and the genetic vulnerability explained by the score by itself might not capture the functional alterations across all patients.

The finding of the association of PRS with the right inferior frontal gyrus in BD is interesting, as this structure has been showed to be dysfunctional on BD. This structure is usually hypo- or hyperactivated in BD compared to healthy controls, depending on the patients mood state. Euthymic states are associated with hyperactivation of the right frontal gyrus while during a manic state BD patients show a hypoactivation of this region (Hajek , Alda, Hajek, & Ivanoff, 2013). Therefore, it is important to assess the patient's mood state at the time of acquisition, as this factor seems to be highly associated with the direction of the results.

The results for the diagnosis-specific effect of PRS on task-modulated connectivity are heterogeneous and difficult to interpret, as there are no studies on the literature analyzing this effect. In summary, I found that an increasing PRS is associated with greater connectivity of the left inferior frontal gyrus with the left angular gyrus (in BD) and the left thalamus, right lingual gyrus and right calcarine (in relatives), that is greater during word generation than repetition, and the opposite effect is present in SCZ on the cerebellar vermis and the right occipital gyrus.

The angular gyrus is a structure of the inferior parietal lobe that is involved complex language processes such as the semantic processing, reading and comprehension of words. It is seen as a visual memory center of language, mediating the written language with the spoken language and vice-versa (Seghier, 2013). The lingual gyrus is a structure that belongs to the visual cortex and seems to be associated with the identification of letters and words, contributing to language comprehension (Ghosh, Basu, Kumaran, & Khushu, 2010). The cerebellum is widely known as a structure that contributes to motor control, but it also has an important role in language as it is involved in word association (De Smet, Paquier, Verhoeven, & Mariën, 2013). Finally, the calcarine fissure does not seem to be associated with language or psychosis. Although the occipital structures in SCZ seem to be altered in terms of volume, grey and white matter, those variations don't include the area of the calcarine fissure and surrounding cortex (Tohid, Faizan, & Faizan, 2015).

4.3.3 Diagnosis x PRS interaction

Uncorrected effects for these contrasts on brain activation were found on the calcarine, right parahippocampal gyrus and right lingual gyrus. Additionally, it was also showed through the plot of the contrast estimates that the PRS is strongly associated with a negative activation of the right calcarine for SCZ and very a small positive activation (almost no relation) of this area on controls and BD groups. Although the parahippocampal and lingual gyri have been associated with SCZ symptoms or language functions, it seems that the calcarine fissure does not have any relation with SCZ or with the paradigm, as stated before.

As for the uncorrected results of the diagnosis x PRS interaction on the PPI analysis, associations on the cerebellum, on the right occipital gyrus, on the left thalamus, bilateral calcarine, bilateral lingual gyrus and right caudate nucleus were found – all areas, except the calcarine, are linked to VF paradigms or associated with language processes. From the results obtained, it seems that PRS has a greater effect on the healthy groups, when compared to SCZ, on the correlation of the cerebellum with the interaction term. Moreover, the PRS has a larger effect on relatives than on controls on the correlation of the interaction term with the left thalamus, bilateral calcarine and bilateral lingual gyrus.

4.4 Additional analyses

I did not find suprathreshold regions on spheres defined using the peak coordinates of the previous studies listed on Table 2.2, probably due to the fact that none has used the VF paradigm – as

seen, most areas associated with PRS were found to be associated with the task. As for the case where the search region was restricted to areas activated by the contrast word generation > repetition, two different regions of the contrast of the main effect of PRS on brain deactivation were found on the areas covered by the mask – although none has reached a corrected threshold. This indicates that effectively several areas that were found to be associated with the main effect of PRS are overlapping with areas associated with the task, such as the left inferior frontal gyrus and the left middle temporal gyrus.

More robust effects of PRS were obtained in the multiple regression model where the diagnosis factor was not taken into account, i.e., one region reached the significance threshold and the trends were associated with smaller p_{FWE} and larger cluster sizes. This indicates that PRS and diagnosis factor might share some variance which possibly reduces the power to detect effects of PRS on the full factorial ANOVAs used on the regional brain activation and connectivity analysis, has the shared variance is not assigned to either.

The task difficulty analysis revealed that there are no differences between the areas recruited by easy and hard trials during word generation > repetition and that the main effect of PRS does not differ for different difficulty levels. The only effect that was statistically different between the two difficulty levels was the effect of PRS on brain activation of the healthy control group, suggesting that the negative effect of PRS on the brain activation (of the left postcentral gyrus) of this group is driven by easy trials.

5. Conclusions and future works

5.1 Conclusions

The main goal of this work was to study the effect of PRS on brain function, during a VF paradigm, on a group of participants that included SCZ and BD patients, healthy controls and relatives. I found that PRS has a negative effect on brain activation between word generation and repetition on areas associated with the task, such as the left inferior frontal gyrus and the right insula. The negative association between PRS and brain activation was also found individually on all diagnostic groups. Particularly on healthy controls the effect of PRS was more pronounced, suggesting that PRS effect captures dysfunctions associated with genetic vulnerability, instead of dysfunctions associated with symptomatic phenotypes, but also possibly explained by the lower sample size in the patient groups.

The effect of PRS on task-modulated connectivity was also analyzed; although there are no main effects of PRS at an uncorrected level on the connectivity of the left inferior frontal gyrus (seed) with brain regions, trends were found for the diagnosis-specific effect of PRS on brain connectivity. Moreover, the findings suggest that an increasing PRS is associated with a more robust connectivity during task blocks than repetition blocks, of the seed with areas associated with the VF paradigm, namely the left angular gyrus (in BD), the left thalamus, the right lingual gyrus and right calcarine (in relatives). Also, an increasing PRS in SCZ is associated with reduced connectivity during task blocks than repetition blocks of the seed with the cerebellar vermis and the right occipital gyrus. There were no effects of PRS on the task-modulated connectivity in controls.

The results suggest that the PRSs calculated using several risk-variants for SCZ affect brain function and in particular regional brain activation during a VF paradigm, and that this effect more robust on healthy controls than on psychiatric patients.

5.2 Limitations and future works

Several limitations, present in this study, may be associated with the presence of false positives and false negatives on the statistical images and lack of powerful results. False positives, also called type I errors, appear when the null hypothesis is rejected incorrectly, which often happens when an uncorrected p-value for multiple comparisons is used. In this work, as the uncorrected thresholds used were set to 0.001, 0.1% is the probability of rejecting the null hypothesis given that it is true. False negatives are associated with the failure to reject the null hypothesis when it is false and it is related with the power of a test.

First, functional images were acquired on a MRI scanner with a field strength of 1.5T, which produces images with a lower resolution than nowadays research standard. Thus, at this field strength, the fMRI images have an intrinsic low signal-to-noise ratio (SNR) (Edelstein, Glover, Hardy & Redington, 1986) and low BOLD contrast, as the magnetic susceptibility difference between dHB and HB is not so

pronounced (Turner et al., 1993). On future studies, a MRI scanner with increased field strength (at least 3T) should be used to acquire the images.

Also, the large voxel size ($3.75 \times 3,75 \times 8mm^3$) combined with a large smoothing kernel (8mm full-width at half maximum Gaussian) leads to marked partial volume effects, where the boundaries of different structures are averaged on a single voxel, resulting on an inaccurate signal intensity and an insuficient spatial resolution, compromising the spatial location of effects on detailed structures. Additionally, the signal of a particular voxel might be spread across neighboring voxels – in particular, the grey matter structures signal can reach the white matter, which could explain the findings localized on white matter. However, the large smoothing kernel applied on the functional scans is recommended on images with worse resolution, as it helps increasing the SNR and results on a normalized distributed error on GLM.

The error term on GLM is assumed to be normally distributed, however this is frequently not the case: data can show significant temporal correlations that are due to physiological noise (Weisskoff et al., 1993). Physiological noise can arise from metabolic and hemodynamic fluctuations, due to breathing and heartbeat.

Some preprocessing steps may affect the anatomical localization of several structures, mainly coregistration and spatial normalization, although I have applied quality control procedures to verify the accuracy of these methods, I only managed to visually analyze images from 3 randomly selected participants. An additional analysis without the coregistration of the functional images to the structural space could be done in the future to better understand the effects of this step on regional brain activation.

The addition of motion parameters to the single-level analysis is also questionable (Bright & Murphy, 2015). A study from Jonhstone et al. concluded that the inclusion of these nuisance covariates may decrease the sensitivity to detect activations (Johnstone et al., 2006). Thus, there is a trade-off between sensitivity and the removal of motion artifacts. I have also performed an analysis where the motion parameters were not include, although the results were not showed. The absence of motion parameters as covariates was associated with larger clusters but less significance, thus I decided to exclude this analysis from the main findings.

In terms of power, the sample size in the SCZ patient group is less than the recommended number of 20 participants for fMRI analysis (Thirion et al., 2007). Therefore, any comparisons involving this group might have resulted in false positives due to sampling bias, or false negatives due to lack of power to detect a true effect, explaining the lack of significant effects of PRS on brain activation and connectivity on this group.

The treatment with different antipsychotics or antidepressants and their dosage might also affect the performance of the participants. Ideally, it should be possible to control for the type of medication and dosage, by selecting individuals that receive the same treatment. Another solution would be to

include the dosage and type treatment as covariates of no interest on the group-level model. Additionally, the assessment of BD participants' mood state and measures of SCZ patients' positive and negative symptoms should be included on the group-level analysis, as the intermediated phenotypes they reveal during fMRI experiments is dependent on these factors.

Other factors with impact on brain activation and connectivity are the environmental and neurodevelopmental factors, since they contribute to the onset of the psychotic disorders and their cognitive functioning. High-genetic-risk participants might not show cognitive dysfunction due to the absence of other non-genetic risk factors. Thus, the interaction between the genetic and environmental factors should be assessed and included in the model.

In this work, the effect of PRS on brain function was studied. It would also be interesting to understand if the PRS has an effect on structural phenotypes and if the effect is in concordance with the studies listed on Table 1.1. Structural phenotypes could be total brain volume, white matter volume or cortical thickness.

The PRSs used were obtained at a p_T<0.1, as it was associated with the greatest proportion of variance. It is possible that among the PRS genetic risk variants there are some originally carrying a false positive effect, as they were selected using a non-stringent threshold, and thus might be adding noise to the PRS and masquerading the true effect of other variants. Moreover, in the future, the p-values obtained at different thresholds should also be used in a new analysis to understand if, as assumed, the larger proportion of variance is reflected in more significant results, and to analyze the influence of the false-positive rate on the final results.

The results reported here can only be validated after replication on an independent sample. Therefore, future imaging genetic studies with larger samples should be conducted to disentangle the complex relationship between the psychiatric genetic risk and the endophenotypes revealed by the participants during cognitive tasks. This would be essential to understand the link between genetic risk factors and the neurobiological mechanisms associated with the development of disorders of the psychosis spectrum.

References

American Psychiatric Association. (1994). *Diagnostic and statistical manual of mental disorders* (4th ed.). Washington, DC: Author.

American Psychiatric Association. (2013). *Diagnostic and statistical manual of mental disorders* (5th ed.). Washington, DC: Author.

Ashburner, J. (2009). Computational anatomy with the SPM software. *Magnetic resonance imaging*, *27*(8), 1163-1174.

Ashburner, J., & Friston, K. J. (2005). Unified segmentation. *Neuroimage*, *26*(3), 839-851.

Baldo, J. V., Schwartz, S., Wilkins, D., & Dronkers, N. F. (2006). Role of frontal versus temporal cortex in verbal fluency as revealed by voxel-based lesion symptom mapping. *Journal of the international neuropsychological society*, *12*(6), 896-900.

Birn, R. M., Kenworthy, L., Case, L., Caravella, R., Jones, T. B., Bandettini, P. A., & Martin, A. (2010). Neural systems supporting lexical search guided by letter and semantic category cues: a self-paced overt response fMRI study of verbal fluency. *Neuroimage*, *49*(1), 1099-1107.

Boksman, K., Théberge, J., Williamson, P., Drost, D. J., Malla, A., Densmore, M., ... & Neufeld, R. W. (2005). A 4.0-T fMRI study of brain connectivity during word fluency in first-episode schizophrenia. *Schizophrenia research*, *75*(2), 247-263.

Bright, M. G., & Murphy, K. (2015). Is fMRI "noise" really noise? Resting state nuisance regressors remove variance with network structure. *NeuroImage*, *114*, 158-169.

Buxton, R. B. (2001). The elusive initial dip. *Neuroimage*, *13*(6), 953-958.

Callicott, J. H., Bertolino, A., Mattay, V. S., Langheim, F. J., Duyn, J., Coppola, R., ... & Weinberger, D. R. (2000). Physiological dysfunction of the dorsolateral prefrontal cortex in schizophrenia revisited. *Cerebral cortex*, *10*(11), 1078-1092.

Cannon, T. D., Kaprio, J., Lönnqvist, J., Huttunen, M., & Koskenvuo, M. (1998). The genetic epidemiology of schizophrenia in a Finnish twin cohort: a population-based modeling study. *Archives of general psychiatry*, *55*(1), 67-74.

Chang, C. C., Chow, C. C., Tellier, L. C., Vattikuti, S., Purcell, S. M., & Lee, J. J. (2015). Second-generation PLINK: rising to the challenge of larger and richer datasets. Gigascience, *4*(1), 1-16.

Chernick, M. R., & Friis, R. H. (2003). *Introductory Biostatistics for the Health Sciences: Modern Applications Including Bootstrap*. Hoboken, NJ: Wiley-Interscience.

Collignon, A., Maes, F., Delaere, D., Vandermeulen, D., Suetens, P., & Marchal, G. (1995). Automated multi-modality image registration based on information theory. In *Information processing in medical imaging*, *3*(6), 263-274.

Cosgrove, D., Harold, D., Mothersill, O., Anney, R., Hill, M. J., Bray, N. J., ... & Owen, M. (2017). MiR-137-derived polygenic risk: effects on cognitive performance in patients with schizophrenia and controls. *Translational psychiatry*, *7*(1), 1012.

Costafreda, S. G., David, A. S., & Brammer, M. J. (2009). A parametric approach to voxel-based meta-analysis. *Neuroimage*, *46*(1), 115-122.

Costafreda, S. G., Fu, C. H., Lee, L., Everitt, B., Brammer, M. J., & David, A. S. (2006). A systematic review and quantitative appraisal of fMRI studies of verbal fluency: role of the left inferior frontal gyrus. *Human brain mapping*, *27*(10), 799-810.

Costafreda, S. G., Fu, C. H., Picchioni, M., Toulopoulou, T., McDonald, C., Kravariti, E., ... & McGuire, P. K. (2011). Pattern of neural responses to verbal fluency shows diagnostic specificity for schizophrenia and bipolar disorder. *BMC psychiatry*, *11*(1), 18.

Craddock, N., & Jones, I. (1999). Genetics of bipolar disorder. *Journal of medical genetics*, *36*(8), 585-594.

Craddock, N., & Owen, M. J. (2005). The beginning of the end for the Kraepelinian dichotomy. *The British journal of psychiatry,* 186(5) 364-366.

Craddock, N., & Sklar, P. (2009). Genetics of bipolar disorder: successful start to a long journey. *Trends in genetics*, *25*(2), 99-105.

Craddock, N., & Sklar, P. (2013). Genetics of bipolar disorder. *The Lancet*, *381*(9878), 1654-1662.

Curtis, V. A., Bullmore, E. T., Brammer, M. J., Wright, I. C., Williams, S. C., Morris, R. G., ... & McGuire, P. K. (1998). Attenuated frontal activation during a verbal fluency task in patients with schizophrenia. *American journal of psychiatry*, *155*(8), 1056-1063.

De Smet, H. J., Paquier, P., Verhoeven, J., & Mariën, P. (2013). The cerebellum: its role in language and related cognitive and affective functions. *Brain and language*, *127*(3), 334-342.

Dima, D., de Jong, S., Breen, G., & Frangou, S. (2016). The polygenic risk for bipolar disorder influences brain regional function relating to visual and default state processing of emotional information. *Neuroimage: clinical*, *12*, 838-844.

Dronkers, N. F. (1996). A new brain region for coordinating speech articulation. *Nature*, *384*(6605), 159-161,

Edelstein, W. A., Glover, G. H., Hardy, C. J., & Redington, R. W. (1986). The intrinsic signal-to-noise ratio in NMR imaging. *Magnetic resonance in medicine*, *3*(4), 604-618.

Escartí, M. J., de la Iglesia-Vayá, M., Martí-Bonmatí, L., Robles, M., Carbonell, J., Lull, J. J., ... & Sanjuán, J. (2010). Increased amygdala and parahippocampal gyrus activation in schizophrenic patients with auditory hallucinations: an fMRI study using independent component analysis. *Schizophrenia research*, *117*(1), 31-41.

Euesden, J., Lewis, C. M., & O'Reilly, P. F. (2014). PRSice: polygenic risk score software. Bioinformatics, 31(9), 1466-1468.

Fiez, J. A. (1997). Phonology, semantics, and the role of the left inferior prefrontal cortex. *Human brain mapping*, 5(2), 79-83.

Fox, P. T., Raichle, M. E., Mintun, M. A., & Dence, C. (1988). Nonoxidative glucose consumption during focal physiologic neural activity. *Science*, *241*(4864), 462-464.

Freedman, R. (2003). Schizophrenia. *The new England journal of medicine,* 349(18), 1738-1749.

Friston, K. J. (2005). Models of brain function in neuroimaging. *Annual review of psychology*, *56*, 57-87.

Friston, K. J., Buechel, C., Fink, G. R., Morris, J., Rolls, E., & Dolan, R. J. (1997). Psychophysiological and modulatory interactions in neuroimaging. *Neuroimage*, *6*(3), 218-229.

Friston, K. J., Fletcher, P., Josephs, O., Holmes, A., Rugg, M. D., & Turner, R. (1998). Event-related fMRI: characterizing differential responses. *Neuroimage*, *7*(1), 30-40.

Friston, K. J., Frith, C. D., Liddle, P. F., & Frackowiak, R. S. J. (1991). Comparing functional (PET) images: the assessment of significant change. *Journal of cerebral blood flow & metabolism*, *11*(4), 690-699.

Friston, K. J., Frith, C. D., Liddle, P. F., & Frackowiak, R. S. J. (1993). Functional connectivity: the principal-component analysis of large (PET) data sets. *Journal of cerebral blood flow & metabolism*, *13*(1), 5-14.

Friston, K. J., Frith, C. D., & Frackowiak, R. S. J. (1993). Time-dependent changes in effective connectivity measured with PET. *Human brain mapping*, *1*(1), 69-79.

Friston, K. J., Holmes, A. P., Worsley, K. J., Poline, J. P., Frith, C. D., & Frackowiak, R. S. (1995). Statistical parametric maps in functional imaging: a general linear approach. *Human brain mapping*, *2*(4), 189-210.

Fu, C. H., Morgan, K., Suckling, J., Williams, S. C., Andrew, C., Vythelingum, G. N., & McGuire, P. K. (2002). A functional magnetic resonance imaging study of overt letter verbal fluency using a clustered acquisition sequence: greater anterior cingulate activation with increased task demand. *Neuroimage*, *17*(2), 871-879.

Fu, C. H., Suckling, J., Williams, S. C., Andrew, C. M., Vythelingum, G. N., & McGuire, P. K. (2005). Effects of psychotic state and task demand on prefrontal function in schizophrenia: an fMRI study of overt verbal fluency. *American journal of psychiatry*, *162*(3), 485-494.

Gawryluk, J. R., Mazerolle, E. L., & D'Arcy, R. C. (2014). Does functional MRI detect activation in white matter? A review of emerging evidence, issues, and future directions. *Frontiers in neuroscience*, *8*, e239.

Gejman, P. V., Sanders, A. R., & Kendler, K. S. (2011). Genetics of schizophrenia: new findings and challenges. *Annual review of genomics and human genetics*, *12*, 121-144.

Ghosh, S., Basu, A., Kumaran, S. S., & Khushu, S. (2010). Functional mapping of language networks in the normal brain using a word-association task. *The Indian journal of radiology & imaging*, *20*(3), 182-187.

Gitelman, D. R., Penny, W. D., Ashburner, J., & Friston, K. J. (2003). Modeling regional and psychophysiologic interactions in fMRI: the importance of hemodynamic deconvolution. *Neuroimage*, *19*(1), 200-207.

Goodwin, F. K., & Jamison, K. R. (2007). *Manic-depressive illness: bipolar disorders and recurrent depression*. New York, NY: Oxford University Press.

Gottesman, I. I., & Gould, T. D. (2003). The endophenotype concept in psychiatry: etymology and strategic intentions. *American journal of psychiatry*, *160*(4), 636-645.

Grande, I., Berk, M., Birmaher, B., & Vieta, E. (2016). Bipolar disorder. *The Lancet*, *387*(10027), 1561-1572.

Gregory, M. L., Burton, V. J., & Shapiro, B. K. (2015). *Neurobiology of brain disorders: biological basis of neurological and psychiatric disorders*. London. Elsevier Inc.

Gurung, R., & Prata, D. P. (2015). What is the impact of genome-wide supported risk variants for schizophrenia and bipolar disorder on brain structure and function? A systematic review. *Psychological medicine*, *45*(12), 2461-2480.

Hajek, T., Alda, M., Hajek, E., & Ivanoff, J. (2013). Functional neuroanatomy of response inhibition in bipolar disorders–combined voxel based and cognitive performance meta-analysis. *Journal of psychiatric research*, *47*(12), 1955-1966.

Handwerker, D. A., Ollinger, J. M., & D'Esposito, M. (2004). Variation of BOLD hemodynamic responses across subjects and brain regions and their effects on statistical analyses. *Neuroimage*, *21*(4), 1639-1651.

Harrisberger, F., Smieskova, R., Vogler, C., Egli, T., Schmidt, A., Lenz, C., ... & Borgwardt, S. (2016). Impact of polygenic schizophrenia-related risk and hippocampal volumes on the onset of psychosis. *Translational psychiatry*, *6*(8), e868.

Hashimoto, R., Ohi, K., Yamamori, H., Yasuda, Y., Fujimoto, M., Umeda-Yano, S., ... & Takeda, M. (2015). Imaging genetics and psychiatric disorders. *Current molecular medicine*, *15*(2), 168-175.

Heckers, S., Barch, D. M., Bustillo, J., Gaebel, W., Gur, R., Malaspina, D., ... & Van Os, J. (2016). Structure of the Psychotic Disorders Classification in DSM-5. *Focus*, *14*(3), 366-369.

Henriksen, M. G., Nordgaard, J., & Jansson, L. B. (2017). Genetics of Schizophrenia: Overview of Methods, Findings and Limitations. *Frontiers in human neuroscience*, *11*, e322.

Henry, J., & Crawford, J. (2005). A meta-analytic review of verbal fluency deficits in schizophrenia relative to other neurocognitive deficits. *Cognitive neuropsychiatry*, *10*(1), 1-33.

Hudson, J. I., Javaras, K. N., Laird, N. M., VanderWeele, T. J., Pope Jr, H. G., & Hernán, M. A. (2008). A structural approach to the familial coaggregation of disorders. *Epidemiology*, *19*(3), 431-439.

International Schizophrenia Consortium (2009). Common polygenic variation contributes to risk of schizophrenia that overlaps with bipolar disorder. *Nature*, *460*(7256), 748-752.

Jeong, B., Wible, C. G., Hashimoto, R. I., & Kubicki, M. (2009). Functional and anatomical connectivity abnormalities in left inferior frontal gyrus in schizophrenia. *Human brain mapping*, *30*(12), 4138-4151.

Johnstone, T., Ores Walsh, K. S., Greischar, L. L., Alexander, A. L., Fox, A. S., Davidson, R. J., & Oakes, T. R. (2006). Motion correction and the use of motion covariates in multiple-subject fMRI analysis. *Human brain mapping*, *27*(10), 779-788.

Kauppi, K., Westlye, L. T., Tesli, M., Bettella, F., Brandt, C. L., Mattingsdal, M., ... & Djurovic, S. (2014). Polygenic risk for schizophrenia associated with working memory-related prefrontal brain activation in patients with schizophrenia and healthy controls. *Schizophrenia bulletin*, *41*(3), 736-743.

Keefe, R. S., Silva, S. G., Perkins, D. O., & Lieberman, J. A. (1999). The effects of atypical antipsychotic drugs on neurocognitive impairment in schizophrenia: a review and meta-analysis. *Schizophrenia bulletin*, *25*(2), 201-222.

Keshavan, M. S., Morris, D. W., Sweeney, J. A., Pearlson, G., Thaker, G., Seidman, L. J., ... & Tamminga, C. (2011). A dimensional approach to the psychosis spectrum between bipolar disorder and schizophrenia: the Schizo-Bipolar Scale. *Schizophrenia research*, *133*(1), 250-254.

Kim, D., Kim, J., Koo, T., Yun, H., & Won, S. (2015). Shared and distinct neurocognitive endophenotypes of schizophrenia and psychotic bipolar disorder. *Clinical psychopharmacology and neuroscience*, *13*(1), 94-102.

Krabbendam, L., Arts, B., van Os, J., & Aleman, A. (2005). Cognitive functioning in patients with schizophrenia and bipolar disorder: a quantitative review. *Schizophrenia research*, *80*(2), 137-149.

Kraepelin, E. (1896). *Textbook of Psychiatry*.

Krug, A., Nieratschker, V., Markov, V., Krach, S., Jansen, A., Zerres, K., ... & Mühleisen, T. W. (2010). Effect of CACNA1C rs1006737 on neural correlates of verbal fluency in healthy individuals. *Neuroimage*, *49*(2), 1831-1836.

La, C., Garcia-Ramos, C., Nair, V. A., Meier, T. B., Farrar-Edwards, D., Birn, R., ... & Prabhakaran, V. (2016). Age-Related Changes in BOLD Activation Pattern in Phonemic Fluency Paradigm: An Investigation of Activation, Functional Connectivity and Psychophysiological Interactions. *Frontiers in aging neuroscience*, *8*, e110.

Lancaster, T. M., Ihssen, N., Brindley, L. M., Tansey, K. E., Mantripragada, K., O'donovan, M. C., ... & Linden, D. E. (2016a). Associations between polygenic risk for schizophrenia and brain function during probabilistic learning in healthy individuals. *Human brain mapping*, *37*(2), 491-500.

Lancaster, T. M., Linden, D. E., Tansey, K. E., Banaschewski, T., Bokde, A. L., Bromberg, U., ... & Frouin, V. (2016b). Polygenic risk of psychosis and ventral striatal activation during reward processing in healthy adolescents. *JAMA psychiatry*, *73*(8), 852-861.

Lewis, C. M., Levinson, D. F., Wise, L. H., DeLisi, L. E., Straub, R. E., Hovatta, I., ... & Brzustowicz, L. M. (2003). Genome scan meta-analysis of schizophrenia and bipolar disorder, part II: Schizophrenia. *the american journal of human genetics*, *73*(1), 34-48.

Li, X., Branch, C. A., & DeLisi, L. E. (2009). Language pathway abnormalities in schizophrenia: a review of fMRI and other imaging studies. *Current opinion in psychiatry*, *22*(2), 131-139.

Li, Y., Li, P., Yang, Q. X., Eslinger, P. J., Sica, C. T., & Karunanayaka, P. (2017). Lexical-Semantic Search Under Different Covert Verbal Fluency Tasks: An fMRI Study. *Frontiers in behavioral neuroscience*, *11*, e131.

Lindquist, M. A., Loh, J. M., Atlas, L. Y., & Wager, T. D. (2009). Modeling the hemodynamic response function in fMRI: efficiency, bias and mis-modeling. *Neuroimage*, *45*(1), S187-S198.

Logothetis, N. K., Pauls, J., Augath, M., Trinath, T., & Oeltermann, A. (2001). Neurophysiological investigation of the basis of the fMRI signal. *Nature*, *412*(6843), 150-157.

Lurito, J. T., Kareken, D. A., Lowe, M. J., Chen, S. H. A., & Mathews, V. P. (2000). Comparison of rhyming and word generation with FMRI. *Human brain mapping*, *10*(3), 99-106.

Markov, V., Krug, A., Krach, S., Whitney, C., Eggermann, T., Zerres, K., ... & Rietschel, M. (2009). Genetic variation in schizophrenia-risk-gene dysbindin 1 modulates brain activation in anterior cingulate cortex and right temporal gyrus during language production in healthy individuals. *Neuroimage*, *47*(4), 2016-2022.

Matsuo, K., Watanabe, A., Onodera, Y., Kato, N., & Kato, T. (2004). Prefrontal hemodynamic response to verbal-fluency task and hyperventilation in bipolar disorder measured by multi-channel near-infrared spectroscopy. *Journal of affective disorders*, *82*(1), 85-92.

Mechelli, A., Fusar-Poli, P., Prata, D., Papagni, S. A., Tognin, S., Kambeitz, J., ... & Bramon, E. (2012). Genetic vulnerability to psychosis and cortical function: epistatic effects between DAAO and G72. *Current pharmaceutical design*, *18*(4), 510-517.

Mechelli, A., Prata, D. P., Fu, C. H., Picchioni, M., Kane, F., Kalidindi, S., ... & Murray, R. (2008). The effects of neuregulin1 on brain function in controls and patients with schizophrenia and bipolar disorder. *Neuroimage*, *42*(2), 817-826.

Meinzer, M., Flaisch, T., Wilser, L., Eulitz, C., Rockstroh, B., Conway, T., ... & Crosson, B. (2009). Neural signatures of semantic and phonemic fluency in young and old adults. *Journal of cognitive neuroscience*, *21*(10), 2007-2018.

Millier, A., Schmidt, U., Angermeyer, M. C., Chauhan, D., Murthy, V., Toumi, M., & Cadi-Soussi, N. (2014). Humanistic burden in schizophrenia: a literature review. *Journal of psychiatric research*, *54*, 85-93.

Moore, D. J., Savla, G. N., Woods, S. P., Jeste, D. V., & Palmer, B. W. (2006). Verbal fluency impairments among middle-aged and older outpatients with schizophrenia are characterized by deficient switching. *Schizophrenia research*, *87*(1), 254-260.

Mubarik, A., & Tohid, H. (2016). Frontal lobe alterations in schizophrenia: a review. *Trends in psychiatry and psychotherapy*, *38*(4), 198-206.

Muñoz, M. K. E., Hyde, M. L. W., & Hariri, A. R. (2009). Imaging genetics. *Journal of the American academy of child and adolescent psychiatry*, *48*(4), 356.

Neill, E., Gurvich, C., & Rossell, S. L. (2014). Category fluency in schizophrenia research: Is it an executive or semantic measure? *Cognitive neuropsychiatry*, *19*(1), 81-95.

Neilson, E., Bois, C., Gibson, J., Duff, B., Watson, A., Roberts, N., ... & Whalley, H. C. (2017). Effects of environmental risks and polygenic loading for schizophrenia on cortical thickness. *Schizophrenia research*, *184*, 128-136.

Nelson, H. E., & Willison, J. R. (1991). The revised national adult reading test–test manual. Windsor, UK*:* *NFER-Nelson*.

Netter, F. H. (2006). *Atlas of Human Anatomy*. 4th ed. Philadelphia, PA*:* Saunders Elsevier.

Ng, M. Y., Levinson, D. F., Faraone, S. V., Suárez, B. K., DeLisi, L. E., Arinami, T., ... & Pulver, A. E. (2009). Meta-analysis of 32 genome-wide linkage studies of schizophrenia. *Molecular psychiatry*, *14*(8), 774-785.

Nishimura, Y., Takahashi, K., Ohtani, T., Ikeda-Sugita, R., Kasai, K., & Okazaki, Y. (2014). Dorsolateral prefrontal hemodynamic responses during a verbal fluency task in hypomanic bipolar disorder. *Bipolar disorders*, *17*(2), 172-183.

Noll, R. (2009). *The encyclopedia of schizophrenia and other psychotic disorders*. New York, NY: Infobase Publishing.

Oertel-Knöchel, V., Lancaster, T. M., Knöchel, C., Stäblein, M., Storchak, H., Reinke, B., ... & Tansey, K. E. (2015). Schizophrenia risk variants modulate white matter volume across the psychosis spectrum: evidence from two independent cohorts. *NeuroImage: clinical*, *7*, 764-770.

Ogawa, S., Lee, T. M., Kay, A. R., & Tank, D. W. (1990). Brain magnetic resonance imaging with contrast dependent on blood oxygenation. *Proceedings of the national academy of sciences*, *87*(24), 9868-9872.

O'Reilly, J. X., Woolrich, M. W., Behrens, T. E., Smith, S. M., & Johansen-Berg, H. (2012). Tools of the trade: psychophysiological interactions and functional connectivity. *Social cognitive and affective neuroscience*, *7*(5), 604-609.

Owen M., Sawa A., Mortensen P. (2016) Schizophrenia. *The Lancet*, 388(10039), 86-97.

Papiol, S., Mitjans, M., Assogna, F., Piras, F., Hammer, C., Caltagirone, C., ... & Spalletta, G. (2014). Polygenic determinants of white matter volume derived from GWAS lack reproducibility in a replicate sample. *Translational psychiatry*, *4*(2), e362.

Pauling, L., & Coryell, C. D. (1936). The magnetic properties and structure of hemoglobin, oxyhemoglobin and carbonmonoxyhemoglobin. *Proceedings of the national academy of sciences*, *22*(4), 210-216.

Perälä, J., Suvisaari, J., Saarni, S. I., Kuoppasalmi, K., Isometsä, E., Pirkola, S., ... & Härkänen, T. (2007). Lifetime prevalence of psychotic and bipolar I disorders in a general population. *Archives of general psychiatry*, *64*(1), 19-28.

Phelps, E. A., Hyder, F., Blamire, A. M., & Shulman, R. G. (1997). FMRI of the prefrontal cortex during overt verbal fluency. *Neuroreport*, *8*(2), 561-565.

Pouget, J. G., & Müller, D. J. (2014). Pharmacogenetics of antipsychotic treatment in schizophrenia. *Pharmacogenomics in drug discovery and development*, 557-587.

Prata, D. (2008). *Effect of dopamine regulating genes on regional brain function during verbal fluency in healthy individuals and in patients with schizophrenia* (Doctoral dissertation, University of London, King's College London, Institute of Psychiatry).

Prata, D. P., Papagni, S. A., Mechelli, A., Fu, C. H., Kambeitz, J., Picchioni, M., ... & Toulopoulou, T. (2012). Effect of D-amino acid oxidase activator (DAOA; G72) on brain function during verbal fluency. *Human brain mapping*, *33*(1), 143-153.

Psychiatric GWAS Consortium Bipolar Disorder Working Group. (2011). Large-scale genome-wide association analysis of bipolar disorder identifies a new susceptibility locus near ODZ4. *Nature genetics*, *43*(10), 977-983.

Ramnani, N., Behrens, T. E., Penny, W., & Matthews, P. M. (2004). New approaches for exploring anatomical and functional connectivity in the human brain. *Biological psychiatry*, *56*(9), 613-619.

Raucher-Chéné, D., Achim, A. M., Kaladjian, A., & Besche-Richard, C. (2017). Verbal fluency in bipolar disorders: A systematic review and meta-analysis. *Journal of affective disorders*, *207*, 359-366.

Ripke, S., O'Dushlaine, C., Chambert, K., Moran, J. L., Kähler, A. K., Akterin, S., ... & Kim, Y. (2013). Genome-wide association analysis identifies 13 new risk loci for schizophrenia. *Nature genetics*, *45*(10), 1150-1159.

Robert, P. H., Lafont, V., Medecin, I., Berthet, L., Thauby, S., Baudu, C., & Darcourt, G. U. Y. (1998). Clustering and switching strategies in verbal fluency tasks: comparison between schizophrenics and healthy adults. *Journal of the international neuropsychological society*, *4*(6), 539-546.

Rolls, E. T., Joliot, M., & Tzourio-Mazoyer, N. (2015). Implementation of a new parcellation of the orbitofrontal cortex in the automated anatomical labeling atlas. *Neuroimage*, *122*, 1-5.

Schizophrenia Psychiatric Genome-Wide Association Study (GWAS) Consortium. (2011). Genome-wide association study identifies five new schizophrenia loci. *Nature genetics*, *43*(10), 969-976.

Schizophrenia Working Group of the Psychiatric Genomics Consortium, Ripke, S., Neale, B. M., Corvin, A., Walters, J. T., Farh, K.-H., … O'Donovan, M. C. (2014). Biological insights from 108 schizophrenia-associated genetic loci. *Nature*, 511(7510), 421–427.

Seghier, M. L. (2013). The angular gyrus: multiple functions and multiple subdivisions. *The Neuroscientist*, *19*(1), 43-61.

Smee, C., Krabbendam, L., O'Daly, O., Prins, A. M., Nalesnik, N., Morley, L., ... & Shergill, S. (2011). An fMRI study of prefrontal dysfunction and symptomatic recovery in schizophrenia. *Acta psychiatrica scandinavica*, *123*(6), 440-450.

Soleman, R. S., Schagen, S. E., Veltman, D. J., Kreukels, B. P., Cohen-Kettenis, P. T., Lambalk, C. B., ... & Delemarre-van de Waal, H. A. (2013). Sex differences in verbal fluency during adolescence: a functional magnetic resonance imaging study in gender dysphoric and control boys and girls. *The journal of sexual medicine*, *10*(8), 1969-1977.

Sung, K., Gordon, B., Vannorsdall, T. D., Ledoux, K., Pickett, E. J., Pearlson, G. D., & Schretlen, D. J. (2012). Semantic clustering of category fluency in schizophrenia examined with singular value decomposition. *Journal of the international neuropsychological society*, *18*(3), 565-575.

Terwisscha van Scheltinga, A. F., Bakker, S. C., van Haren, N. E., Derks, E. M., Buizer-Voskamp, J. E., Boos, H. B., ... & Kahn, R. S. (2013). Genetic schizophrenia risk variants jointly modulate total brain and white matter volume. *Biological psychiatry*, *73*(6), 525-531.

Tesli, M., Kauppi, K., Bettella, F., Brandt, C. L., Kaufmann, T., Espeseth, T., ... & Westlye, L. T. (2015). Altered brain activation during emotional face processing in relation to both diagnosis and polygenic risk of bipolar disorder. *PloS one*, *10*(7), e0134202.

Thames, A. D., Foley, J. M., Wright, M. J., Panos, S. E., Ettenhofer, M., Ramezani, A., ... & Hinkin, C. H. (2012). Basal ganglia structures differentially contribute to verbal fluency: evidence from Human Immunodeficiency Virus (HIV)-infected adults. *Neuropsychologia*, *50*(3), 390-395.

Thirion, B., Pinel, P., Mériaux, S., Roche, A., Dehaene, S., & Poline, J. B. (2007). Analysis of a large fMRI cohort: Statistical and methodological issues for group analyses. *Neuroimage*, *35*(1), 105-120.

Thomas, D. (2010). Gene-environment-wide association studies: emerging approaches. *Nature reviews. Genetics*, *11*(4), 259-272.

Thulborn, K. R., Waterton, J. C., Matthews, P. M., & Radda, G. K. (1982). Oxygenation dependence of the transverse relaxation time of water protons in whole blood at high field. *Biochimica et biophysica acta – general subjects, 714*(2), 265-270.

Tohid, H., Faizan, M., & Faizan, U. (2015). Alterations of the occipital lobe in schizophrenia. *Neurosciences*, *20*(3), 213-224.

Turner, R., Jezzard, P., Wen, H., Kwong, K. K., Le Bihan, D., Zeffiro, T., & Balaban, R. S. (1993). Functional mapping of the human visual cortex at 4 and 1.5 Tesla using deoxygenation contrast EPI. *Magnetic resonance in medicine*, *29*(2), 277-279.

Tyburski, E., Sokołowski, A., Chęć, M., Pełka-Wysiecka, J., & Samochowiec, A. (2015). Neuropsychological characteristics of verbal and non-verbal fluency in schizophrenia patients. *Archives of psychiatric nursing*, *29*(1), 33-38.

Utevsky, A. V., Smith, D. V., & Huettel, S. A. (2014). Precuneus is a functional core of the default-mode network. *Journal of neuroscience*, *34*(3), 932-940.

Van Snellenberg, J. X., & de Candia, T. (2009). Meta-analytic evidence for familial coaggregation of schizophrenia and bipolar disorder. *Archives of general psychiatry*, *66*(7), 748-755.

Vassos, E., Di Forti, M., Coleman, J., Iyegbe, C., Prata, D., Euesden, J., ... & Newhouse, S. (2016). An examination of polygenic score risk prediction in individuals with first-episode psychosis. *Biological psychiatry*, *81*(6), 470-477.

Vöhringer, P. A., Barroilhet, S. A., Amerio, A., Reale, M. L., Alvear, K., Vergne, D., & Ghaemi, S. N. (2013). Cognitive impairment in bipolar disorder and schizophrenia: a systematic review. *Frontiers in psychiatry*, *4*, e87.

Voineskos, A. N., Felsky, D., Wheeler, A. L., Rotenberg, D. J., Levesque, M., Patel, S., ... & Malhotra, A. K. (2016). Limited evidence for association of genome-wide schizophrenia risk variants on cortical neuroimaging phenotypes. *Schizophrenia bulletin*, *42*(4), 1027-1036.

Walton, E., Geisler, D., Lee, P. H., Hass, J., Turner, J. A., Liu, J., ... & Gollub, R. L. (2013). Prefrontal inefficiency is associated with polygenic risk for schizophrenia. *Schizophrenia bulletin*, 40(6), 1263–1271.

Walton, E., Turner, J., Gollub, R. L., Manoach, D. S., Yendiki, A., Ho, B. C., ... & Ehrlich, S. (2012). Cumulative genetic risk and prefrontal activity in patients with schizophrenia. *Schizophrenia bulletin*, *39*(3), 703-711.

Webb, A. (2003). *Introduction to biomedical imaging*. Hoboken, NJ: Wiley-Interscience.

Wechsler, D. (1981). WAIS-R manual: Wechsler adult intelligence scale-revised. *Psychological Corporation.*

Wechsler D. (1997). Wechsler Adult Intelligence Scale-Third Edition. *Psychological Corporation.*

Wechsler, D. (2008). Wechsler adult intelligence scale – Fourth Edition (WAIS–IV). San Antonio, TX: *NCS Pearson.*

Weisskoff, R. M., Baker, J., Belliveau, J., Davis, T. L., Kwong, K. K., Cohen, M. S., & Rosen, B. R. (1993). Power spectrum analysis of functionally-weighted MR data: what's in the noise. *Proceedings of the international society for magnetic resonance in medicine, 1*(7).

Whalley, H. C., Hall, L., Romaniuk, L., Macdonald, A., Lawrie, S. M., Sussmann, J. E., & McIntosh, A. M. (2014). Impact of cross-disorder polygenic risk on frontal brain activation with specific effect of schizophrenia risk. *Schizophrenia research*, *161*(2), 484-489.

Whalley, H. C., Papmeyer, M., Romaniuk, L., Johnstone, E. C., Hall, J., Lawrie, S. M., ... & McIntosh, A. M. (2012a). Effect of variation in diacylglycerol kinase eta (DGKH) gene on brain function in a cohort at familial risk of bipolar disorder. *Neuropsychopharmacology*, *37*(4), 919-928.

Whalley, H. C., Papmeyer, M., Sprooten, E., Romaniuk, L., Blackwood, D. H., Glahn, D. C., ... & McIntosh, A. M. (2012b). The influence of polygenic risk for bipolar disorder on neural activation assessed using fMRI. *Translational psychiatry*, *2*(7), e130.

Wing, J. K., Babor, T., Brugha, T., Burke, J., Cooper, J. E., Giel, R., ... & Sartorius, N. (1990). Scan: Schedules for clinical assessment in neuropsychiatry. *Archives of general psychiatry*, *47*(6), 589-593.

Worsley, K. J., Taylor, J. E., Tomaiuolo, F., & Lerch, J. (2004). Unified univariate and multivariate random field theory. *NeuroImage*, *23(1)*, S189-S195.

Wray, N. R., Lee, S. H., Mehta, D., Vinkhuyzen, A. A., Dudbridge, F., & Middeldorp, C. M. (2014). Research review: polygenic methods and their application to psychiatric traits. *Journal of child psychology and psychiatry*, *55*(10), 1068-1087.

Wylie, K. P., & Tregellas, J. R. (2010). The role of the insula in schizophrenia. *Schizophrenia research*, *123*(2), 93-104.

Yoshimura, Y., Okamoto, Y., Onoda, K., Okada, G., Toki, S., Yoshino, A., ... & Yamawaki, S. (2014). Psychosocial functioning is correlated with activation in the anterior cingulate cortex and left lateral prefrontal cortex during a verbal fluency task in euthymic bipolar disorder: a preliminary fMRI study. *Psychiatry and clinical neurosciences*, *68*(3), 188-196.

Yurgelun-Todd, D.A., Waternaux C.M., Cohen B.M., Gruber S.A., English C.D., Renshaw P.F. (1996). Functional magnetic resonance imaging of schizophrenic patients and comparison subjects during word production. *American journal of psychiatry*, *153*(2), 200-205.

Appendix

Appendix A – Z-standardization of the IQ scores

To allow comparisons between the different tests used to evaluate the IQ, the scores obtained for each test were z-standardized. The z-score for each score is given by

$$Z = \frac{x - \mu}{\sigma} \quad \text{(A.1)}$$

Where x is the IQ score of each participant on a given test and μ is the average and σ the standard deviation of the IQ scores for the controls assessed on the same test. Since several participants were assessed using more than one test, the z-scores selected to be included on the analysis were dependent on the frequency of each test. First, the z-scores of the test most frequent were assigned to the participants assessed through that test, then the z-scores of the second most used test were assigned to the participants…. The order of tests (from most used to less used test) was WASI4 (assessed on 39 participants) - NART (assessed on 35 participants) - WAIS-R (assessed on 34 participants) - WASI3 (assessed on 33 participants). After assigning to each participant the standardized z-score, it was necessary to calculate a standardized IQ-score for the ones in each the IQ was not measured (8 participants). The missing values were correspondent to the average value of the standardized z-score for each diagnostic group.

Appendix B – Correlation between PRS and demographic variables

In order to understand if the with PRS is linearly related with demographic variables present on Table 2.1, I have calculated the Pearson's or Spearman's correlation coefficient and its respective p-value for each pair PRS – demographic variable. The Spearman's correlation coefficient, a non-parametric equivalent of Pearson's, was used to understand if the PRS was correlated with Gender, a binary variable. All coefficients and their respective p-values were calculated using the MATLAB function `corr(x)`, that computes p-values for the correlation coefficient r through a students' t-distribution. The t-test statistic for a correlation coefficient r is given by

$$t_{df} = \frac{r\sqrt{n-2}}{\sqrt{1-r^2}} \tag{B.1}$$

Where df are equal to n-2 and n is the number of observations (Chernick & Friis, 2003).

The Pearson's and Spearman's coefficients and their respective p-values obtained are summarized on Table B.1. The only pair with p-value<0.05 is the PRS-Gender, which means that these two variables are (slighlty) statistically correlated. PRS is not correlated with any other variable tested.

Table B.1 - Correlation coefficients and respective p-values for the pairs PRS-Age, PRS-IQ, PRS-YE and PRS-Gender.

	Correlation coefficients	p-value
PRS-Age	-0.072	0.50
PRS-IQ (z-scores)	-0.18	0.071
PRS-YE	-0.10	0.30
PRS-Gender	-0.24	0.015

Appendix C – Histogram plots of the incorrect responses during the task

To understand if the number of incorrect responses given by the participants during the task, on easy, on hard and on both versions of the task combined, for each group analyzed individually, follow a normal distribution, the histogram plots of these variables were obtained using MATLAB 8.1.0.604 (Figure C.1; C.2 and C.3), where the x axis represents the number of incorrect responses and its respective frequency, for each group. A visual inspection of these plots suggests that the number of incorrect responses does not follow a normal distribution.

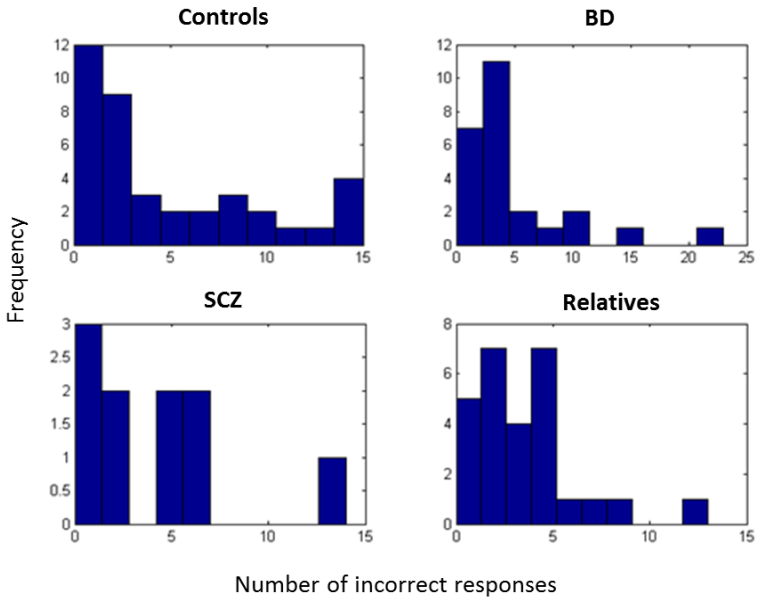

Figure C.1 - Histogram of the number of incorrect responses during easy trials.

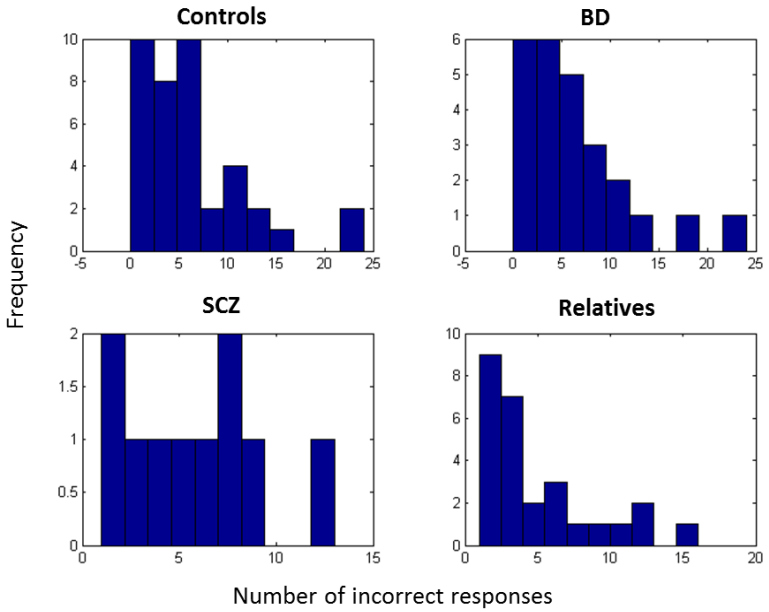

Figure C.2 - Histogram of the number of incorrect responses during hard trials.

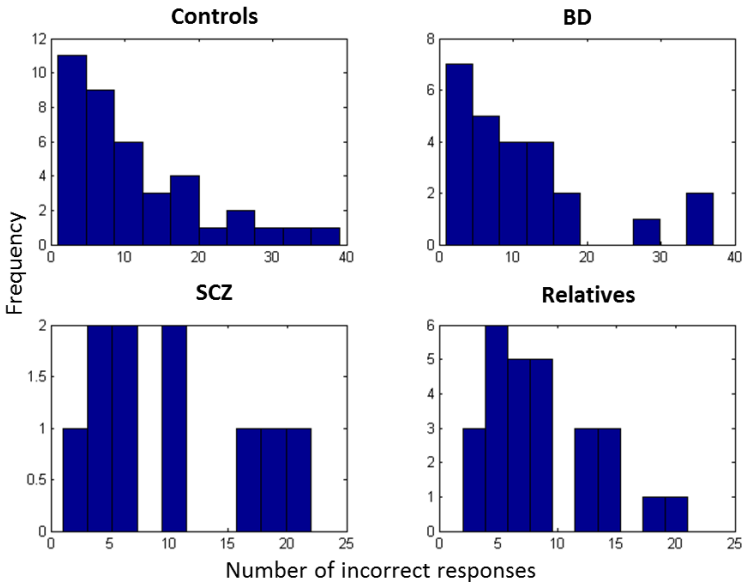

Figure C.3 - Histogram of the total number of incorrect responses during the VF task.

Appendix D – Automated Anatomical Labeling 2 (AAL2)

AAL2 is a software available as an extension for SPM that enables anatomical labeling of clusters and local maxima (Rolls, Joliot, & Tzourio-Mazoyer, 2015). On Table D.1 there is a list of the anatomical descriptions of the regions defined in AAL2 and their respective indexes and abbreviations.

Table D.1 – AAL2 anatomical regions descriptions and their respective indices and abbreviations.

Indexes	Anatomical descriptions	Abbreviations
1	Left precentral gyrus	Precentral_L
2	Right precentral gyrus	Precentral_R
3	Left superior frontal gyrus, dorsolateral	Frontal_Sup_2_L
4	Right superior frontal gyrus, dorsolateral	Frontal_Sup_2_R
5	Left middle frontal gyrus	Frontal_Mid_2_L
6	Right middle frontal gyrus	Frontal_Mid_2_R
7	Left inferior frontal gyrus, opercular part	Frontal_Inf_Oper_L
8	Right inferior frontal gyrus, opercular part	Frontal_Inf_Oper_R
9	Left inferior frontal gyrus, triangular part	Frontal_Inf_Tri_L
10	Right inferior frontal gyrus, triangular part	Frontal_Inf_Tri_R
11	Left inferior frontal gyrus, pars orbitalis	Frontal_Inf_Orb_2_L
12	Right inferior frontal gyrus, pars orbitalis	Frontal_Inf_Orb_2_R
13	Left rolandic operculum	Rolandic_Oper_L
14	Right rolandic operculum	Rolandic_Oper_R
15	Left supplementary motor area	Supp_Motor_Area_L
16	Right supplementary motor area	Supp_Motor_Area_R
17	Left olfactory cortex	Olfactory_L
18	Right olfactory cortex	Olfactory_R
19	Left superior frontal gyrus, medial	Frontal_Sup_Medial_L
20	Right superior frontal gyrus, medial	Frontal_Sup_Medial_R
21	Left medial orbital gyrus	Frontal_Med_Orb_L
22	Right medial orbital gyrus	Frontal_Med_Orb_R
23	Left gyrus rectus	Rectus_L
24	Right gyrus rectus	Rectus_R
25	Left medial orbital gyrus	OFCmed_L
26	Right medial orbital gyrus	OFCmed_R
27	Left anterior orbital gyrus	OFCant_L
28	Right anterior orbital gyrus	OFCant_R
29	Left posterior orbital gyrus	OFCpost_L
30	Right posterior orbital gyrus	OFCpost_R
31	Left lateral orbital gyrus	OFClat_L
32	Right lateral orbital gyrus	OFClat_R
33	Left insula	Insula_L
34	Right insula	Insula_R
35	Left anterior cingulate & paracingulate gyri	Cingulate_Ant_L
36	Right anterior cingulate & paracingulate gyri	Cingulate_Ant_R
37	Left middle cingulate & paracingulate gyri	Cingulate_Mid_L
38	Right middle cingulate & paracingulate gyri	Cingulate_Mid_R
39	Left posterior cingulate gyrus	Cingulate_Post_L
40	Right posterior cingulate gyrus	Cingulate_Post_R
41	Left hippocampus	Hippocampus_L
42	Right hippocampus	Hippocampus_R
43	Left parahippocampal gyrus	ParaHippocampal_L

44	Right parahippocampal gyrus	ParaHippocampal_R
45	Left amygdala	Amygdala_L
46	Right amygdala	Amygdala_R
47	Left calcarine fissure and surrounding cortex	Calcarine_L
48	Right calcarine fissure and surrounding cortex	Calcarine_R
49	Left cuneus	Cuneus_L
50	Right cuneus	Cuneus_R
51	Left lingual gyrus	Lingual_L
52	Right lingual gyrus	Lingual_R
53	Left superior occipital gyrus	Occipital_Sup_L
54	Right superior occipital gyrus	Occipital_Sup_R
55	Left middle occipital gyrus	Occipital_Mid_L
56	Right middle occipital gyrus	Occipital_Mid_R
57	Left inferior occipital gyrus	Occipital_Inf_L
58	Right inferior occipital gyrus	Occipital_Inf_R
59	Left fusiform gyrus	Fusiform_L
60	Right fusiform gyrus	Fusiform_R
61	Left postcentral gyrus	Postcentral_L
62	Right postcentral gyrus	Postcentral_R
63	Left superior parietal gyrus	Parietal_Sup_L
64	Right superior parietal gyrus	Parietal_Sup_R
65	Left inferior parietal gyrus	Parietal_Inf_L
66	Right inferior parietal gyrus	Parietal_Inf_R
67	Left supramarginal gyrus	SupraMarginal_L
68	Right supramarginal gyrus	SupraMarginal_R
69	Left angular gyrus	Angular_L
70	Right angular gyrus	Angular_R
71	Left precuneus	Precuneus_L
72	Right precuneus	Precuneus_R
73	Left paracentral lobule	Paracentral_Lobule_L
74	Right paracentral lobule	Paracentral_Lobule_R
75	Left caudate nucleus	Caudate_L
76	Right caudate nucleus	Caudate_R
77	Left lenticular nucleus, putamen	Putamen_L
78	Right lenticular nucleus, putamen	Putamen_R
79	Left lenticular nucleus, pallidum	Pallidum_L
80	Right lenticular nucleus, pallidum	Pallidum_R
81	Left thalamus	Thalamus_L
82	Right thalamus	Thalamus_R
83	Left Helschl's gyrus	Heschl_L
84	Right Helschl's gyrus	Heschl_R
85	Left superior temporal gyrus	Temporal_Sup_L
86	Right superior temporal gyrus	Temporal_Sup_R
87	Left temporal pole: superior temporal gyrus	Temporal_Pole_Sup_L
88	Right temporal pole: superior temporal gyrus	Temporal_Pole_Sup_R
89	Left middle temporal gyrus	Temporal_Mid_L
90	Right middle temporal gyrus	Temporal_Mid_R
91	Left temporal pole: middle temporal gyrus	Temporal_Pole_Mid_L
92	Right temporal pole: middle temporal gyrus	Temporal_Pole_Mid_R
93	Left inferior temporal gyrus	Temporal_Inf_L
94	Right inferior temporal gyrus	Temporal_Inf_R

95	Left crus I of cerebellar hemisphere	Cerebelum_Crus1_L
96	Right crus I of cerebellar hemisphere	Cerebelum_Crus1_R
97	Left crus II of cerebellar hemisphere	Cerebelum_Crus2_L
98	Right crus II of cerebellar hemisphere	Cerebelum_Crus2_R
99	Left lobule III of cerebellar hemisphere	Cerebelum_3_L
100	Right lobule III of cerebellar hemisphere	Cerebelum_3_R
101	Left lobule IV, V of cerebellar hemisphere	Cerebelum_4_5_L
102	Right lobule IV, V of cerebellar hemisphere	Cerebelum_4_5_R
103	Left lobule VI of cerebellar hemisphere	Cerebelum_6_L
104	Right lobule VI of cerebellar hemisphere	Cerebelum_6_R
105	Left lobule VIIB of cerebellar hemisphere	Cerebelum_7b_L
106	Right lobule VIIB of cerebellar hemisphere	Cerebelum_7b_R
107	Left lobule VIII of cerebellar hemisphere	Cerebelum_8_L
108	Right lobule VIII of cerebellar hemisphere	Cerebelum_8_R
109	Left lobule IX of cerebellar hemisphere	Cerebelum_9_L
110	Right lobule IX of cerebellar hemisphere	Cerebelum_9_R
111	Left lobule X of cerebellar hemisphere	Cerebelum_10_L
112	Right lobule X of cerebellar hemisphere	Cerebelum_10_R
113	Lobule I, II of vermis	Vermis_1_2
114	Lobule III of vermis	Vermis_3
115	Lobule IV, V of vermis	Vermis_4_5
116	Lobule VI of vermis	Vermis_6
117	Lobule VII of vermis	Vermis_7
118	Lobule VIII of vermis	Vermis_8
119	Lobule IX of vermis	Vermis_9
120	Lobule X of vermis	Vermis_10